

Matter under extreme conditions

C. Adami^a and G.E. Brown^b

^a *W.K. Kellogg Radiation Laboratory 106-38, California Institute of Technology, Pasadena, CA 91106, USA*

^b *Physics Department, State University of New York at Stony Brook, Stony Brook, NY 11794, USA*

Received April 1993; editor: G.E. Brown

Abstract:

We study scenarios for chiral symmetry restoration and deconfinement at finite temperature and/or density, based on assuming universal scaling relations for some hadron masses. We explore and discuss consequences of this scaling assumption in nuclear structure and show that most experiments support the scaling. The relevance of soft and hard scales as pertaining to chiral symmetry restoration and deconfinement is emphasized, and scaling relations for nonstrange and strange Goldstone bosons are presented. Theoretical support for the scaling relations is found from the analysis of effective Lagrangians in hot and dense matter, as well as finite-temperature and finite-density QCD sum rules. Both approaches suggest the validity of approximate scaling relations and identify sources of violation of the latter.

Finite-temperature hadron masses can be compared to the results of QCD lattice gauge calculations. We show that large screening masses above T_c merging into chiral multiplets are consistent with thermal, rather than dynamically generated, quark masses on the lattice. The results are consistent with vanishing dynamically generated masses above T_c , where T_c is interpreted as the chiral symmetry restoration temperature.

We review the “dynamical confinement” scenario of hot quarks and show that the hadronic wavefunctions obtained above T_c are consistent with those obtained from recent measurements of the latter in lattice QCD. This suggests that there are strong quark/antiquark correlations in the vector meson channels.

We conclude that for finite-temperature QCD, chiral symmetry above T_c is realized in terms of essentially massless multiplets of chiral partners, and that chiral symmetry restoration is the only phase transition.

Contents:

1. Introduction	3	6.1. The ρ -meson at finite temperature	35
2. Universal scaling and scale invariance: its breaking and restoration	4	6.2. The nucleon at finite temperature	41
3. Two scales: chiral and conformal restoration	13	7. QCD sum rules at finite density and the nuclear many-body problem	45
4. Effective restoration of explicit chiral symmetry breaking	20	7.1. Vector-meson masses	46
4.1. Density dependence of π and K -masses	20	7.2. Nucleon mass and nuclear matter equation of state	47
4.2. Kaon condensation and neutron stars	22	7.3. Saturation of nuclear matter	50
4.3. Relativistic heavy ion collisions	25	8. The hadron to quark/gluon transition	52
5. Evidence for scaling in nuclei	27	8.1. The Hagedorn scenario	53
5.1. K^+ -nucleus scattering	27	8.2. Lattice gauge simulations	56
5.2. Missing longitudinal strength	30	8.3. Dynamical confinement	61
5.3. Axial charge renormalization at finite density	32	9. Conclusions	67
6. Hadronic properties and scaling from QCD sum rules at finite temperature	34	References	68

MATTER UNDER EXTREME CONDITIONS

C. ADAMI

*W.K. Kellogg Radiation Laboratory 106-38, California Institute of Technology,
Pasadena, CA 91106, USA*

and

G.E. BROWN

Physics Department, State University of New York at Stony Brook, Stony Brook, NY 11794, USA



NORTH-HOLLAND

1. Introduction

Progress in the understanding of hot and dense matter seems to be impeded mainly on two accounts: On the one hand, experiments recreating the hot and dense environment are very difficult, and data, while abundant, are hard to analyze and quantify. On the other hand, the underlying theory, QCD, is nonperturbative. Historically, most of the attention was brought to the investigation of the high-temperature phase, where new physics was most likely to be found. The main tools in this undertaking turned out to be relativistic quantum field theory in an attempt to describe the thermodynamics of the plasma phase microscopically, and hydrodynamic models focusing on dynamics and global aspects of the phase. While yielding important insights, both approaches are limited: the quantum field theoretic one because of persistent nonperturbative effects even at high temperatures, the hydrodynamic one because in the relativistic heavy-ion collision environment thermodynamic equilibrium does not seem to be achieved. The low temperature and density phase (“low” in this context meaning below the respective critical values), on the other hand, was considered uninteresting in the sense that the global properties, and in particular the mass spectrum, were assumed not to differ from the zero temperature and density ones. On the whole, this attitude seems more and more surprising. Indeed, it is generally believed that all dimensionful parameters in QCD are related to the one true scale of the theory, Λ_{QCD} (as the quark masses are believed to arise from the symmetry breaking mechanism of the electroweak sector). One such dimensionful parameter, the quark condensate, was shown to change with temperature already in early-eighties lattice QCD calculations, from which it might have been straightforward to surmise that, if $\langle \bar{q}q \rangle \sim \Lambda_{\text{QCD}}^3$, then since e.g. $m_N \sim \Lambda_{\text{QCD}}$ we should conclude that all hadron masses should change accordingly. In retrospect, we recognize that this conclusion was not drawn due to our ignorance of just how to relate the dynamically generated scales to the fundamental one. No matter how complicated these unknown coefficients are, however, in the absence of a symmetry principle it would seem surprising if a change in Λ_{QCD} would be exactly counterbalanced by a commensurate change in the said coefficient.

As a consequence of these severe constraints, two very useful tools, lattice gauge calculations, and effective model building, have gained prominence complementing the standard approach sketched above. We attempt in this report to use these tools to outline a general picture of hot and dense matter that reflects the qualitative features that have emerged from experiments and lattice calculations. While this scenario and some of its consequences have been proposed earlier [1–3], it is really the recent “discovery”, in lattice gauge theory calculations, that the QCD transition is very probably of second order, more akin to a smooth crossover of thermodynamic variables [4–7], that has provided a serious shake-up of firmly held beliefs. Indeed, the notion of gradual restoration of chiral symmetry seems to imply that physical hadron masses below T_χ must be affected by this “reordering” taking place in the QCD vacuum. Secondly, the notion of a deconfined phase of quarks and gluons above a certain critical temperature is under serious reconsideration stemming from the observation, again in lattice QCD, of hadronic modes above T_χ [8], area-law behaviour of the Wilson loop above T_χ [9], and confined bound-state wave functions [10]. We will attempt here to tie these observations together, and provide a rough framework in which these phenomena can be understood. Naturally, as the framework relies mostly on effective models, not altogether consistent with each other, we do not claim to have a theory of hot and dense matter. Rather, we

hope to stir discussions, and provide a somewhat novel point of view.

In section 2 we will present the hypothesis of Brown–Rho scaling as developed in ref. [11], and proceed with a description of the Campbell, Ellis, and Olive [12,13] effective theory that provides a mechanism for several of these scaling relations. We also point out effects that lead to a violation of Brown–Rho scaling. In the third section we address the apparent contradiction between the emergence of two independent scales (the gluonic scale set by the trace anomaly to one-loop order, and the quark scale set by the quark condensate), and the universal scaling hypothesis. Indeed we find that there are two rather different scales in the problem, namely a “soft” scale, related to the cube root of the quark condensate $|\langle\bar{q}q\rangle|^{1/3}$, which sets the scale for chiral symmetry restoration (this is the quantity we believe should be associated with the average background field $\bar{\chi}_*$ introduced in section 2), and a “hard” scale, related to the fourth root of the gluon condensate $\langle G_{\mu\nu}^2\rangle^{1/4}$, which should be associated with the order parameter of restoration of conformal symmetry; equivalently, with the fourth root of the bag constant $B^{1/4}$, which enters into the hadron to quark/gluon transition. This plays a crucial role in the quark/gluon phase transition, and will turn out to be $B^{1/4} = 245$ MeV for two flavors^{*)}. We shall also show, by calculating the energy associated with chiral restoration, that we can define an effective bag constant $B_{\text{eff}}^{1/4}$ which sets the scale for chiral restoration. The fact that these scales are quite different will have important consequences for the transition from hadrons to quarks and gluons.

In section 4 we analyze density effects on the Goldstone bosons in the effective Lagrangian approach. We point out the origin of the weak density dependence of the pion mass, and obtain the density dependence of strange meson masses in the framework set forth by Kaplan and Nelson [14, 15]. This is an instance where scaling is obtained in a model dependent way (chiral perturbation theory). Yet, the consequences, for e.g. kaon condensation, are striking. Section 5 is devoted to a review of the experimental evidence for scaling in nuclei.

We show how the apparent contradiction between the emergence of two scales and universal scaling relations can be resolved to a certain degree in the QCD sum rule formalism in section 6, where we discuss the temperature dependence of hadron masses and widths using as input temperature dependent vacuum condensates. Section 7 then is devoted to a review of QCD sum rule calculations at finite density, with applications to hadron masses and the nuclear binding problem. In section 8 we explore the consequences of the scaling hypothesis for the hadron to quark/gluon transition proper, and try to connect our predictions with those of lattice gauge theory. Furthermore, we sketch a schematic model that reproduces the general features of dynamical confinement as observed in recent lattice calculations. We offer some conclusionary comments in the last section.

2. Universal scaling and scale invariance: its breaking and restoration

The hypothesis of universal scaling, or Brown–Rho scaling, can be put succinctly: We claim that many discrepancies between theory and experiment in nuclear physics can be understood if meson masses decrease with increasing density at about the same rate as the nucleon effective mass. We denote this temperature and density dependent fraction by Φ , i.e.,

$$\Phi = \frac{m_N^*}{m_N} = \frac{m_\rho^*}{m_\rho} = \frac{m_\omega^*}{m_\omega} = \frac{m_\sigma^*}{m_\sigma} = \frac{f_\pi^*}{f_\pi} = \frac{\Lambda^*}{\Lambda}. \quad (2.1)$$

^{*)} There is a weak flavor dependence in B , as will be shown later on.

Here, and in the following, “starred” quantities are to be taken “in medium”, meaning temperature and/or density, depending on the context. This concept of a universal, single, scale, can be argued for directly from QCD, as apart from quark masses the theory indeed only possesses one such scale, usually taken to be Λ_{QCD} . While this might be true in general, it does not seem to be a useful concept by itself, as we are as yet incapable of calculating any low-energy observables directly from QCD armed with just the knowledge of Λ_{QCD} . Also, violations must arise at temperatures and densities where $T, \mu \sim \Lambda_{\text{QCD}}$.

Initially [16, 17] the argument for the scaling (2.1) as an, at least approximate, universal scaling, was made in terms of a dynamical model, in which pions were viewed as basic building blocks of the mesons. The scaling behavior was detached from this particular microscopic model in refs. [18, 19], where the need for a single scale in the broken symmetry regime of QCD was argued for. The scaling of f_π^*/f_π was shown to follow [20, 21], at least at low momentum scales, from the Goldberger–Treiman relation. While Nambu–Jona-Lasinio (NJL)-type theories produce the scaling $m_N^*/m_N = m_\sigma^*/m_\sigma$ [22], they do not allow for decreases in the vector meson masses unless the cutoff Λ is also allowed to scale [23]. Arguments for the latter were put forward by the present authors recently in ref. [24]. There, we suggested that extending the zero-range interaction of the NJL theory to finite range requires $\Lambda^*/\Lambda = m_\sigma^*/m_\sigma$, while obtaining a formula for the nucleon mass very much similar to the well-known Ioffe formula [25], obtained from QCD sum rules. This scaling of the Nambu–Jona-Lasinio cutoff does not appear to follow directly from an extension of the model to finite temperature and density. This, however, can be traced back to the explicit breaking of scale symmetry in the process of obtaining the effective theory from the QCD effective action, as gluon masses have to be introduced in intermediate steps (see, e.g., ref. [26]). However, it was also realized by Kusaka and Weise that it is unreasonable to restore scale invariance in the NJL Lagrangian by the introduction of a hard (gluonic) scale only [27]. A re-investigation of the NJL Lagrangian systematically keeping track of the scaling properties of the operators and restoring scale symmetry appropriately shows that it can be modified so as to yield results roughly compatible with our scaling hypothesis [28].

Independently of these developments, it was realized [21] that finite-density QCD sum rules would predict hadron masses that, at least approximately, would scale according to (2.1). This was demonstrated convincingly by Hatsuda and Lee [29] and Hatsuda et al. [30].

On an entirely different level, Campbell, Ellis and Olive [12, 13] analyzed the QCD phase transition in an effective field theory. They point out that low-energy effective Lagrangians for spontaneously broken chiral symmetry do not correctly reflect the operator scaling properties of QCD. Whereas massless QCD is scale invariant at the tree level, some terms in the low-energy effective Lagrangian do not have the correct scale dimension to be invariant. We will in the following repeat Campbell, Ellis, and Olive’s arguments in a slightly more general way, and draw our own conclusions about the implications for the phase transition.

The low-energy Lagrangian for spontaneously broken chiral symmetry may be written as

$$\mathcal{L} = \frac{1}{4}f_\pi^2 \text{Tr}(\partial_\mu U \partial^\mu U^\dagger) + \frac{1}{4}\epsilon^2 \text{Tr}[L_\mu, L_\nu]^2 - c \text{Tr}\{M_q(U + U^\dagger)\} + \dots \quad (2.2)$$

in an expansion in derivatives and quark masses. Here

$$U(x) = \exp\left(i \sum_{i=0}^8 \frac{\lambda_i \phi_i(x)}{f_\pi}\right) \quad (2.3)$$

is the “order-parameter field”, or more precisely, the phase of an order-parameter field (this terminology is argued for below), and $M_q = \text{diag}(m_u, m_d, m_s)$ is the quark mass matrix. Furthermore,

c is a dimensionful constant to be determined later, and $L_\mu = U^\dagger \partial_\mu U$. We neglect the $U_A(1)$ anomaly, but include the fourth-order ‘‘Skyrme term’’ not considered by Campbell et al. This will lead to some interesting consequences.

Spontaneous breaking of chiral symmetry arises through a nonvanishing vacuum expectation value for the order-parameter field $U(x)$. This may be related to the global order parameter $\langle \bar{q}q \rangle$ through a suitable average

$$\langle 0|\bar{q}q|0\rangle = \frac{-c}{V} \int_V d^3x \langle 0|\text{Tr}(U + U^\dagger)|0\rangle. \quad (2.4)$$

Skyrmions (nucleons) arise through topological defects in the order parameter (solitons), and fluctuations of the order parameter may be associated with the Goldstone bosons of the spontaneously broken symmetry. This explains the parameterization (2.3) by pseudoscalar meson fields.

Although each term in the Lagrangian (2.2) has mass dimension four so as to give a dimensionless action $\int d^4x \mathcal{L}(x)$, they do not (except for the fourth-order Skyrme term) correctly reflect the operator scaling properties of QCD. Under scale transformations, a field ϕ transforms as

$$\phi(x) \rightarrow e^{\alpha d} \phi(e^\alpha x), \quad (2.5)$$

where d is in general a matrix. Its eigenvalue, which should be 1 for bosons, and $\frac{3}{2}$ for fermions, is called the *scale dimension* of the field. The infinitesimal form of (2.5) is

$$\delta\phi = (d + x_\mu \partial^\mu) \phi(x), \quad (2.6)$$

where we left out the infinitesimal parameter α . The operators $G_{\mu\nu}(x)G^{\mu\nu}(x)$ and $\bar{\psi}(x) \overleftrightarrow{D} \psi(x)$ appearing in the QCD Lagrangian have scale dimension 4, so that

$$\delta S_{\text{QCD}} = \int d^4x \delta \mathcal{L}_{\text{QCD}} = \int d^4x (4 + x_\mu \partial^\mu) \mathcal{L}_{\text{QCD}} = 0, \quad (2.7)$$

where $\delta \mathcal{L}_{\text{QCD}}$ is the change in \mathcal{L}_{QCD} due to dilatation and the final equation results from a partial integration. Hence, massless QCD is scale invariant at the tree level, while quark mass terms have scale dimension $d=3$ and thus break scale invariance explicitly. On the other hand, the two terms in the effective Lagrangian (2.2) have scale dimension $d=2$ and $d=0$, respectively. Low energy effective Lagrangians of the type (2.2) are usually obtained ‘‘from QCD’’ by integrating out the quark fields on the path integral level and expanding the resulting fermion determinant in terms of derivatives. The scaling properties of the original Lagrangian are not preserved by this operation, as it requires the introduction of an ultraviolet cutoff parameter as a regulator, which explicitly breaks scale invariance. In the usual lore this cutoff is then related to f_π to represent the dynamically generated scale. Indeed, it is precisely the dimensionful parameter f_π that spoils the scaling properties of the effective Lagrangian (2.2). In the following we shall take the stance that, while (2.2) is a good starting point, there is nothing sacred about it, particularly as the concept of an ultraviolet cutoff governing the low-energy behavior in the guise of a pion decay constant seems suspect. More specifically, we strive to restore the scaling properties of the QCD Lagrangian which were lost in the regularization procedure. In addition to that, we will mimic the breaking of scale invariance at the quantum level in QCD, through the emergence of a trace anomaly, by adding an effective potential term to (2.2) that breaks scale invariance explicitly, and can be thought of as arising through the Coleman–Weinberg mechanism [31].

The minimal possibility [32] for restoring scale symmetry is to introduce a flavor singlet field χ with scale dimension $d = 1$. The correct tree-level QCD scaling properties can be restored by multiplying each of the terms in (2.2) by appropriate powers of (χ/χ_0) and introducing a kinetic term for the χ -field:

$$\begin{aligned} \mathcal{L} = & \frac{1}{4}f_\pi^2 (\chi/\chi_0)^2 \text{Tr} \partial_\mu U \partial^\mu U^\dagger + \frac{1}{2} \partial_\mu \chi \partial^\mu \chi \\ & - c (\chi/\chi_0)^3 \text{Tr} \{M_q(U + U^\dagger)\} + \frac{1}{4} \epsilon^2 \text{Tr}[L_\mu, L_\nu]^2. \end{aligned} \quad (2.8)$$

Here, χ_0 is the expectation value of the χ -field, at zero temperature and density. This should of course be nonzero and arise dynamically as the minimum of the effective potential for χ introduced below, thus replacing the dimensionful coupling constants (dimensional transmutation).

At the quantum level the QCD Lagrangian develops the well-known trace anomaly [33], which breaks scale invariance explicitly. As we mentioned earlier, we mimic this by adding an effective potential to (2.2). Such an effective potential breaks scale invariance much in the same way as the trace anomaly does. We thus add ^{*)} (b is a dimensionless constant)

$$V_{\text{eff}} = \frac{1}{2} b \chi^4 \left\{ \log (\chi/\chi_0)^2 - \frac{1}{2} \right\} \quad (2.9)$$

to the Lagrangian such that

$$\begin{aligned} \delta \int d^4x (\mathcal{L} + V_{\text{eff}}) &= \int d^4x \left(c (\chi/\chi_0)^3 \text{Tr} \{M_q(U + U^\dagger)\} + b \chi^4 \right) \\ &= \int d^4x \theta_\mu^\mu, \end{aligned} \quad (2.10)$$

where $\theta_{\mu\nu}$ is the energy–momentum tensor. In the chiral limit we obtain

$$\langle \theta_\mu^\mu \rangle = b \chi_0^4. \quad (2.11)$$

In QCD, the expectation value of the trace anomaly is related to the bag constant, as the latter is just the energy of the vacuum. Again in the chiral limit we have then

$$\theta_\mu^\mu = -\frac{\beta(g)}{2g} (G_{\mu\nu}^a)^2, \quad (2.12)$$

where $\beta(g)$ is the QCD beta-function, g is the quark–gluon coupling constant, and $G_{\mu\nu}^a$ is the QCD field strength tensor. The bag constant then is just

$$B = \frac{1}{4} \langle 0 | \theta_\mu^\mu | 0 \rangle = \frac{1}{4} b \chi_0^4. \quad (2.13)$$

Comparing the energy–momentum tensors (2.10) and (2.12) we observe that the expectation value $\langle \chi^4 \rangle$ should be proportional to the gluon condensate $\langle G^2 \rangle$, as

$$b \chi^4 = -\frac{\beta(g)}{2g} (G_{\mu\nu}^a)^2. \quad (2.14)$$

At zero temperature, the effective potential for the χ -field forces the field configuration to take on the minimal configuration χ_0 . This is a situation reminiscent of spontaneous magnetization,

^{*)} This parameterization of the trace anomaly is unique up to nonminimal terms (see ref. [34] for a thorough discussion of this point).

where the asymmetric vacuum has a lower energy than the symmetric one. Stability of the vacuum requires that fluctuations around χ_0 be small. These fluctuations are analogous to the spin waves in a ferromagnet, and they are associated here with scalar glueball states, with a mass

$$M_\chi^2 = \delta^2 V_{\text{eff}}(\chi) / \delta\chi^2|_{\chi=\chi_0} = 4b\chi_0^2. \quad (2.15)$$

The scale of these fluctuations is presumably $M_\chi > 1$ GeV, and we do not expect to be able to describe these accurately in this approach.

The instanton-liquid picture of the QCD vacuum (see ref. [35]) suggests to interpret χ_0 as the instanton background. Under the assumption that the trace anomaly is entirely due to instantons, we would find

$$\chi^4 = \frac{1}{b} (11 - \frac{2}{3}N_f) (N + \bar{N}), \quad (2.16)$$

where N, \bar{N} are the instanton and anti-instanton densities, respectively. While this (the saturation of the gluon condensate by instantons) is an extreme point of view, it demonstrates that $\langle\chi^4\rangle$ must at least contain a piece that vanishes with chiral symmetry restoration, simply because it is known that the long range instanton structure dissolves in that limit [36].

The precise form of χ_0 is determined by solving the coupled equations of motion resulting from $\mathcal{L}_{\text{eff}} + V_{\text{eff}}$. This was done some time ago by Gomm et al. [37] (in the absence of explicit chiral symmetry breaking) and revealed the dual nature of χ_0 , in the sense that it can describe bag formation (chiral symmetry restoration inside the nucleon), or scale symmetry breaking, depending on the magnitude of $B = \frac{1}{4}b\chi_0^4$. This duality will be discussed in more detail in sections 3 and 6. Here we shall organize our expansion in such a way that *the averaged finite-temperature/density expectation value* of χ is small, and therefore describes the approach to chiral restoration (see below). Let us first discuss the separation of the classical from the quantum pieces of the field at zero temperature/density. Specifically we shall treat χ_0 as another order parameter (initially associated with scale symmetry breaking), and denote fluctuations of the order parameter with χ' :

$$\chi = \chi_0 + \chi'. \quad (2.17)$$

At finite temperature and/or density, the equations of motion force χ to develop an *in medium* expectation value

$$\chi_\star = \langle\star|\chi|\star\rangle. \quad (2.18)$$

There is an intricate interplay of temperature and density effects on the order-parameter fields, which we would like to elucidate in the following. Let us first redefine the order-parameter field associated with chiral symmetry breaking as

$$\sigma_\star(\mathbf{x}) = \frac{1}{4}f_\pi\langle\star|\text{Tr}\{U(\mathbf{x}) + U^\dagger(\mathbf{x})\}|\star\rangle \quad (2.19)$$

and rewrite the explicit symmetry breaking term as

$$\mathcal{L}_{\text{sb}} = -c'\chi^3\sigma, \quad (2.20)$$

which suggests that the quark mass term is the source of explicit chiral as well as scale symmetry breaking. The σ -field is not dynamical, and does not propagate. The constant c' may be estimated via the Gell-Mann–Oakes–Renner relation

$$c' = m_\pi^2 f_\pi / \chi_0^3. \quad (2.21)$$

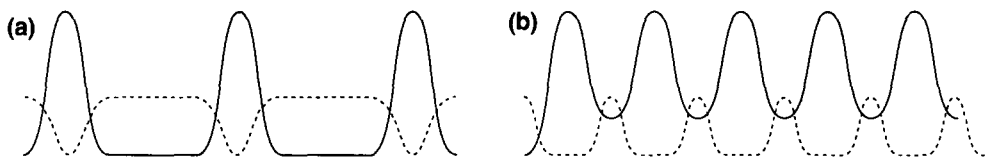


Fig. 2.1. Sketch of Skyrmon profile (solid line) and dilaton field (dashed line) in a Skyrmon crystal (estimated, arbitrary units). (a) Low density, (b) high density.

In explicit Skyrme-model calculations at finite density (baryon number N_B) it can be shown [38, 39] that the space average of σ_* tends to zero with increasing baryon number (in the absence of explicit chiral symmetry breaking). In fact, this quantity is used as the order parameter for chiral symmetry restoration in ref. [38]. The vanishing of the space average of $\sigma_*(\mathbf{x})$, $\bar{\sigma}_*$, is easily understood seeing that for total winding number (baryon number) N_B we find in a sphere with radius R

$$\bar{\sigma}_* = \frac{1}{V} \int dV \frac{1}{4} f_\pi \langle * | \text{Tr}(U + U^\dagger) | * \rangle = f_\pi \frac{3}{2R^3} \int_0^R r^2 dr \cos \theta(r), \quad (2.22)$$

where $\theta(r)$ is the N_B -Skyrmion solution with boundary conditions

$$\theta(r) \rightarrow 0 \quad (r \rightarrow \infty), \quad \theta(0) = N_B \pi. \quad (2.23)$$

Thus, for large N_B the space average of the order parameter tends to zero although $\sigma_*(\mathbf{x})$ does not vanish everywhere. In ref. [37] the authors found that in the “small-bag-constant scenario” the coupling between the order-parameter fields (at zero temperature in the one-baryon sector) force χ_0 to vanish close to the nucleon center. Tentatively generalizing these results to the Skyrmon crystal (this was done explicitly only on the hypersphere by Reinhardt and Dang [39]) we expect χ_* to vanish almost everywhere except between nucleon sites (see fig. 2.1). This would suggest that there are in fact two ways in which the quark condensate can vanish at finite density. Generalizing eq. (2.4) we define

$$\langle \bar{q}q \rangle^* = -c \frac{1}{V} \int d^3x \langle * | (\chi/\chi_0)^3 \text{Tr}(U + U^\dagger) | * \rangle. \quad (2.24)$$

We now introduce a finite-density/temperature quantum field χ' by

$$\chi = \chi_* + \chi' \quad (2.25)$$

and insert into (2.24) such that

$$\begin{aligned} \langle \bar{q}q \rangle^* &= -c \frac{1}{V} \int d^3x (\chi_*/\chi_0)^3 \langle * | \text{Tr}(U + U^\dagger) | * \rangle d^3x \\ &\simeq -c (\bar{\chi}_*/\chi_0)^3 \bar{\sigma}_* \end{aligned} \quad (2.26)$$

obtained by neglecting the quantum fluctuations in the space average. Here, we introduced the space average of the gluonic order parameter

$$\bar{\chi}_* = \frac{1}{V} \int d^3x \chi_*(\mathbf{x}). \quad (2.27)$$

Thus, the *in medium* quark condensate can vanish either because the average of the order-parameter phase $\bar{\sigma}_*$ vanishes, or because $\bar{\chi}_*$ does. We would like to stress again that this does not imply that scale symmetry is restored inside the nucleon. Our choice of splitting the quantum field χ (see eq. (2.33) below) isolates the piece of χ associated with chiral symmetry restoration, since this is the piece we are interested in. Other choices (for example expanding around the unaveraged χ_*), while possible, will result in effective Lagrangians that reliably describe the physics at a different scale.

Let us now consider the case of vanishing baryon number. This case is in some respects more tricky in this approach, as the behavior of σ_* with temperature has not yet been worked out numerically. We might surmise, however, that at zero density and finite temperature

$$\sigma_* = \frac{1}{4}f_\pi \langle * | \text{Tr}(U + U^\dagger) | * \rangle \simeq \frac{1}{4}f_\pi \langle 0 | \text{Tr}(U + U^\dagger) | 0 \rangle = f_\pi \quad (2.28)$$

as in the trivial ($N_B = 0$) sector $U \simeq 1$. With the above definition of bulk quark condensates, we find

$$\langle \bar{q}q \rangle^* / \langle \bar{q}q \rangle = (\bar{\chi}_* / \chi_0)^3, \quad (2.29)$$

which leads to one of the scaling relations we are advertising. In case (2.28) is violated through temperature effects on $\text{Tr}(U + U^\dagger)$, the detailed behavior of σ_* will change, but none of our relations will be significantly altered.

The change in χ_* is induced by finite-temperature corrections to the Coleman–Weinberg effective potential. Very generally, these tend to shift the minimum of the effective potential towards $\chi_* = 0$, and the transition to a $\chi_* = 0$ vacuum can occur either smoothly or by tunneling. While this depends on the precise nature of the temperature corrections, it can be said in generality that the vacuum with $\chi_* = 0$ (melted instantons, vanishing gluon condensate) cannot support glueball fluctuations, as the effective potential is odd in χ and an expansion of the form (2.25) around $\chi_* = 0$ does not make sense. However, we expect this to happen only at temperatures well outside of the range considered here.

In order to select a suitable order parameter for the expansion, let us return to the instanton-liquid picture. Equation (2.16) suggests that χ_*^4 describes finite-temperature instanton, or caloron, fields. This caloron background is highly nonlinear. As noted by Shuryak [35]

$$\langle G^2 G^2 \rangle / \langle G^2 \rangle^2 \sim 8, \quad (2.30)$$

which indicates strong spatial fluctuations in the gluon fields. However, quarks are only weakly affected by the nonlinearity. Indeed, in the simple picture where quarks condense due to zero modes in the energy spectrum of quarks propagating in the instanton background, the quark effective mass is given by (neglecting current-quark masses) [40]

$$M_{\text{eff}} = -\frac{2}{3}\pi^2 \langle \bar{q}q \rangle \rho^2, \quad (2.31)$$

where ρ is the instanton radius. Consequently, quark–instanton interactions are governed by the much smoother quark condensate for which [35]

$$\langle \bar{q}q\bar{q}q \rangle / \langle \bar{q}q \rangle^2 \simeq 1.2. \quad (2.32)$$

The smoothness of $\langle \bar{q}q\bar{q}q \rangle$ is due to its being composed chiefly of spatially constant fermionic zero modes. In order to describe quark–background interactions we would therefore like to extract a

piece from χ for which the vacuum saturation hypothesis is approximately valid. This is clearly the space averaged expectation value (2.27). Therefore, in the following, we would like to expand around the order parameter $\bar{\chi}_*$ and in this way include all long-wavelength fluctuations, while the high-frequency ones (nonlinear pieces) will be lumped into the (redefined) quantum fluctuations χ' [11],

$$\chi = \bar{\chi}_* + \chi'. \quad (2.33)$$

This procedure leads to scaling relations in the following manner. Substituting (2.33) into (2.8), and neglecting the terms involving the fluctuations χ' yields the following effective theory with renormalized coefficients:

$$\mathcal{L} = \frac{1}{4}f_\pi^2 (\bar{\chi}_*/\chi_0)^2 \text{Tr} \partial_\mu U \partial^\mu U^\dagger - c (\bar{\chi}_*/\chi_0)^3 \text{Tr} \{M_q(U + U^\dagger)\} + \frac{1}{4}\epsilon^2 \text{Tr}[L_\mu, L_\nu]^2. \quad (2.34)$$

The neglected higher powers of χ' represent purely gluonic fluctuations which couple only weakly to the quarks as noted earlier. These fluctuations are associated with true gluonic degrees of freedom, the scale of which is not $(\bar{\chi}_*)^4$ but rather $\bar{\chi}_*^4$. The latter quantity sets a higher scale and should be related to the gluon condensate $\langle G^2 \rangle$. We estimate that the neglected terms are of the order of magnitude of the gluon condensate contribution to hadron masses in QCD sum rule calculations (see section 6). These were shown to enter at the 15% level in the expressions for masses of hadrons made up of light up and down quarks in ref. [41], and they lead in principle to violations of Brown–Rho scaling due to the emergence of the glueball mass scale. Explicit calculations (see sections 6 and 7), however, show that the coefficients of these corrections are themselves suppressed, such that the overall effect is more akin to a renormalization of the quark condensate.

Let us return to the effective Lagrangian (2.34). The expansion and truncation leads to an introduction of factors $\bar{\chi}_*/\chi_0$, which assure that each dynamically generated scale is renormalized. For example we find an *in medium* renormalized pion decay constant

$$f_\pi^* = (\bar{\chi}_*/\chi_0) f_\pi. \quad (2.35)$$

At finite temperature and vanishing baryon density, this (in conjunction with (2.29)) leads to the scaling law

$$\langle \bar{q}q \rangle^* / \langle \bar{q}q \rangle = (f_\pi^*/f_\pi)^3, \quad (2.36)$$

which is the relation discussed in ref. [21].

Equations (2.35) and (2.36) are remarkable in several respects. Indeed, $\bar{\chi}_*$ plays the role of the σ in the linear sigma model, although it is not a dynamical field. In the nonlinear sigma model, the “elementary” $\bar{q}q$ scalar field is eliminated and does not propagate, in contrast to, e.g., the Nambu–Jona-Lasinio model, which is more akin to a linear sigma model and which has a scalar meson below 1 GeV. The latter model can be bosonized by replacing the $\bar{q}q$ field by $\phi(x)U(x)$, where $\phi(x)$ is the modulus, and $U(x)$ the phase of the order parameter. When the bosonized version is made scale invariant by coupling to a dilaton field [28], an additional scalar is introduced and one witnesses mixing between scalar meson and glueball states. In the nonlinear approach, the role of the modulus $\phi(x)$ is played by the gluonic field $\chi_*(x)$, and therefore encompasses the quark and gluon scales at the same time. Once again, the space-averaged field $\bar{\chi}_*$ describes the approach towards chiral restoration via eq. (2.26), although it originated as a gluonic field.

Another scaling relation [11] can be obtained quite trivially by considering the scaling properties of the so-called Skyrme term,

$$\mathcal{L}_{\text{Sky}} = \frac{1}{4}\epsilon^2 \text{Tr}[L_\mu, L_\nu]^2. \quad (2.37)$$

This term is the only possible fourth-order term quadratic in the time derivatives, is clearly scale invariant from the outset and does not require powers of (χ/χ_0) . It can be obtained in the hidden local gauge symmetry scheme of Bando et al. [42] by integrating out the vector meson degrees of freedom. In this approach, the arbitrary coefficient of the Skyrme term is identified as

$$\epsilon^2 = 1/(8g^2), \quad (2.38)$$

where g is the hidden vector-meson gauge coupling. Furthermore, analysis of the hidden-gauge Lagrangian reveals that the Kawarabayashi–Suzuki–Riazuddin–Fayyazuddin (KSRF) relation is fulfilled, thus

$$m_V^2 = 2g^2 f_\pi^2. \quad (2.39)$$

Ignoring $\mathcal{O}(1/N_c)$ corrections and setting $m_V = m_\rho = m_\omega$ we can then rewrite the coefficient of the Skyrme term,

$$\mathcal{L}_{\text{Sky}} = \frac{1}{16} (m_\rho^2/f_\pi^2) \text{Tr} [L_\mu, L_\nu]^2. \quad (2.40)$$

This is another demonstration of the power of the effective Lagrangian approach, as the scale invariance of the Skyrme term assures that there is no renormalization of the vector coupling at finite temperature/density, a result that squares nicely with the well-known nonrenormalization of the ρ -meson coupling (ρ -universality) observed at zero temperature/density (see, e.g., ref. [43]). At the mean-field level (where $g_A = 1$) we thus obtain

$$m_\rho^*/m_\rho = f_\pi^*/f_\pi. \quad (2.41)$$

It has been known for some time that effective Lagrangians of the type (2.34) possess soliton solutions, which can be identified with the nucleons [44]. The mass of the latter is of course related to the pion decay constant, and scales like it: $m_N \sim f_\pi$. As f_π is renormalized at finite temperature/density, we expect from a Skyrme-type model to find

$$m_N^* \sim f_\pi^*. \quad (2.42)$$

Whereas it appears that as a consequence the nucleon mass drops as f_π^* , we should point out the following. While indeed the effective mass m_N^* scales with f_π^* ,

$$m_N^*/m_N = f_\pi^*/f_\pi, \quad (2.43)$$

the energy of the nucleon also depends on the vector condensate (vector field), which develops as a collective field of the nucleons at finite density. Thus, the chemical potential μ_N of the nucleon does not obey a scaling law as in (2.1); in fact, it clearly increases as densities increase above nuclear matter density ρ_0 . As a consequence, the nucleon energy does *not* obey the scaling law (2.1); rather it stays approximately constant up to densities comparable with ρ_0 .

Finally, we would like to comment on the scaling of scalar excitations in this model. This issue is somewhat obscured in this approach, as it does not allow for a dynamical scalar meson. The “nuclear-physics scalar” of mass $m_\sigma \simeq 4m_\pi$ is a substitute for correlated pairs of pions coupled to angular momentum $J = 0$. These correlations may be thought of as arising from pairs of pions scattering on each other chiefly via t -channel ρ -meson exchange. While the latter does scale, the connection to the scaling of m_σ is not immediate. It does, however, arise in *linear* sigma-model

Lagrangians, and we therefore include it in the list (2.1). We shall return to a discussion of this effect in section 7. The scaling of the scalar glue-ball states is even less clear, as from (2.15)

$$M_\chi^*/M_\chi = \chi_*/\chi_0. \quad (2.44)$$

However, no averaging enters into (2.44), and as a consequence the scaling of glue-ball states is not immediately connected to chiral restoration, and thus not accessible in this approach.

3. Two scales: chiral and conformal restoration

The idea that two scales effectively control low-energy strong interaction physics is by no means new. Shuryak [45] pointed out over ten years ago that two fundamental scales emerge in the guise of the confinement radius R_{conf} , and the constituent quark size R_Q . The disparity in these scales, he concluded, should be reflected in different temperatures for deconfinement and chiral symmetry restoration. We would like to pursue this idea in the light of more recent developments, and point out the connection of the scales mentioned above, to the fundamental vacuum condensates of QCD, the quark and the gluon condensates. As we would like to show, these give rise to two rather different bag constants, one related to chiral symmetry restoration, the other to scale symmetry restoration. Mainly, however, we would like to emphasize the *duality* inherent in this two-scale picture. Indeed, it is clear that the two scales cannot be totally independent. For example, it seems intuitively obvious that in order to have a quark condensate, condensed gluons must be present. A condensate is, after all, just the expectation value of the relevant quantity in the vacuum. Quarks must be held together, at a fundamental level, by gluons in order to condense in the vacuum. Thus, a condensate of quarks has both an expectation value $\langle \bar{q}q \rangle$ as well as $\langle (\alpha_s/\pi)G^2 \rangle$. This is most obvious for the heavy-quark condensate, for which the heavy-quark expansion yields [41]

$$\langle \bar{q}q \rangle = -\frac{1}{12}m_Q^{-1}\langle (\alpha_s/\pi)G^2 \rangle + \mathcal{O}(m_Q^{-2}). \quad (3.1)$$

As a model for the duality of descriptions (in terms of quarks or in terms of gluons), we would like to present a simple scenario which shares some of the salient features that we would like to elucidate. Instead of the “elementary” condensates, let us consider a hadronic one, e.g. the pion condensate. The usual pion condensate is, in a simpler language, a spin–isospin ordered state of nucleons. The criterion for forming such a state is that the small-amplitude spin–isospin sound becomes unstable. Consider specifically a π^- condensate in a neutron star. The condensed pion field can be described as a classical field, connected to its source by the equation

$$(\mu_\pi^2 - m_\pi^2 + \nabla^2)\langle \phi(r) \rangle = J(r), \quad (3.2)$$

where $J(r)$ is the nucleon source

$$J(r) = \sqrt{2} \frac{f}{m_\pi} \nabla \cdot \langle \psi_p^\dagger \sigma \psi_n \rangle \quad (3.3)$$

and f the pseudovector coupling constant. The chemical potential μ_π is related to neutron and proton chemical potentials by

$$\mu_{\pi^-} = \mu_n - \mu_p \quad (3.4)$$

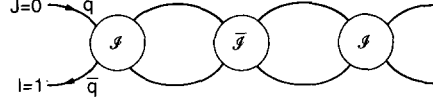


Fig. 3.1. Instanton polymer model of the pion [46]. \mathcal{I} denotes an instanton, $\bar{\mathcal{I}}$ an anti-instanton.

and serves as the energy of the pion field. The density of (negatively charged) pions in the condensate is

$$\langle \rho_{\pi^-} \rangle_C = 2\mu_\pi |\langle \phi(r) \rangle|^2. \quad (3.5)$$

In the above equations, the brackets indicate the expectation value *in the condensate*, which can be thought of as describing the new vacuum, the one with a condensate present. The energy of the new vacuum must, of course, be lower than that of the perturbative (bare) vacuum if it is to be the true ground state. We have dealt with the charged π^- condensate here, rather than the neutral π^0 one, in order to have a nonvanishing charge density (3.5).

We now have equivalent order parameters for the condensate, either the classical condensed pion field $\langle \phi(r) \rangle$ or the condensed source function $\nabla \cdot \langle \psi_p^\dagger \sigma \psi_n \rangle$. Both of these are pseudoscalars, so in order for either of these operators to develop a vacuum expectation value, the symmetry of the bare vacuum must be broken. We can, then, equivalently talk about a pion condensate, or about a $\psi_p^\dagger \sigma \psi_n$ condensate, the two being linked by the classical field equation (3.3).

A possible, more microscopic, description of the pion condensate is to consider [46] the pion as an instanton polymer, composed of a quark and an antiquark rescattering through instantons and anti-instantons. Clearly, in the graph of fig. 3.1, it is possible to cut the quark and antiquark lines so as to determine the $\bar{q}q$ content of the pion, or to cut the instanton and anti-instanton, in order to determine the gluon content, much like in the pion-condensate picture presented above.

Incidentally, rather than coupling the \bar{q} and q to an isospin $I = 1, J = 0^-$ state, in order to represent the pion, we can also couple them to $I = 0, J = 0^+$ giving rise to a scalar excitation, part of the σ -meson. In order to have a complete description of the problem of interacting pions and nucleons, or of scalar particles σ and nucleons, we should also give the nucleons a description in terms of quarks and gluons, as well as the interaction between nucleon and pion or σ .

Roughly, we can think of the two scales in this problem as the energies associated with the restoration of two (approximate) symmetries of the perturbative QCD Lagrangian: The energy associated with scale-symmetry restoration (which we shall denote by the bag constant B), and the energy associated with chiral symmetry restoration (denoted by $B_{\chi\text{SR}}$). As noted earlier, the true bag constant for the QCD transition from hadronic matter to perturbative quark/gluon matter is given by the trace (conformal) anomaly as [47]

$$B = -\frac{1}{4} \langle 0 | [\beta(g)/2g] (G_{\mu\nu}^a)^2 | 0 \rangle, \quad (3.6)$$

where

$$\beta(g) = -\frac{g^3}{16\pi^2} \left(11 - \frac{2}{3} N_f \right) \quad (3.7)$$

is the beta function of QCD to one loop, and N_f is the number of flavors. The value of the gluon condensate

$$\frac{g^2}{4\pi^2} \langle 0 | (G_{\mu\nu}^a)^2 | 0 \rangle \simeq (330 \text{ MeV})^4 \quad (3.8)$$

is well pinned down from the states of charmonium using the QCD sum rules [41]. For N_f flavors we then find

$$B^{1/4} = 165 \left(\frac{33 - 2N_f}{6} \right)^{1/4} \text{ MeV}, \quad (3.9)$$

which, for two flavors, becomes

$$B^{1/4} = 245 \text{ MeV} \quad (\text{two flavors}). \quad (3.10)$$

This is the “hard” scale, the scale for conformal restoration or, equivalently, the decondensation of gluons. Up until this decondensation, matter is not perturbative, even though with chiral restoration it may be more convenient to use the language of quarks and antiquarks rather than that of mesons. These quarks and antiquarks must, however, be connected by line integrals of the gauge potential if the description is to be gauge invariant, in the sector of broken conformal invariance. Consequently, they do not make up a perturbative quark gas. We will return to this question in section 8.3, when we sketch a schematic model for dynamical confinement.

In order to obtain an estimate for the energy associated with chiral symmetry restoration, we have to make use of a model description. An interesting and instructive hadronic model that is easily extended to finite temperature and density is the model of Nambu and Jona-Lasinio [48]. It naturally incorporates a chiral symmetry restoring transition, and can be used to predict the finite-temperature and/or density dependence of hadron parameters [23, 22, 49]. In the sense discussed in the previous section, this model is more akin to a linear sigma model, and as such the pole in the scalar propagator turns out to be rather low. In other aspects, the model predicts a more or less linearly decreasing constituent quark mass as the density is increased, and a mean-field type decrease of the quark mass with temperature (see ref. [50] for a rather complete analysis, and references therein). As mentioned earlier, however, these calculations are performed with a fixed cutoff in order not to perturb the fragile fitting of parameters. Since the cutoff of the Nambu–Jona-Lasinio model should be thought of as mimicking a physical (dimensionful) parameter of the theory, the former procedure appears to be arbitrary in the light of the scaling relations. Scaling the cutoff Λ of the NJL model with the glue-ball mass leads to the restoration of scale invariance together with that of chiral invariance [27, 28], which is not supported empirically. However, the NJL Lagrangian can be modified in such a way [28] that Brown–Rho scaling [11] results. In the following, we take a much simpler approach by just *assuming* a scaling behavior for the cutoff as dictated by (2.1). In this scenario we would like to calculate the vacuum-energy difference between the (chiral) symmetry-restored vacuum *inside* the nucleon, and the broken phase outside, and associate this energy with the soft scale, the bag constant as it appears in the MIT bag model, which we denote by $B_{\chi\text{SR}}$.

In the Nambu–Jona-Lasinio model, the vacuum develops an expectation value for the scalar field. A simple model for this is to consider a system of fermions in negative-energy states, cut off at some momentum Λ , held together by the scalar field [51]. Since we wish to calculate the quark condensate, it is convenient here to consider the fermions to be constituent quarks. The vacuum develops an expectation value of the scalar field because the vacuum energy is lowered by the quarks developing masses. Specifically, it is lowered by [51]

$$-B_{\chi\text{SR}} = E_{\text{vac}} = -12 \left\{ \int_0^\Lambda \frac{d^3k}{(2\pi)^3} \sqrt{k^2 + m_Q^2} - \frac{1}{2} \int_0^\Lambda \frac{d^3k}{(2\pi)^3} \frac{m_Q^2}{\sqrt{k^2 + m_Q^2}} \right\} + \frac{3\Lambda^4}{2\pi^2}. \quad (3.11)$$

Here, m_Q is the constituent quark mass,

$$m_Q \simeq 313 \text{ MeV} . \quad (3.12)$$

The term $3A^4/2\pi^2$ subtracts off the energy of the sea of massless quarks; i.e., E_{vac} is the lowering in energy by the constituent quarks developing masses, or in other words the energy difference between the Wigner and Goldstone vacuum. The quark mass m_Q is determined by solving the self-consistent equation in the Goldstone phase, and is related to the quark condensate. The cutoff A is set to reproduce the value

$$\langle 0|\bar{u}u|0\rangle \simeq -(240 \text{ MeV})^3 , \quad (3.13)$$

which follows from the Gell-Mann–Oakes–Renner relation

$$f_\pi^2 m_\pi^2 = -\hat{m}\langle 0|\bar{u}u + \bar{d}d|0\rangle , \quad (3.14)$$

where $\hat{m} \sim 6 \text{ MeV}$ is the isospin-averaged quark mass. The cutoff is then

$$A \simeq 550 \text{ MeV} . \quad (3.15)$$

Performing the integrals, one finds

$$B_{\chi\text{SR}} \simeq (140 \text{ MeV})^4 \simeq 50 \text{ MeV}/\text{fm}^3 , \quad (3.16)$$

just the typical value employed in the MIT bag model. For the cutoff (3.15) a similar value was obtained in refs. [52] and [53].

Note that, while the quark condensate in this model depends strongly on the cutoff, $B_{\chi\text{SR}}$ depends on it only logarithmically. In fact, it is easy to show that to lowest order in the quark mass

$$B_{\chi\text{SR}} \sim m_Q^4 \quad (3.17)$$

and therefore with our assumption (2.1) we see that at finite temperature/density, $B_{\chi\text{SR}} \rightarrow B_{\chi\text{SR}}^*$, where

$$B_{\chi\text{SR}}^* = B_{\chi\text{SR}} \Phi^4 . \quad (3.18)$$

$B_{\chi\text{SR}}^*$ denotes the value of $B_{\chi\text{SR}}$ at finite temperature or density, and Φ is our common scaling (2.1); e.g., $\Phi = m_N^*/m_N$. Incidentally, this scaling is also obtained from our arguments in section 2. Continuing (2.13) to finite temperature/density and averaging over space yields

$$B_{\chi\text{SR}}^* \sim (\bar{\chi}_*)^4 , \quad (3.19)$$

which obviously scales as (3.18). This scaling of $B_{\chi\text{SR}}^{*1/4}$ was noted in ref. [52]. As is clear from refs. [52] and [53], this quantity is simply the energy of the vacuum per fm^3 . As such, it is analogous to the energy from nucleon loops obtained by extending Walecka mean field calculations. Although $B_{\chi\text{SR}}$ is small compared to the bag constant B , it is still significant. At nuclear matter density of $1/6$ nucleon per fm^3 , it would contribute $\sim 300 \text{ MeV}/\text{nucleon}$ to the energy, as follows from (3.16). It is this value that renormalizes the nucleon energy, and the changes with density of the subtraction are substantial compared with the $16 \text{ MeV}/\text{nucleon}$ binding energy of nuclear matter. As a consequence, caution is required in applying these results. Furthermore, the justification of

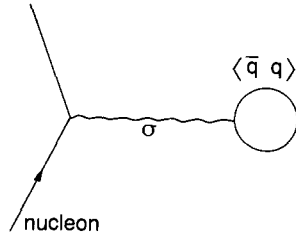


Fig. 3.2. Graphical representation of the mean-field relation giving rise to the nucleon mass in the NJL model.

eq. (3.11) for so large a number is in terms of an effective field theory. Whereas the general picture should be correct, we do not know whether it is also correct quantitatively.

A more satisfactory approach is in terms of effective chiral Lagrangians. Brown–Rho scaling is applied to these at the mean-field level. Loop calculations are then carried out in the heavy-fermion modification of chiral perturbation theory [54, 55]. In this formulation, effects of the negative-energy sea are suppressed by factors of p/m_N .

Of course, the Nambu–Jona-Lasinio model can be used equally successfully to predict hadron masses. In a simplified approach, the nucleon mass can be written as

$$m_N = -G\langle\bar{q}q\rangle, \quad (3.20)$$

where the quark condensate is

$$\langle\bar{q}q\rangle = -g \int_0^A \frac{d^3k}{(2\pi)^3} \frac{m_Q}{\sqrt{k^2 + m_Q^2}}, \quad (3.21)$$

with g the degeneracy and G a dimensionful constant. As previously, A can be determined in order to give the condensate its known value from the Gell-Mann–Oakes–Renner relation.

In the light of the NJL model, it is convenient [21] to consider m_N to result from the mean field relation

$$m_N = -\frac{2}{3} \frac{g_{\sigma NN}}{m_\sigma^2} \langle\bar{q}q\rangle, \quad (3.22)$$

which is shown graphically in fig. 3.2. In fact, this can be thought of as an extended-range version of the model. The $2/3$ arises because there are only up and down quarks for the nucleon to couple to in the negative-energy sea, although there are three quarks in the nucleon. Now in the Nambu–Jona-Lasinio model [23] m_σ^* scales like m_N^* , as shown in (2.1). This results rather trivially, because the nucleon mass is made out of three constituent quarks, and the σ out of a constituent quark and antiquark. In both cases the interactions can be neglected.

Thus, in continuing (3.22) to finite density or temperature we have

$$m_N^* = -\frac{2}{3} \frac{g_{\sigma NN}^2}{(m_\sigma^*)^2} \langle\bar{q}q\rangle^*. \quad (3.23)$$

Let us interpret $\langle\bar{q}q\rangle^*$ as meaning that we not only replace m_Q by m_Q^* , but also A by A^* on the

right hand side of (3.21), choosing Λ^*/Λ to obey the scaling (2.1). Then we can rewrite (3.23) as

$$m_N^* = -\frac{2}{3} \frac{g_{\sigma NN}^2}{m_\sigma^2} \frac{\langle \bar{q}q \rangle^*}{(m_\sigma^*/m_\sigma)^2} \quad (3.24)$$

$$= -G \frac{\langle \bar{q}q \rangle^*}{(m_\sigma^*/m_\sigma)^2}, \quad (3.25)$$

where we have equated (3.20) and (3.22) in order to replace $\frac{2}{3}g_{\sigma NN}^2/m_\sigma^2$ by G .

In practice, $\Lambda \gg m_Q$, so that to a good approximation

$$\langle \bar{q}q \rangle \simeq -C\Lambda^2 m_Q \quad (3.26)$$

with some constant C , and similarly $\langle \bar{q}q \rangle^* \simeq -C\Lambda^{*2} m_Q^*$. Thus

$$\frac{\langle \bar{q}q \rangle^*}{\langle \bar{q}q \rangle} \simeq \frac{\Lambda^{*2} m_Q^*}{\Lambda^2 m_Q}, \quad (3.27)$$

and, assuming the scaling (2.1) we can cancel the $(\Lambda^*/\Lambda)^2$ against the $(m_\sigma^*/m_\sigma)^{-2}$ in (3.25), arriving at

$$m_N^* = -G \langle \bar{q}q \rangle_{\text{NJL}}^*, \quad (3.28)$$

where we defined

$$\langle \bar{q}q \rangle_{\text{NJL}}^* = -g \int_0^\Lambda \frac{d^3k}{(2\pi)^3} \frac{m_Q^*}{\sqrt{k^2 + m_Q^{*2}}}. \quad (3.29)$$

We therefore see that, although in our extension of NJL to finite range as shown in (3.22), all masses m_N , m_σ and m_Q as well as Λ scale when extending the formula to finite density or temperature, it is equivalent to consider Λ to be constant when a zero range interaction is used, as shown in eqs. (3.28) and (3.29).

The quark condensate does not appear, however, only in the Nambu–Jona-Lasinio formula, but, especially in the QCD sum rules, often in other contexts. It should be clear from our preceding discussion that the correct quark condensate at finite temperature or density is the one in which $\Lambda \rightarrow \Lambda^*$ and $m_Q \rightarrow m_Q^*$, following the scaling in (2.1). It is interesting to note that a formula quite similar to (3.23) appears in the QCD sum-rule formalism, applied to the nucleon channel, at zero density/temperature. Dropping higher-order terms we obtain [25]

$$m_N \simeq -2(2\pi)^2 \langle \bar{q}q \rangle / M^2, \quad (3.30)$$

where M is the Borel mass (see ref. [25], or section 6). The usual procedure is to choose $M \sim m_N$, which results in the Ioffe formula

$$m_N = \left[-2(2\pi)^2 \langle \bar{q}q \rangle \right]^{1/3}. \quad (3.31)$$

This formula, however, does not have a consistent N_c dependence, as both m_N and $\langle \bar{q}q \rangle$ are linear in N_c . It was suggested by the present authors [24] that M could be thought of as simulating the mass of the scalar m_σ , which has no N_c dependence. The numerics of (3.31) are unchanged because

[21] $m_\sigma \simeq m_N$. In QCD sum rule calculations m_σ turns out to be [56] (see also the appendix in ref. [21])

$$m_\sigma \simeq 1 \text{ GeV}, \quad (3.32)$$

so the interpretation put forward in ref. [24], besides having some interesting consequences, at least seems to be consistent.

Let us now tie together our discussion of the glue-ball mean field $\bar{\chi}_*$ and the fluctuation field χ' , with the concept of two scales: those of chiral and conformal restoration. From the structure of the effective Lagrangian (2.34), and especially the rewritten coupling term (2.20), one can see that $\bar{\chi}_*$ is coupled to the chiral field U . As discussed earlier, $\bar{\chi}_*$ governs the rate of chiral restoration, although it is made up of the (highly nonlinear) glue field. In fact, it can vanish, restoring the “soft” symmetry breaking (vanishing of $B_{\chi\text{SR}}$), and yet gluon condensates (“hard” symmetry breaking) can remain, since $\langle *|\chi^4|* \rangle$ can be large even if $(\int d^3x \langle *|\chi|* \rangle)^4$ is small. Indeed, we would like to associate $\langle *|\chi^4|* \rangle$ with the trace anomaly (2.12), while $\bar{\chi}_*^4$ should be identified with $B_{\chi\text{SR}}$.

Another aspect of the interplay of scales is evident from QCD sum rule calculations, which we will cover in considerable detail in sections 6 and 7. However, we would like to mention some key results here as far as they apply to the concept of two scales.

To a reasonable ($\sim 15\%$) approximation, the nucleon mass is determined by the quark condensate $\langle \bar{q}q \rangle$ as in eq. (3.30), the Ioffe formula^{*)}. Both continuum corrections and gluon condensates, as well as a $\langle \bar{q}q \rangle^2$ correction in the OPE are neglected here. Using perturbation theory, one finds that the correction to (3.30) from the gluon condensate is [using the value of the gluon condensate given in eq. (3.8)]

$$m_N \simeq -2(2\pi)^2 \frac{\langle \bar{q}q \rangle}{M^2} \left\{ 1 - \pi^2 \frac{\langle 0 | (\alpha_s/\pi) G^2 | 0 \rangle}{M^4} \right\} = 1 - \frac{0.12 \text{ GeV}^4}{M^4}, \quad (3.33)$$

where the Borel mass M is usually taken to lie in the vicinity of m_N . Consequently, the gluon term gives an $\sim 15\%$ correction, and violations of the scaling law (2.1) should appear at the same order of magnitude. Incidentally, this correction is of similar size for the ρ -meson mass. The above arguments, however, do not take into account changes in the Wilson coefficients brought about by chiral restoration at finite temperature. The Wilson coefficient of the gluonic correction tends to zero as the mass drops, such that chiral restoration occurs at nearly the same temperature as the one where hadrons go massless, while opposite parity states become nearly degenerate slightly before. As a result, scaling is observed to a much better degree than the previous estimate, simply because the gluon condensate contribution that inherently violates scaling is suppressed. This mechanism is discussed in detail in the case of the ρ meson in section 6.

This scenario is different from the one advocated by De Tar and Kunihiro [58], who describe the chiral restoration and concomitant parity doubling in terms of an extension of the Gell-Mann–Levy σ -model. The latter extension involves for the opposite parity hadrons a “nonscaling” mass m_0 , which is the mass of the parity doublet after chiral restoration. De Tar and Kunihiro determine m_0 to be ~ 270 MeV. While this is not particularly large, it is not supported by the present QCD sum rule analysis, which suggests that the nonscaling mass vanishes (see section 6). However, this conclusion is based on the approximation of neglecting all higher-order condensates. It is entirely conceivable, though hard to quantify, that the nonscaling mass is set by these neglected condensates. Lattice gauge calculations which we will discuss later on do not seem to be accurate enough to determine m_0 and thus to distinguish between the proposed scenarios.

^{*)} The Ioffe formula [25] is summarized conveniently by Reinders [57].

4. Effective restoration of explicit chiral symmetry breaking

There is an intricate interplay between the role of the density and temperature dependence in pion and kaon effective masses, which signals an effective restoration of explicit chiral symmetry breaking, and the restoration of spontaneously broken chiral symmetry.

4.1. Density dependence of π and K -masses

Kaplan and Nelson [14, 15], in their description of strangeness condensation in the many-body system, noted that kaon effective masses were surprisingly density dependent. We begin, however, with discussing [59, 51] the behavior of the pion effective mass m_π^* , along the lines suggested in refs. [14, 15]. The same argument will apply later for m_K^* , the kaon effective mass, but it is instructive to discuss the pion first. The latter will be shown to be insensitive to changes in density due to a loop correction that cancels the attractive interaction that would otherwise cause the effective pion mass to drop. The situation is different with respect to the kaon, however.

It is well known that there is an attractive interaction in pion–nucleon scattering that is due to vector-meson exchange. We want to focus here, however, on a contribution that is relevant at the so-called Cheng–Dashen point, and which involves the explicit chiral symmetry breaking term only. In the chiral Lagrangian language it can be written as [see eq. (2.2)]

$$\delta\mathcal{L} = -c \operatorname{Tr} \{ M_q (U + U^\dagger) \} . \quad (4.1)$$

In the $SU(2) \times SU(2)$ case we can take M_q to be the diagonal matrix $M_q = \operatorname{diag}(\hat{m}, \hat{m})$, where $\hat{m} = (m_u + m_d)/2$, since we will neglect isospin breaking at the moment.

This correction is of scalar nature, and may be thought of as arising from a scalar *interaction*, an effective scalar-meson exchange between the pion and the nucleon. In the Jenkins–Manohar effective Lagrangian [54, 55] this is written as

$$\delta\mathcal{L} = -\mathcal{C} (\bar{N}N) \hat{m} \operatorname{Tr} \{ \frac{1}{4} (U + U^\dagger) \} , \quad (4.2)$$

which can be extended to finite density straightforwardly. In the vacuum, in the single-nucleon channel we should obtain the well-known pion–nucleon sigma term from the expectation value of (4.2), which sets our constant \mathcal{C} ,

$$\langle \bar{N} | \delta H | N \rangle \equiv \Sigma_{\pi N} = 2\hat{m} \langle N | \bar{q}q | N \rangle = \mathcal{C} \hat{m} . \quad (4.3)$$

Consequently, we write

$$\delta\mathcal{L} = -\Sigma_{\pi N} (\bar{N}N) \operatorname{Tr} \{ \frac{1}{4} (U + U^\dagger) \} = -\Sigma_{\pi N} (\bar{N}N) \cos(\pi/f_\pi) . \quad (4.4)$$

Expanding,

$$\delta\mathcal{L} \simeq -\Sigma_{\pi N} (\bar{N}N) (1 - \pi^2/2f_\pi^2) . \quad (4.5)$$

This gives a density-dependent attractive interaction between nucleon scalar density and pion field of

$$\delta H = -(\Sigma_{\pi N}/2f_\pi^2) (\bar{N}N) \pi^2 . \quad (4.6)$$

The interaction (4.6) gives the pion an effective mass

$$\left(\frac{m_\pi^*}{m_\pi}\right)^2 = 1 - \frac{\Sigma_{\pi N}}{f_\pi^2} \frac{(\overline{N}N)}{m_\pi^2}, \quad (4.7)$$

which goes to zero as $(\overline{N}N) \rightarrow n_{\text{crit}}$ with

$$n_{\text{crit}} = f_\pi^2 m_\pi^2 / \Sigma_{\pi N}. \quad (4.8)$$

Using linear chiral perturbation theory, the critical density was found [59] to be (for heavy nucleons we ignore the difference between scalar and vector densities)

$$\rho_{\text{crit}} = 2.2 \rho_0. \quad (4.9)$$

The $\Sigma_{\pi N}$ has recently been recalculated [60] and shown to be ~ 45 MeV with a 15% error. Replacing f_π in eq. (4.8) by f_π^* brings ρ_{crit} down to [59]

$$\rho_{\text{crit}} \simeq 1.6 \rho_0. \quad (4.10)$$

As mentioned earlier, this scaling in the pion mass is equivalent to an attractive scalar potential acting on the pion. Consider the nucleons as giving rise to an attractive effective scalar field

$$S \sim \overline{N}N / f_\pi^2 \quad (4.11)$$

coupled to the pion with a ‘‘coupling constant’’ $\lambda = -\Sigma_{\pi N}/2$,

$$\delta\mathcal{L} \sim -\lambda S \pi^2. \quad (4.12)$$

This scalar field renormalizes (through its ‘‘vacuum’’ expectation value) m_π^2 in the medium to an effective one $m_\pi^{*2} = m_\pi^2 - \lambda(S)$. No such attractive potential is seen, however, in pionic atoms. This situation has been clarified recently by Delorme et al. [61], who show that the range term in pion–nucleon scattering (in the following denoted by β) cancels the attraction found above. More precisely, they find for the on-shell isospin symmetric pion–nucleon scattering length

$$a^{(+)} = \Sigma_{\pi N} / 4\pi f_\pi^2 - \beta m_\pi^2, \quad (4.13)$$

where the range term β is obtained from Fubini and Furlan [62],

$$\beta = m_\pi^{-1} \left(a^{(+2)} + 2a^{(-2)} \right) + \frac{1}{4\pi^2} \int_{4m_\pi^2}^{\infty} d\omega \frac{B^{(+)}(\omega) - B^{(+)}(m_\pi)}{\omega(\omega^2 - m_\pi^2)^{1/2}} \quad (4.14)$$

and $B^{(+)}$ is determined by the imaginary part of the isospin-symmetric s -wave πN -scattering amplitude $T_0^{(+)}$,

$$B^{(+)} = \frac{\text{Im} T_0^{(+)}}{m_N (\omega^2 - m_\pi^2)^{1/2}}. \quad (4.15)$$

The range term should bring $a^{(+)}$ back to the very small empirical value $a^{(+)} = -0.01 m_\pi^{-1}$ [61]. In chiral perturbation theory, the range term β must come from loop corrections (as is obvious from its form).

For the kaon scattering length, the correction due to the range term is the object of ongoing work. Indeed, the form of the range term, with coefficient β in the case of pion scattering [see eqs. (4.13) and (4.14)] is precisely that arising from higher-order corrections in chiral perturbation theory [63]. In calculating the s -wave scattering lengths the relevant higher-order terms can be written as

$$\mathcal{L}_{\text{int}} = \frac{\Sigma_{KN}}{f_K^2} (\bar{N}N) \left\{ (\bar{K}K) - \frac{D'}{m_K^2} \partial_t \bar{K} \partial_t K \right\} \quad (4.16)$$

with an unknown constant D' that can in principle be determined by including all counterterms, but in practice is obtained by comparing to experimental phase shifts. The second term in (4.16) turns out to be $\sim D'(\omega_K^2/m_K^2)\bar{K}K$ and ensures that at threshold, where $\omega_K = m_K$, the correction to the isoscalar scattering length obtained from \mathcal{L}_{int} is cut down by a factor $(1 - D')$. In the case of the pion it turns out that $D' \sim 1$ to fit the measured quantity, or in other words there is no remnant scalar attractive interaction. The scattering length for the kaon, however, is less well determined experimentally, and it is thus harder to quantify D' in this case. Calculations of D' in heavy fermion chiral perturbation theory [63] give D' somewhat less than unity. Let us try instead to understand the kaon scattering length in a mean-field language.

The most complete analysis of $\bar{K}N$ scattering has been carried out in the boson-exchange model by Müller-Groeling et al. [64]. These authors include vector meson exchanges with essentially the same couplings as in chiral Lagrangians while omitting explicit chiral symmetry breaking. Instead, they include the exchange of a scalar meson between kaon and nucleon, a vertex that is absent in the chiral Lagrangian. As mentioned [see eqs. (4.11) and (4.12)], the explicit chiral symmetry breaking term (4.16) emulates precisely such an interaction, an effective attractive scalar interaction. The effective coupling turns out to be roughly the same as that of the explicit scalar interaction in ref. [64]. We shall return to the mean-field picture in the context of kaon condensation in neutron stars.

Of course, the same term should be used in the K^+N sector [65]. The situation here is more complicated, as a very strong short-range repulsion from the fictitious scalar exchange of mass 1200 MeV is needed. This strong repulsion is of the same nature as that of the very strong repulsion in the nucleon–nucleon interaction which exists on top of the repulsion from ω -meson exchange. It has been suggested that such a repulsion results from the topological nature of the nucleon [66, 67]. In topological models such as the chiral bag model, a meson with a nonstrange quark encounters a nucleon with a filled grand-spin $K = 0$ level. In the composite system, the nonstrange quark has to fill the next higher level, which costs a considerable amount of energy. Indeed, this would happen in either NN or K^+N scattering, but not for K^-N as these mesons do not contain nonstrange quarks and the repulsion would therefore be absent. This is in accordance with ref. [64]. K^- condensation, which can happen as a consequence of the attractive interaction, turns out to be rather insensitive to the precise value of D' , as we discuss in the next section.

4.2. Kaon condensation and neutron stars

As the kaon energy is lowered by the attractive interaction, at high enough density it may become favorable for the kaon to condense [68]. Equations (4.6)–(4.8) are immediately adaptable to kaon condensation by changing the pion to a kaon field, f_π to f_K and $\Sigma_{\pi N}$ to Σ_{KN} , where

$$\Sigma_{KN} = \frac{1}{2}(m_u + m_s) \langle N | \bar{u}u + \bar{s}s | N \rangle. \quad (4.17)$$

Note that Σ_{KN} is large, due to m_s , even if $\langle N|\bar{s}s|N\rangle = 0$. Strangeness condensation does not require a large strangeness content of the nucleon. With $\langle N|\bar{s}s|N\rangle$ assumed zero,

$$\Sigma_{KN} \gtrsim (m_s/4\hat{m})\Sigma_{\pi N}, \quad (4.18)$$

giving a lower limit $\Sigma_{KN} \gtrsim 2m_\pi$. Thus, naively,

$$n_{\text{crit}} = \frac{f_K^2 m_K^2}{\Sigma_{KN}} \lesssim \frac{f_K^2 m_K^2}{(m_s/4\hat{m})\Sigma_{\pi N}}. \quad (4.19)$$

Calculations to date in dense matter [69, 70] obtain a critical density $\rho \sim 3\rho_0$ for K^- condensation in dense matter. These do not include loop corrections, which tend to increase the critical density ρ_c , nor do they include the Brown–Rho scaling of eq. (2.1), which also tends to lower ρ_c . Inclusion of all these effects [63] does not seem to considerably affect the earlier estimates of ref. [70].

In the neutron star environment, a lower critical density is achieved by the presence of a chemical potential. For a negative charge, the m_K^2 in the numerator of (4.19) is replaced by $m_K^2 - \mu_c^2$, which can substantially lower the critical density. K^- condensation is also helped by the attractive K^- –neutron interaction from vector meson exchange (see below). Note that the mass terms involved in calculating the critical density for a negative kaon condensate to form are slightly different from those for the neutral one; indeed, the Σ_{KN} must be replaced by a quantity that is $\sim 15\%$ less than the one used above. Explicit formulae are given in ref. [69], where it is shown that this K^- condensate is extremely robust.

Let us explore the equivalent (to the chiral Lagrangian description) but more physical description of kaon condensation in the mean-field language, beginning with the concept of kaon effective mass,

$$\frac{m_K^{*2}}{m_K^2} = 1 - \frac{\Sigma_{KN} \bar{N}N}{f_K^2 m_K^2}, \quad (4.20)$$

obtained in a way completely analogous to the pion effective mass, eq. (4.7). In the presence of vector-meson exchange interactions, the inverse kaon propagator in neutron matter is (we set the proton fraction to zero)

$$D_K^{-1}(\omega) = k^2 + m_K^{*2} + 2\omega V(\rho) - \omega^2, \quad (4.21)$$

where $V(\rho)$ is the self-energy which arises from the vector-meson exchange interactions in matter. [We neglect the higher-order term $\mathcal{O}(V^2)$.] We may write it quite generally as

$$V(\rho) = -g_{\omega KN}^2 \frac{\rho}{m_\omega^2} + g_{\rho KN}^2 \frac{\rho}{m_\rho^2}. \quad (4.22)$$

Using the approximate SU(3) relations $g_{\omega KN}^2 = \frac{1}{3}g_{\omega NN}^2$, $g_{\rho KN}^2 = \frac{1}{3}g_{\omega KN}^2$ and $g_{\omega NN}^2 = 9g_{\rho NN}^2$ to relate these couplings to the universal ρ coupling $g_\rho^2/4\pi \approx 2.74$ [note that in the nuclear physics convention $g_{\rho NN}^2 = \frac{1}{4}g_\rho^2$], we can use the KSFR relation

$$m_\rho^2 = 2g_\rho^2 f_\pi^2 \quad (4.23)$$

to relate the mean-field interaction (4.22) to

$$V(\rho) = -\rho/4f_\pi^2, \quad (4.24)$$

as is obtained from the Jenkins–Manohar chiral Lagrangian to lowest order. Note that this effective potential only describes the interaction due to ρ and ω mesons, *not* the attraction in the scalar channel. This is buried in the kaon effective mass.

The general condition for a condensate is that [71]

$$D_K^{-1}(\omega) = 0|_{\omega=\mu} ; \quad (4.25)$$

i.e., that the propagator develops a pole under the constraint that the kaon energy equals the chemical potential. From (4.21) and (4.25) we can see why the negative condensate can be achieved at lower densities. Suppose that the μ_- is established by the electron chemical potential in neutron stars. Then (4.21) and (4.25) say that for kaon condensation, the *in medium* kaon energy

$$\omega_K(\rho) = \sqrt{k^2 + m_K^{*2}} + V(\rho) \quad (4.26)$$

has to come down to the electron energy μ_- , not to zero as in the case of a neutral condensate, before condensation can take place. When $\omega_K(\rho) = \mu_- = \mu_{e^-}$, electrons can change into kaons (and vice versa). From equilibrium, one has

$$\mu_n - \mu_p = \mu_{e^-} = \mu_{K^-} \quad (4.27)$$

because the weak interactions

$$\begin{aligned} n &\rightarrow p + e^- + \bar{\nu}, & p + e^- &\rightarrow n + \nu, \\ e^- &\rightarrow K^- + \nu, & K^- &\rightarrow e^- + \bar{\nu}, \end{aligned} \quad (4.28)$$

all have time to equilibrate the system even though the interactions are weak. The low-energy neutrinos of thermal energies in these reactions simply escape from the star. The critical density for kaon condensation as derived from (4.25) turns out to be $\rho_c = (3-4)\rho_0$ for $\Sigma_{KN} = (2-3)m_\pi$ [63].

Let us now briefly discuss why the kaon condensation scenario appears to be so robust. While the size of the factor D' multiplying the counter term in (4.16) significantly affects the $\bar{K}N$ scattering lengths (a D' of unity resulting in vanishing scattering lengths as in the pion case), it does not seem to significantly affect the threshold for kaon condensation [63]. This is to a large extent due to the time derivatives in the counter term, which result in a factor ω_K^2/m_K^2 (as noted above). As the density increases, the kaon energy drops rapidly and the counter term becomes less and less important. Kaon condensation thus appears through a bootstrap mechanism: Kaons can condense because the kaon energy is lowered, and this lowering of the kaon energy at finite density makes kaon condensation possible in the first place (by suppressing higher-order corrections that could spoil the strong attraction). There is thus no contradiction between little attraction found in $\bar{K}N$ scattering lengths and considerable attraction in the same channel at higher densities.

In earlier work with conventional equations of state, Bethe et al. [72] found that only with a stiff nuclear equation of state could a smooth transition from conventional nuclear matter to strange quark matter be made. With K^- condensation, the situation changes. Hadronic matter becomes strange through strangeness condensation. The equation of state is sufficiently soft that the transition to strange *quark matter* is not made, at least not until very high densities of the order $\rho \sim 10\rho_0$ [73]. Indeed, the equation of state is so soft that the maximum mass for neutron stars drops to

$$m_{\max} \sim 1.5 M_\odot . \quad (4.29)$$

This implies the possibility that Supernova 1987a went into a black hole *after* the explosion [74]. Evidently, K^- condensation in dense matter has startling and important consequences.

4.3. Relativistic heavy ion collisions

We would like to point out in this section that restoration of explicit chiral symmetry breaking can also occur at finite temperature, and indeed in the pion channel.

With increase in temperature, as in relativistic heavy ion reactions, an effective scalar interaction (4.12) arises from the original explicit chiral symmetry breaking at the Higgs scale, magnified by the vacuum condensate that is produced by scalar interactions. As noted, the effective *nuclear physics* scale is that of the scalar σ , of mass ~ 600 MeV. The effective scalar interaction (4.12) should, therefore, survive temperatures of $T \sim 150\text{--}200$ MeV. In other words, it is relatively robust. This would not be expected to be so for the higher-order many-body effects, the evaluation of which involves integration over intermediate states. As the initial states become distributed more and more widely with increasing temperature, the principal value integral over intermediate energy for the higher-order effect receives both positive and negative contributions and the net effect becomes small. We can talk about the many-body effects being “boiled off”. Thus, for high temperatures there is nothing to cancel the attractive interaction (4.12) and the pion mass is substantially decreased for $(\bar{N}N) > \rho_0$. In ref. [59] evidence from the CERN relativistic heavy ion collisions is adduced to suggest that, when the pions are emitted at high temperature and densities $\rho \sim 1.5\rho_0$, they behave as if they were massless. The basic experimental evidence is the excess of soft pions at low p_T , as shown in a NA35 [75] result for ^{16}O on ^{197}Au in fig. 4.1. As p_T goes to zero, free pions would have a Boltzmann factor $\sim e^{-m_\pi/T} \sim e^{-1}$, where the approximate equality results because $T \sim m_\pi$. If, however, the thermal distribution of the pions is determined when they are essentially massless, this factor would be missing, so there would be an apparent excess of pions of $\sim e$ as

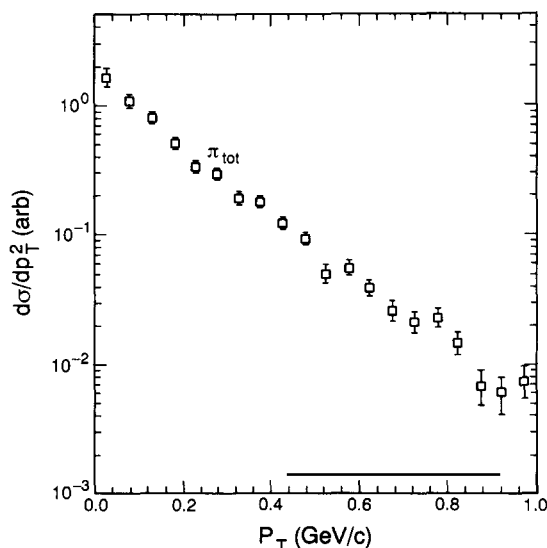


Fig. 4.1. Pion differential cross section in the NA35 experiment plotted versus p_T . Note that the experimental points continue to rise with decreasing p_T right down to $p_T = 0$. If they were to retain their rest mass, they would have a Boltzmann factor $\exp(-m_\pi/T)$ as $p_T \rightarrow 0$ and the curve would bend over.

$p_T \rightarrow 0$. Because some pions come from resonance decay, the excess is even greater; this and how to handle off-shell effects is discussed in ref. [59].

In ref. [76], Schukraft plotted the number of low p_T excess pions as a function of rapidity, finding that at target rapidity in the $^{16}\text{O} + ^{197}\text{Au}$ collisions, there were about four times more low p_T pions than at central rapidity. This strongly suggests that the higher density provided by the target nucleus favors soft pions. It is estimated [59] that the pions are emitted from the hot fire cylinder into the target rapidity region at a density $\rho \sim 1.5\rho_0$, whereas it would be closer to $0.5\rho_0$ in the central rapidity region. That the high density as well as the high temperature is needed is supported by the fact that in the central 200 GeV/nucleon S on S experiments at CERN, where the decay of the fire cylinder occurs without the “casing” afforded by the Au in the case of the $^{16}\text{O} + ^{197}\text{Au}$ collisions, there is essentially no excess of low p_T pions.

Let us now consider the case of strangeness. In relativistic heavy-ion collisions there is insufficient time to develop strangeness through the weak interactions, but K^+K^- pairs can be produced [14,15]. The scenario for this has been worked out in some detail for the Brookhaven AGS collaboration of 14.6 GeV/nucleon ^{28}Si on ^{197}Au [77]. Also, η -condensation is nearly as favorable as kaon condensation [68] for chemical potential zero, so if the latter is hindered, η -condensation may occur. Our scenario bodes ill for the use [78] of enhanced strangeness in relativistic heavy-ion collisions as a signal for the formation of a quark–gluon plasma. The argument was that strangeness production is much easier in the quark–gluon plasma, where one has only to pay for the strange quark masses, than in the broken symmetry sector, where strange hadrons are much more massive than nonstrange ones. This argument fails, however, if kaons lose most of their mass at densities already achieved in the Brookhaven AGS collisions of 12 GeV/nucleon Au on Au collisions. The scenario of a smooth transition between hadronic and partonic phase suggests that at the transition a strange baryon may either be described by its quark content or as a hadron, with no change in mass. To estimate the strangeness in baryons formed at higher densities, we should, however, take into account the production rate of $\bar{K}K$ or K^+K^- pairs at finite density. This depends sensitively on the kaon energy (4.26). The vector potential $V(\rho)$ in eq. (4.26) is repulsive for K^+ and attractive for K^- , and thus their effect cancels. As a consequence, the driving term for enhanced kaon pair production is the interaction (4.16) together with the enhanced phase space due to the lower mass. Then, however, the precise value of the strength of the counterterm D' is important as the interaction is reduced by its presence. Calculations to date [63] give (after isospin averaging) $D' \sim 0.4$. Thus, the enhancement for kaon pair production due to the dropping kaon mass is somewhat reduced by the presence of the counterterm.

The K^+/π^+ ratio in the Brookhaven E802 experiment [79] is enhanced to 0.2 from the 0.05 found in pp collisions. Although the freeze-out temperature in this experiment was determined to be $T_{f0} \simeq 150$ MeV [80], initial temperatures are probably not much higher, so that it seems unlikely that a quark–gluon plasma is formed at Brookhaven energies. Given, however, that kaons can become massless at the high densities $\rho \geq 3\rho_0$ formed in the collision, it is relatively easy [77] to produce $\bar{K}K$ pairs, the \bar{K} 's then mostly combining with nucleons to form strange baryons. In 200 GeV/nucleon S on S collisions at CERN [81], the K_S^0/π^- ratio is found to be about 0.11. This can be related by isospin symmetry to a K^+/π^+ ratio of 0.22. Thus, the strangeness production in the heavy-ion collision hardly increases from Brookhaven to CERN energies, even though it does somewhat in pp collisions. This is indicative of the system formed at higher energies going through a similar freeze-out stage to that at lower temperatures. We will come back later to a discussion of effects of temperature dependence which further aid kaon condensation (although most of the empirical information comes from the pions). Here we note that the density dependent effects seem to be substantially larger than the temperature dependent ones.

Kaons formed in a massless state, or in the kaon condensed state, will of course go back on-shell on the way to the detector, as the effective scalar field (4.12) which suppresses their mass decreases as the system expands. In fact, using this effect, Lissauer and Shuryak [82] obtain an important temperature dependent decrease in the kaon mass, which is due to the pion density $n_\pi = 0.37 T^3$.

It is amusing that in present relativistic heavy-ion experiments, the effective restoration of explicit chiral symmetry breaking may be as important as the movement towards restoration of the spontaneously broken chiral symmetry.

5. Evidence for scaling in nuclei

The nuclear many-body problem has been handled quite successfully in the conventional picture in which hadron masses are taken to be constant, independent of density. Because of the many past successes of the conventional scenario, we shall first give arguments why our scenario of scaling masses preserves these, and then later see what our scaling masses do for discrepancies between theory and experiment. Of course, historically, the development came the other way around: first the discrepancies were noted.

The reason why in most quantities the changes induced by scaling masses is not large is easily understood. When all masses scale equally, there is no net effect in dimensionless quantities. In the nuclear or neutron matter problem, the masses can be scaled out [18, 19] of the Hamiltonian:

$$H(m_i^*, r) = \lambda H(m_i, x), \quad (5.1)$$

where $H(m_i^*, r)$ denotes the Hamiltonian with effective masses,

$$\lambda = m_i^*/m_i, \quad x = \lambda r. \quad (5.2)$$

Thus, one can transform back to the Hamiltonian with the bare masses and a new scale x . In terms of r , $r = \lambda^{-1} x$ and since $\lambda < 1$, one can talk of a “swelling” in this transformation. The change introduced in (5.1) by the factor λ is small.

In a rather complete calculation [83], Brown, Mütter and Prakash showed that the nuclear matter problem could be reasonably well described in such a scenario with scaling meson masses. This scaling eliminated the mechanism for saturation found in relativistic mean-field theories (and, more generally, in the relativistic many-body problem). Saturation had to be enforced by a two-loop term, which, however, worked equivalently to the virtual pair term [84] which is responsible for saturation in relativistic theories, and for which there is substantial empirical support in the fits to spin observables in Dirac phenomenology. However, use of such a two-loop term from such an effective theory is unsatisfactory, and nuclear saturation must be properly embedded in QCD. We return to this problem in the context of finite-density QCD sum rules in section 7.

5.1. K^+ -nucleus scattering

Strong empirical support for scaling meson masses is found in the ratio of K^+ scattering off carbon to that off deuterium [1, 85]. The ratio

$$\sigma(K^+C)/6\sigma(K^+D) > 1 \quad (5.3)$$

has been studied experimentally [86, 87] and theoretically (see ref. [88] for a recent analysis, and references therein), yielding a significant discrepancy.

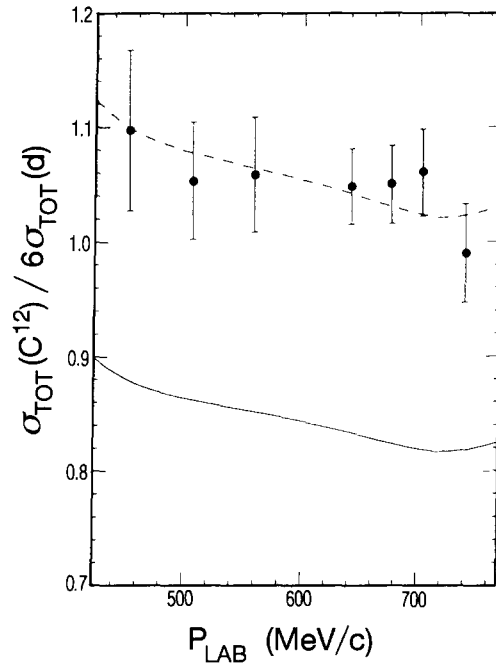


Fig. 5.1. Total cross section for $K^+ {}^{12}\text{C}$ scattering as a function of the K^+ laboratory momentum. The data are from ref. [88]. The solid line is the theoretical prediction using density independent vector meson masses.

The K^+ interaction with nucleons is weak due to the absence of $S = 1$ resonances, so that many-body corrections are well under control. Therefore, because of the large mean free path of the K^+ in the nucleus, the K^+ -nucleus interaction can fairly accurately be viewed as being K^+N scattering, with small corrections. An optical potential model using measured free K^+N scattering phase shifts surprisingly fails to reproduce the data. An earlier successful remedy assumed a nucleon swelling effect to reconcile with the data [85]. It was later shown [1] how the effective nucleon radius swells if the masses of the vector mesons that make up the nucleon cloud are allowed to scale with density. Indeed, assuming vector dominance, the K^+ interaction is mediated mainly through ρ and ω mesons, giving the nucleon a vector radius of the order

$$\langle r^2 \rangle \sim 1/m_V^2. \quad (5.4)$$

Again due to its large mean free path, the K^+ can dive deep into the nucleus, where the density is largest, as opposed to the K^- , which is largely absorbed at the surface. As a consequence the K^+ samples on the average “swollen” nucleons whereas the K^- does not, the rate of swelling being dictated by the scaling of the vector meson masses. Indeed, the cross section ratio (5.3) is nearly one for K^- nucleus scattering. We want to reiterate that although the K^\pm nucleon scattering phase shifts are not well known, conventional calculations using optical model potentials are well outside the error bars [89], and taking the ratio of cross sections as in (5.3) eliminates some of the uncertainties to first order. Recent experimental results on the ratio (5.3) with K^+ beams with lower momenta (and thus even larger mean free path) on the nuclei ${}^6\text{Li}$, ${}^{12}\text{C}$, ${}^{28}\text{Si}$ and ${}^{48}\text{Ca}$ strongly emphasize the need for “nonconventional” nuclear matter effects to explain the discrepancy [90]. This conclusion was also drawn by Chen and Ernst in their thorough analysis of the available experimental data. Their prediction (solid line) from standard scattering theory and density-independent vector meson

masses is shown in fig. 5.1. As can be seen, an $\sim 20\%$ enhancement is required to fit the experimental points. Very roughly, following eq. (5.4), this implies an $\sim 10\%$ decrease in $m_V(\rho)$. This seems reasonable, since the average density in ^{12}C is low, $\rho \sim 0.5\rho_0$, where ρ_0 is nuclear matter density.

In our opinion, the strongest point made in ref. [1] is that the density of nucleons in ^{12}C needed to fit the K^+ scattering can be made consistent with that obtained from electron scattering off ^{12}C if, and only if, meson masses are scaled. This point was made by one of the referees [91] of the paper, ref. [1], and the argument goes as follows.

In a local density approximation, the validity of which we discuss later, the free K^+N t -matrix is modified by the factor (in the linear approximation)

$$F = [1 - \lambda\rho(r)/\rho_0]^{-1}, \quad (5.5)$$

which for small scattering angles (the total cross section is given by the imaginary part of the zero-angle scattering amplitude) takes into account the density dependence of the meson masses in the meson propagator. Here

$$\lambda = 2 [1 - m_N^*(\rho_0)/m_N]. \quad (5.6)$$

Using an idea of Gibbs et al. [92], F can be transformed away to the extent that the nucleon density can be represented by a two-parameter Fermi (2pF) function. The result is that the optical model strength is increased by the factor $(1 - \lambda)^{-1}$ (just the factor $[m_N/m_N^*(\rho(R=0))]^2$ from the inverse meson propagator) and the half-density radius R is replaced by the effective radius

$$R' = R - \lambda a, \quad (5.7)$$

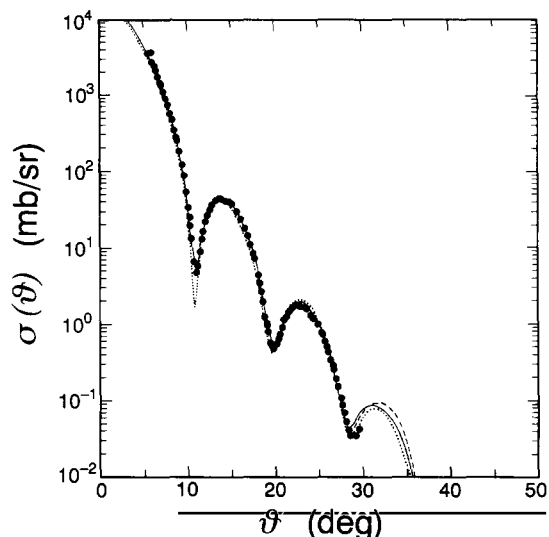


Fig. 5.2. Results of the Tjon-Wallace [95] calculations for the differential cross section for 500 MeV protons scattered off ^{40}Ca . The dotted line refers to IA2 (impulse approximation 2). For the solid line the masses of all mesons except for the pion are scaled as $m_N^*/m_N = 1 - 0.15(\rho/\rho_0)$, the same parameterization as used for K^+ ^{12}C scattering [1]. For the dashed line the ρ -meson mass, as well as the pion mass, are kept constant.

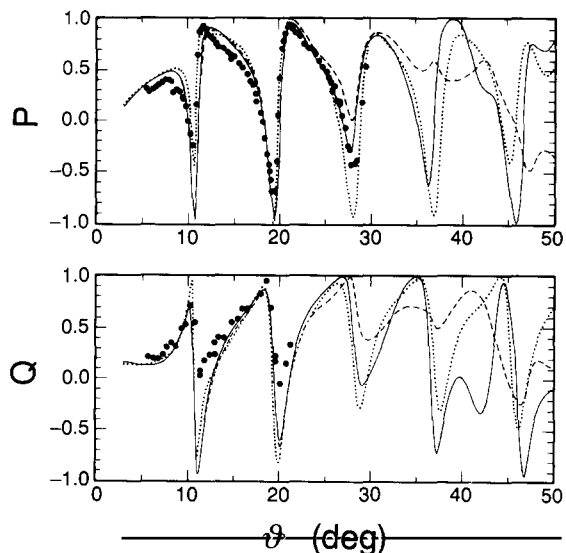


Fig. 5.3. Spin observables (from Tjon and Wallace [95]). See caption of fig. 5.2 for definition of the lines.

where a is the surface thickness of the Fermi function. Basically, the product of two Fermi functions, one representing the optical model potential and the other representing $\rho(r)$ in (5.5), when expanded as $[1 - \lambda\rho(r)/\rho_0]^{-1} \simeq 1 + \lambda\rho(r)/\rho_0$ has a thinner surface thickness than a single Fermi function; hence the foreshortening (5.7) in R results from the effectively contracted surface thickness. It is surprising that the small change $\delta R = -\lambda a$ is substantially more decisive in bringing agreement between theory and experiment in the $K^+ - {}^{12}\text{C}$ scattering than the much larger change $(1 - \lambda)^{-1}$ in the optical model strength. However, the frequency in angle θ of the diffraction pattern can be determined very accurately, whereas there seems to be considerable ambiguity in the overall magnitude of optical model potentials.

Hintz noticed that the same change in radius could remove a longstanding nuclear radius discrepancy [93] in several hundred MeV proton scattering off nuclei. This has been worked out by Brown, Sethi and Hintz [94], and the resulting cross section for proton scattering on ${}^{40}\text{Ca}$ is shown in fig. 5.2. There were worries that scaling masses would upset the spectacularly good fits to spin observables, but preliminary results by Tjon and Wallace [95] show that these fits do not deteriorate with the introduction of density dependent masses. An example is shown in fig. 5.3.

5.2. Missing longitudinal strength

One of the most interesting applications [2] of scaling meson masses was to the problem of the missing longitudinal strength in the quasi-elastic scattering of electrons from nuclei. Whereas the missing strength had been used to motivate an *in medium* swelling of the nucleon, so that its electromagnetic form factor would be cut down, γ -scaling [96] shows no increase in the size of the nucleon with density. The strength in the longitudinal form factors is missing at momentum transfers $\sim 300\text{--}500\text{ MeV}/c$, whereas γ -scaling can first be compared with theory only for higher momentum transfers, $q \gtrsim 1\text{ GeV}$. Thus, quasi-elastic electron scattering probes larger distances than γ -scaling. In the chiral bag model with chiral angle $\theta(R) = \pi/2$, which gives a 50/50 division of charge between quarks in the bag and meson cloud, the latter is chiefly responsible for the long range part of the charge. Contributions to the proton form factor from ref. [97] are shown in fig. 5.4.

Brown and Rho [2] point out that whereas vector dominance works well for a γ -ray with kinematics near the vector-meson pole, space-like γ -rays are relatively far off-shell, and the γ -ray couples only $\sim 50\%$ of the time through the vector meson. In all, the γ -ray arriving at the nucleon is about half vector meson and half γ -ray. Thus, the isoscalar form factor is taken to be

$$F^{I=0}(t) = \frac{A^2 - m_\omega^2}{A^2 - t} \frac{m_\omega^2}{m_\omega^2 - t} + \frac{1}{2} F_{\text{bag}}(t). \quad (5.8)$$

This can be modified to take into account the momentum dependence of the splitting, as for instance for $q \sim 0$ the nucleon appears entirely as a soliton, and for $q \geq 1\text{ GeV}$ the quark part dominates. In the above, A is a cutoff taken to be $A = 2m_\omega$ and $F_{\text{bag}}(t)$ is the form factor from the quarks in the chiral bag for chiral angle $\theta(R) = \pi/2$. As can be seen from fig. 5.4, the fit to the empirical form factor is reasonably good. We define [98] the transverse or longitudinal response to be

$$(T, L)^* = \int d^3r \rho(r) F_{L,T}^* O_{L,T}^*(\rho), \quad (5.9)$$

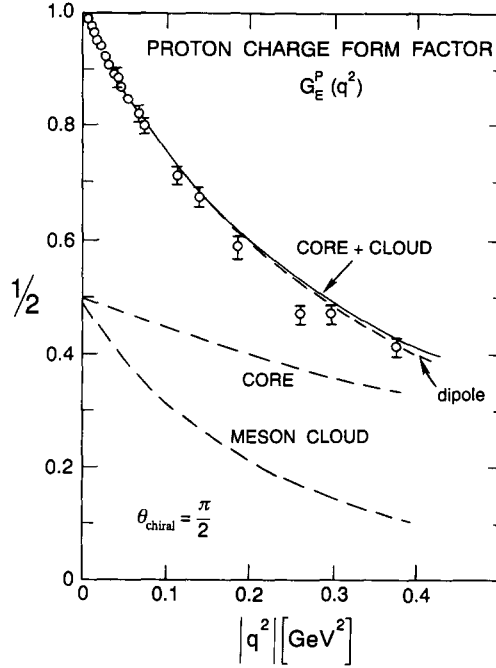


Fig. 5.4. Contributions from the quark core and the meson cloud to the proton charge form factor in a chiral bag model (from ref. [97]).

where $F_{L,T}^*$ are the longitudinal/transverse form factors in medium, and $O_{L,T}^*$ the pertinent operators,

$$O_L = \frac{1}{2} + \frac{1}{2}\tau^3, \quad O_T = \mu_V \frac{\boldsymbol{\epsilon} \cdot [\boldsymbol{\sigma} \times \mathbf{q}]}{2m_N} \tau_3, \quad (5.10)$$

where μ_V is the isovector magnetic moment given by

$$\mu_V = \frac{1}{2}(\mu_p - \mu_n) = 2.353 \quad (5.11)$$

and $\boldsymbol{\epsilon}$ is the photon polarization vector. In medium, the form factors are modified, as $m_\omega \rightarrow m_\omega^*$ and similarly for the cutoff Λ , so that the first term on the right hand side of (5.8) becomes

$$\frac{\Lambda^2 - m_\omega^2}{\Lambda^2 - t} \frac{m_\omega^2}{m_\omega^2 - t} \rightarrow \frac{1}{2} \frac{1}{1 - t/2m_\omega^{*2}} \frac{1}{1 - t/m_\omega^{*2}}. \quad (5.12)$$

In the experiments t is space-like: to a good approximation $t = -q^2$. Thus, the change from m_ω to m_ω^* produces a reduction in strength. Detailed fits to the Saclay data, where separated longitudinal and transverse responses are available, have been carried out by Soyeur et al. [98], and reproduce reasonably well the missing longitudinal strength, while the effect is small for the transverse response. This is due to the additional factor of $m_N^{-1} \rightarrow (m_N^*)^{-1}$ in the transverse operator (5.10), which largely cancels the decrease coming from the form factor. Thus, in the intermediate range of $|q|$ considered, where the decomposition (5.8) seems adequate, the agreement of the prediction and the data is encouraging [98].

In the previous arguments we have assumed a simple scaling relation for the bag form factor,

$$F_{\text{bag}}(q^2) = 1/(1 - q^2/\lambda^2), \quad (5.13)$$

where λ^2 is related to the bag radius R by

$$6/\lambda^2 = \frac{3}{5}R^2. \quad (5.14)$$

This is not true in a purely solitonic description, and an investigation of the density dependence of the Skyrmion radius leads to some interesting details, which we cover in the next section.

5.3. Axial charge renormalization at finite density

In the case of the Skyrmion, the radius goes as

$$R_{\text{Sk}} = \text{const.} \times \sqrt{g_A}/f_\pi. \quad (5.15)$$

Now, it is known [99] that $g_A^* \simeq 1$ in light nuclei, where γ -scaling has been most accurately investigated. The average density is $\sim \frac{1}{2}\rho_0$, so using [100]

$$m_N^*/m_N = 1/(1 + 0.25\rho/\rho_0) \quad (5.16)$$

we can take $m_N^*/m_N = f_\pi^*/f_\pi \simeq 0.9$. Consequently, the ratio $\sqrt{g_A}/f_\pi$ remains essentially constant in going to light nuclei. This is, without exaggeration, quite surprising, as the density in these light nuclei surely is only a fraction of nuclear matter density. Yet, it seems as if g_A is quenched already there. However, we should be careful here. In the vacuum, g_A is defined as the value of the axial form factor at vanishing momentum transfer. For the β -decay of the neutron

$$\int d^4x e^{iqx} \langle p | A_\mu(x) | n \rangle \simeq \bar{u}_p \gamma_\mu \gamma_5 g_A(0) u_n. \quad (5.17)$$

At finite temperature and/or density, however, Lorentz invariance is lost, and the zero component of the axial current can be renormalized differently from the space component. This would be reflected in different axial form factors for the zero and the space components of the axial current, and consequently different g_A 's. A systematic approach to the density dependence of g_A^0 has been developed by Rho and collaborators, as we shall outline below.

Kubodera and Rho [101] made the first attempt in this direction considering experiments by Warburton [102]. In these experiments, the first forbidden β -decays in $A=205$ – 212 nuclei were analyzed, with intriguing results. The conclusion was that the axial charge matrix element in heavy nuclei is enhanced over the impulse approximation by about 100%, with the extracted enhancement factor being

$$\epsilon_{\text{MEC}} = 2.01 \pm 0.05, \quad (5.18)$$

where MEC denotes ‘‘meson exchange currents’’. This enhancement is considerably stronger than anticipated from calculations in light nuclei [103] and calculated more recently [104]. Note that this phenomenon is related to the axial *charge*, i.e. the zero component of the axial current.

Using the universal scaling (2.1) with $\Phi(\rho) = 0.8$, Kubodera and Rho [101] obtain an estimate for ϵ_{MEC} in agreement with the new experiments. It should be stressed here that this effect is due to a change in the vacuum, rather than loop effects. In fact, in ref. [101] the stance is taken that effective Lagrangians should be adequate at tree level, otherwise they simply would not be effective. Loop effects can be taken into account systematically as higher-order terms in a chiral perturbation theory, but should turn out to be small. An attempt at calculating loop effects has

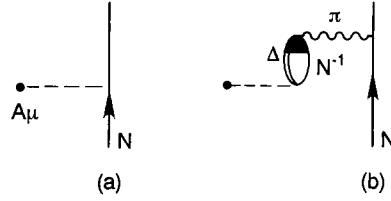


Fig. 5.5. (a) The axial-vector coupling to the nucleon (b) is renormalized in the medium by Δ -particle–nucleon-hole excitations. The blacked-in area at the top of the bubble represents vertex, or local-field, corrections.

been made by Park, Min, and Rho [105]. A number of technical developments, especially the use of heavy-fermion perturbation theory to handle baryons, are outlined there. The net result is that, to one-loop order, the corrections indeed appear to be small. This need not always be the case; in particular, the density dependent loop corrections for the axial form factor as obtained from the space part of the axial current appear to be large. Let us denote this by the usual symbol g_A , and describe a simple model which accounts for the observed quenching of this quantity.

The fact that g_A goes to unity so rapidly is often termed “precocious chiral restoration in g_A ”. While as we have seen this statement has to be taken with a grain of salt, let us proceed here with this notion. The chiral restoration in g_A has been understood [106, 107], at least semiquantitatively, for many years in terms of medium effects consisting of isobar-particle, nucleon-hole insertions (see fig. 5.5).

The calculations of refs. [106, 107] gave a density dependence to g_A^* and f_π^* ,

$$\frac{g_A^*}{g_A} = \left[1 + \frac{8}{9} \left(\frac{f_{\pi N\Delta}}{m_\pi} \right)^2 \frac{\rho g'_{N\Delta}}{\omega_R} \right]^{-1}, \quad (5.19)$$

$$\frac{f_\pi^*}{f_\pi} = 1 - \frac{\frac{8}{9} (f_{\pi N\Delta}/m_\pi)^2 \rho / \omega_R}{1 + \frac{8}{9} (f_{\pi N\Delta}/m_\pi)^2 \rho g'_{N\Delta} / \omega_R}, \quad (5.20)$$

where $f_{\pi N\Delta}^* \simeq 2$ is the $\pi N\Delta$ coupling constant and $\omega_R = m_\Delta - m_N \simeq 300$ MeV. The $g'_{N\Delta}$ is the Ericson–Ericson Lorentz–Lorenz (EELL) vertex correction.

Whereas this accomplishes the decrease in $g_A = 1.25$ to $g_A \sim 1$ as seemed to be needed for s, d -shell nuclei [99], Cohen and Kisslinger [108] have recently called this argument into question. However, the density dependence (5.19) is supported by QCD sum rule calculations [109]. g_A^* should decrease to unity with increasing density as chiral symmetry is restored.

In the Skyrmin description of the nucleon, the $\Delta(33)$ resonance is an excited rotational state, built on the nucleon ground state. Its energy should go inversely with the moment of inertia, which is proportional to the squared radius (5.15). Since g_A goes from 1.25 at $\rho = 0$ to ~ 1 at $\rho = \rho_0$, and f_π^*/f_π scales as m_N^*/m_N , using (5.16) we find

$$E_\Delta^*/E_\Delta \simeq (R_{Sk}^*)^2 / (R_{Sk})^2 \simeq 0.8 \quad \text{for } \rho = \rho_0, \quad (5.21)$$

i.e., a 20% decrease, or a decrease of 60 MeV, in going from zero density to nuclear matter density ρ_0 . This is not seen [110, 111]. However, Brown et al. [112] point out that the EELL correction will move up the $\Delta(33)$ excitations in nuclear matter by

$$\delta E = (g'_0)_{n\Delta} (\rho/\rho_0) m_\pi. \quad (5.22)$$

Hence, for nuclear matter density $\rho = \rho_0$, this many-body effect almost cancels that of the dropping Skyrminion mass (5.21). Beyond ρ_0 we expect E_Δ^* to decrease with increasing density. This will, of course, affect the dispersion curves for densities $\rho > \rho_0$.

Through the above examples we see that, although the scaling (2.1) may govern the general situation, in specific instances different scales, such as that given by the density dependence of g_A^* , can retard the change with density that would follow from the scaling (2.1). This complicates the description of the effects in finite nuclei, not only by the application of rules deduced for infinite systems to finite ones, but also because of the detailed special scales which develop for limited ranges of densities.

There may well be more surprises in heavy nuclei. In ^{232}Th and ^{238}U , the effective parity non-conserving interaction as it enters into low-energy neutron scattering has recently been found to be two orders of magnitude larger than the estimate based on standard meson-exchange models [113]. Scaling meson masses are found to increase the latter estimates by a factor 3–5, thus decreasing the discrepancy. It would be interesting to include loop corrections to this calculation.

6. Hadronic properties and scaling from QCD sum rules at finite temperature

In this section we investigate the changes in hadron properties such as mass and width of a resonance, as well as continuum thresholds, induced by finite temperature, using the powerful method of QCD sum rules [41]. The changes can be traced back to two effects: On the one hand the source is exposed to a heat bath of pions (in the broken-symmetry regime) or of quarks and gluons (in the perturbative regime), which are continually absorbed and emitted. On the other hand finite temperature changes the nonperturbative QCD vacuum, which is characterized by a coupling strength $g(T, A)$, A being the renormalization scale. As the temperature increases, the coupling gets weaker and matrix elements of gauge invariant operators such as $\bar{q}q$ and G^2 change owing to the change taking place in the ground state. In other words: the condensates start to melt. As there is as yet no method to construct the true nonperturbative QCD vacuum, and while the function $g(T, A)$ can only be calculated in the perturbative regime, we have to content ourselves with using phenomenological estimates for the temperature behavior of the condensates, or to take the results from lattice calculations at face value.

We will not here review the application of QCD sum rules at zero temperature. This is done in refs. [56, 57], the latter article serving as a worthwhile introduction while the former provides a wealth of details.

The main ideas connected with the use of finite temperature QCD sum rules were expounded in an article by Bochkarev and Shaposhnikov [114], who first investigated the 1^{--} channel of the ρ -meson. A more thorough investigation coming to different conclusions is that of Adami, Hatsuda, and Zahed [115]. We shall follow this treatment, and go on to describe the changes to the nucleon properties using essentially the same technique [116].

The central idea behind the sum-rule method is to use the analyticity properties of a correlator of currents in a selected channel to relate the real and imaginary parts of this quantity via Cauchy's theorem. For a structure function $\Pi(q_0, |\mathbf{q}|)$ this relation is expressed by the fixed-momentum dispersion relation

$$\Pi(q_0, |\mathbf{q}|) = \frac{1}{\pi} \int \frac{\text{Im } \Pi(\omega, |\mathbf{q}|)}{\omega - q_0} d\omega. \quad (6.1)$$

The imaginary part, being related to a total cross section (measurable or not), is then parametrized

either using input from experiment or by knowledge gained from low-energy effective theories. This treatment of the “right-hand-side” (r.h.s.) of the sum rule (6.1) therefore introduces some uncertainty into the results, which, however, can be minimized by use of the Borel transform as we shall see below. The “left-hand-side” (l.h.s.), i.e. the real part of the correlator, is on the contrary calculated in perturbative QCD at large space-like momentum transfer. The nonperturbative nature of the QCD vacuum introduces power corrections to the leading perturbative result through the occurrence of nonvanishing condensates which summarize the low-frequency aspects of quark and gluon dynamics, inaccessible to perturbation theory. The coefficients of these condensates in turn carry the ultraviolet information. This division, which is implemented by the use of the operator product expansion (OPE) [117] for the l.h.s., shall be maintained at finite temperature in the sense that all temperature dependent pieces which are of perturbative origin should reside in the Wilson coefficients, whereas all nonperturbative effects should be buried in the condensates. This is a nontrivial requirement at finite temperature, as we shall see below.

6.1. The ρ -meson at finite temperature

As is well known [118], it is not the causal correlator that has the required analytic properties in a heat bath, but rather the *retarded* one. Let us therefore consider the retarded correlator of currents with photon quantum numbers,

$$\Pi_{\mu\nu}^R(q^2) = i \int d^4x e^{iqx} \theta(x_0) \langle \langle [J_\mu(x), J_\nu(0)] \rangle \rangle, \quad (6.2)$$

where $\langle \langle \mathcal{O} \rangle \rangle$ denotes the usual temperature average of an operator \mathcal{O} :

$$\langle \langle \mathcal{O} \rangle \rangle = Z^{-1} \sum_n \langle n | \mathcal{O} | n \rangle e^{-\beta \omega_n}, \quad (6.3)$$

β being the inverse temperature and ω_n the energy of the state $|n\rangle$. Z is the partition function,

$$Z = \sum_n \langle n | e^{-\beta H} | n \rangle. \quad (6.4)$$

We shall refer to this definition as the “Gibbs” vacuum.

For simplicity the currents will be restricted to the ρ^0 -channel:

$$J_\mu(x) = \frac{1}{2} (\bar{u}(x) \gamma_\mu u(x) - \bar{d}(x) \gamma_\mu d(x)). \quad (6.5)$$

For use with the l.h.s. of the sum rule we write down the OPE for the operator $[J_\mu(x), J_\nu(0)]$, which is valid at small x and which includes non-Lorentz-invariant operators due to the presence of a heat bath:

$$[J_\mu(x), J_\nu(0)] = C_1(x) \mathbf{1} + C_{\bar{q}q}(x) \bar{q}q + C_{E^2}(x) E^2 + C_{B^2}(x) B^2 + \dots. \quad (6.6)$$

Due to the increasing dimensionality of the operators appearing in the infinite sum in (6.6), the Wilson coefficients C_i must carry increasingly high powers of x such that the series converges at small x . Taking the vacuum expectation value using the Gibbs vacuum defined above, however, reveals that, due to the fact that *all* the temperature dependence, perturbative and nonperturbative, is buried in the state $|0\rangle$, the Wilson coefficients $C_i(x)$, being c -numbers, acquire no temperature dependence whatsoever. In turn, the condensates carry perturbative information, as e.g.

$$\langle \langle B^2 \rangle \rangle = \text{const.} \cdot T^4 + \langle B^2 \rangle_{\text{np}}. \quad (6.7)$$

The first piece is the perturbative (Stefan–Boltzmann) contribution and represents the pressure associated with the thermal (black-body) gluons rather than any nonperturbative information. The latter is contained in the second term of (6.7), and only this piece should be termed “condensate”. While it is not explicitly temperature dependent, it is implicitly so, as the matrix element depends on the coupling strength $g(T, A)$. In order to extract the black-body piece from *all* the condensates appearing in the OPE and to shuffle these into the Wilson coefficients we will use the well known Matsubara approach, in which the temperature dependence is introduced by restricting the integration along the Euclidean time axis over a finite interval. The vacuum in this approach carries no explicit temperature dependence and may be identified with the $|0\rangle_{\text{np}}$ defined above. That this approach achieves the stated purpose will be verified a posteriori. At this point one might wonder about the relevance of an approach where the perturbative contributions to the “pressure” in a condensate are derived using quark and gluonic degrees of freedom, rather than hadronic ones. We would like to point out, however, that the Matsubara approach described below manages to sum up *all* perturbative contributions, which should in principle add up to a result similar to one obtained from summing up all hadronic “perturbative” contributions. The latter, however, has yet to be attempted. Taking into account only the lowest order corrections to the condensates stemming from pions [30] has revealed similarities in the results, but also important differences, which we discuss below.

The Matsubara correlator is defined in Euclidean space–time by

$$\Pi_{\mu\nu}^E(q_0 = i\omega_n, \mathbf{q}) = i \int_0^\beta dx_0 \int d^3x e^{iqx} \langle 0 | T_\tau (J_\mu(x) J_\nu(0)) | 0 \rangle_{\text{np}}, \quad (6.8)$$

and coincides with the Gibbs one at the (discrete) Matsubara frequencies $\omega_n = 2\pi n/\beta$ (see, e.g., ref. [119]). T_τ denotes the operator ordering along the time-like Euclidean axis. However, the Wilson coefficients obtained from the Matsubara approach are temperature dependent, unlike the ones obtained from the Gibbs approach, as discussed above. In fact, they contain the black-body pieces arising from the condensates used in the Gibbs approach, while the condensates of the Matsubara approach should be identical with the $\langle \mathcal{O} \rangle_{\text{np}}$ contribution in the Gibbs approach. While technically it does not matter which approach is used, the results will differ as soon as the OPE is truncated, as of course is inevitable. The truncation in the Matsubara approach neglects terms of the form $\langle \mathcal{O} \rangle_{\text{np}}/(q^2)^m \times (T^2/q^2)^n$ and retains all purely temperature dependent pieces and those powers of temperature multiplying a condensate kept in the expansion. This seems to be a reasonable approximation in the case $\langle \mathcal{O} \rangle_{\text{np}}/(q^2)^m$ is small, which is probable at high temperatures. This is not the case for the factor $\langle \langle \mathcal{O} \rangle \rangle / (q^2)^m$ appearing in neglected terms in the Gibbs approach, as it contains perturbative pieces $\sim (T^2/q^2)^m$ which grow with temperature. In the spirit of Shifman, Vainshtein, and Zakharov [41] (SVZ) we therefore proceed with the Matsubara approach. One might now be tempted to expand the temperature dependent Wilson coefficients in such a way that only terms up to a certain order in q^2 are retained. For example, we might insist that if terms of the order $\langle \bar{q}q \rangle^2/q^6$ are retained, the temperature expansion is carried only to order $(T^2/q^2)^3$ etc. While this seems to be the consistent procedure, it is only reliable for very low temperatures as the temperature expansion is an asymptotic one, with ever growing terms alternating in sign. Whether this reflects the behavior of the underlying OPE is presently unknown.

Most approaches to finite-temperature QCD sum rules [30, 120] neglect the perturbative black-body terms $\sim (T^2/q^2)^n$ altogether on the grounds that $q^2 \gg T^2$. However, as the expansion is really in powers of $(2\pi T)^2/q^2$, and q^2 is ultimately used for values as low as $q^2 \sim m_H^2$, where m_H

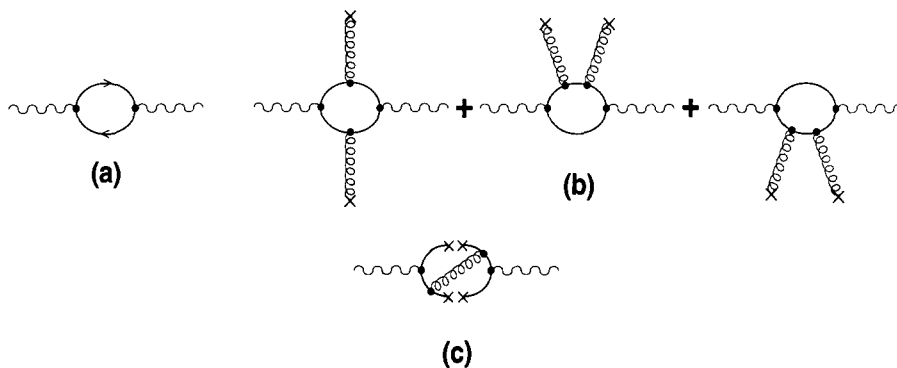


Fig. 6.1. (a) Leading perturbative contribution in the OPE, coefficient C_1 ; (b) contribution of the gluon condensates C_{E2} and C_{B2} ; (c) contribution of the square of the quark condensate $C_{(\bar{q}q)^2}$.

is the relevant hadron mass, the perturbative terms of higher order soon dominate, and cannot be neglected. The recent pion-gas calculations [30] mentioned earlier obtain some of the low temperature behavior seen in the calculations described below. Since the ρ -meson couples strongly to two pions, the pion-gas approximation at low temperatures leads smoothly into the perturbative one at higher temperatures. The properties of the ω -meson, which couples only to three or more pions, are essentially unchanged in the pion-gas model [30]; however, it is expected to follow the behavior of the ρ -meson at higher temperatures.

Lattice gauge calculations [6] confirm directly that energy production in the region of temperatures $T \sim T_c$ is at least approximatively black-body in terms of both quarks and gluons (as these are the variables used in the lattice calculations). To the extent that the gluon energy is black-body, this confirms that the matrix element $\langle\langle 0|G_{\mu\nu}^2|0\rangle\rangle$ must contain the black-body T^4 term [see eq. (6.7)], which is not present in the pion-gas description of Hatsuda et al. [30].

The correlator (6.8) may at finite temperature be decomposed into a longitudinal and a transverse piece (we drop the superscript E which indicated the Euclidean correlator). Defining $Q^2 = -q^2$ we write [121]

$$\Pi_{ij} = \left(\delta_{ij} - \frac{Q_i Q_j}{Q^2} \right) \Pi_T + \frac{Q_i Q_j}{Q^2} Q_0^2 \Pi_L, \quad (6.9)$$

$$\Pi_{00} = Q^2 \Pi_L. \quad (6.10)$$

In the following, we shall put the source at rest in the heat bath, i.e. $\mathbf{Q} \rightarrow \mathbf{0}$. In this case $\Pi_T \rightarrow Q^2 \Pi_L$ and the form factors are related. The dispersion relation for the longitudinal form factor is then (with $Q^2 = Q_0^2$ and not writing out subtractions)

$$\text{Re } \Pi_L(Q^2) = \frac{1}{\pi} \int_0^\infty \frac{\text{Im } \Pi_L(s)}{s + Q^2} ds + \text{subtr.} \quad (6.11)$$

The l.h.s. of (6.11) is calculated in perturbation theory at finite temperature retaining only the contributions shown in fig. 6.1. Only the contribution fig. 6.1b gives a vanishing result as it is proportional to the quark mass and we work in the chiral limit. Explicit expressions for the

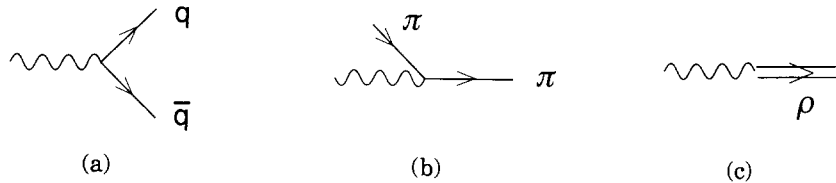


Fig. 6.2. Absorptive processes contributing to the imaginary part of the correlator: (a) quark–antiquark pair formation, (b) Landau damping (virtual pion absorption), (c) ρ -resonance formation.

coefficients can be found in the appendix of ref. [115]. For the r.h.s. we use the “narrow-resonance approximation” of single ρ -pole saturation and a continuum given by the $\rho \rightarrow q\bar{q}$ amplitude-squared at finite temperature. The latter is modelled by taking the imaginary part of the perturbative diagram fig. 6.1a at real momentum transfers starting at an arbitrary threshold s_0 (see fig. 6.2a),

$$\text{Im } \Pi_L^{\text{pair}} = \frac{1}{8\pi} \theta(s - s_0) \tanh(\sqrt{s}/4T). \quad (6.12)$$

This continuum may also be thought of as modelling the emergence of the (broad) A_1 -pole in this channel at around s_0 , through the process $\pi\rho \rightarrow A_1$ enabled by pions from the heat bath, and introducing a mixing of the ρ and A_1 channels [120]. We shall ignore this mixing here for simplicity, burying its effects in the continuum threshold s_0 . Furthermore, at finite temperatures there is a contribution which is associated to the Landau-damping mechanism (fig. 6.2b) and which contributes only at $s \rightarrow 0$. This is adequately modelled by

$$\text{Im } \Pi_L^{\text{ld}} = c_L \pi T^2 \delta(s). \quad (6.13)$$

Here, c_L is a numerical coefficient, which turns out to be $c_L = -1/2$ for Landau damping through quarks in the heat bath, or $c_L = 1/3$ for damping through pions. In the region $s \sim 0$, the latter seems to be the physical choice, and is adopted throughout*).

Including the pole contribution (fig. 6.2c)

$$\text{Im } \Pi_L^{\text{pole}} = f_\rho m_\rho^2 \delta(s - m_\rho^2), \quad (6.14)$$

with a resonance strength f_ρ and a pole position m_ρ^2 , our expression for $\text{Im } \Pi_L$ is just the sum of eqs. (6.12), (6.13), (6.14).

The last ingredient needed here is a parametrization of the temperature dependence of the condensates. In ref. [115] three qualitatively different models were used to probe the stability of the results with respect to different *ansätze* for the condensates. Here, we will be inspired by recent lattice results, which indicate a weak second order transition for the quark condensate [5]. The gluon condensate does not seem to vary appreciably below T_c [123, 115]. Accordingly we take $\langle \bar{q}q \rangle(T) = \langle \bar{q}q \rangle_0 [1 - (T/T_c)^2]^{1/2}$ (see fig. 6.3), and $\langle \langle \mathbf{B}^2 \rangle \rangle = -\langle \langle \mathbf{E}^2 \rangle \rangle = \frac{1}{4} \langle \langle G^2 \rangle \rangle = \frac{1}{4} \langle G^2 \rangle_0$ with $\langle (\alpha_s/\pi) G^2 \rangle^{1/4} = 331 \text{ MeV}$ and $\langle \bar{q}q \rangle_0^{1/3} = -250 \text{ MeV}$.

*) The coefficients differ from the estimates in refs. [114, 115, 122], but are consistent with what is expected from the quark number susceptibility $\chi = -\text{Re } \Pi_{00}(0, \mathbf{0})$.

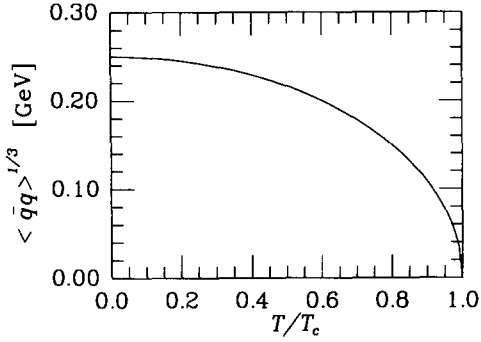


Fig. 6.3. Input temperature dependence of the quark condensate.

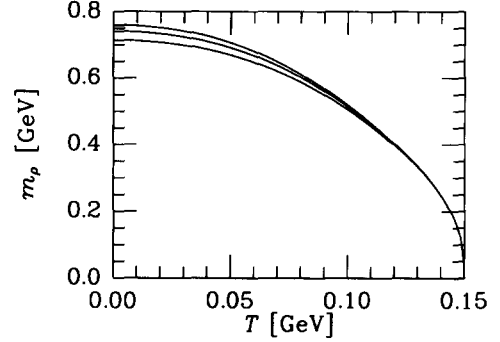


Fig. 6.4. ρ -mass versus temperature as obtained from (6.23) for different continuum thresholds. The upper curve has $s_0 = 1.7 \text{ GeV}^2$, while the middle one was calculated for $s_0 = 1.5 \text{ GeV}^2$. For the lower one we used $s_0 = 1.3 \text{ GeV}^2$ as an input ($T_c = 150 \text{ MeV}$).

The l.h.s. of the sum rule assumes the form

$$\begin{aligned} \text{Re}\Pi_L(Q^2) = & -\frac{1}{8\pi^2} \ln(Q^2/\mu^2) + \frac{1}{\pi^2} \int_0^\infty n_F(p_0) dp_0^2 \frac{p_0^2}{Q^2(p_0^2 + Q^2/4)} - \frac{112}{81} \pi \alpha_s \frac{\langle \bar{q}q \rangle^2}{Q^6} \\ & + \frac{\alpha_s}{18\pi} \left(1 + \frac{1}{2} Q^2 \int_0^\infty n_F(p_0) dp_0^2 \frac{p_0^2 - \frac{3}{4} Q^2}{(p_0^2 + Q^2/4)^3} \right) \left(2\langle \mathbf{B}^2 \rangle - \langle \mathbf{E}^2 \rangle \right) \frac{1}{Q^4}, \end{aligned} \quad (6.15)$$

where $n_F(x)$ denotes the fermionic distribution function $(1 + e^{x/T})^{-1}$.

As was shown by SVZ [41], the convergence of the OPE may be improved by Borel transforming each of the terms arising in the Fourier transform of the series (6.6) by applying the operator

$$\hat{L}_M = \lim_{\substack{n, Q^2 \rightarrow \infty \\ M^2 \equiv Q^2/n}} \frac{1}{(n-1)!} (Q^2)^n (-\partial/\partial Q^2)^n. \quad (6.16)$$

This ensures that a contribution of order $(1/Q^2)^m$ is multiplied by an additional factor $1/m!$ as is easily checked. Furthermore the weight function $1/(s + Q^2)$ appearing on the r.h.s. of the sum rule [see eq. (6.11)] is replaced by

$$\hat{L}_M \frac{1}{s + Q^2} = \frac{1}{M^2} e^{-s/M^2}. \quad (6.17)$$

The arbitrary Borel parameter M^2 is used to match l.h.s. and r.h.s. It is determined in such a way that the dependence of the physical parameters m_ρ , s_0 and f_ρ on M^2 is minimal (see below). Applying \hat{L}_M to the l.h.s. and the r.h.s. we obtain the sum rule

$$8\pi^2 f_\rho \frac{m_\rho^2}{M^2} e^{-m_\rho^2/M^2} = R(M^2, T^2), \quad (6.18)$$

where

$$R(M^2, T^2) = C_1(T^2, M^2) + C_{G^2}(T^2, M^2) \frac{\frac{8}{3}\langle \mathbf{B}^2 \rangle - \frac{4}{3}\langle \mathbf{E}^2 \rangle}{M^4} - C_{\langle \bar{q}q \rangle^2} \frac{\langle \bar{q}q \rangle^2}{M^6}, \quad (6.19)$$

with the definitions

$$C_1(T^2, M^2) = 1 - e^{-s_0/M^2} + 8\pi^2(c_L + \frac{1}{6})\frac{T^2}{M^2} - \int_0^{s_0} \frac{dp_0^2}{M^2} 2n_F(p_0/2)e^{-p_0^2/M^2}, \quad (6.20)$$

$$C_{G^2}(T^2, M^2) = \frac{1}{3}\pi\alpha_s \left\{ 1 - M^2 \int_0^\infty 2n_F(p_0/2) \frac{dp_0^2}{p_0^4} \left[e^{-p_0^2/M^2} \left(1 + \frac{p_0^2}{M^2} + \frac{p_0^4}{2M^4} \right) - 1 \right] \right\}, \quad (6.21)$$

$$C_{(\bar{q}q)^2} = \frac{448}{81}\pi^3\alpha_s. \quad (6.22)$$

In eq. (6.19), we notice a peculiar splitting of magnetic and electric contributions to the gluonic coefficient, in a 2 : 1 ratio. This splitting, however, is entirely frame dependent.

While the parameters f_ρ , m_ρ and s_0 can be found from (6.18) by matching the l.h.s. to the r.h.s. [115], it is more convenient to eliminate the parameter f_ρ by obtaining a second sum rule through differentiation of (6.18). This allows us to derive a formula for the ρ mass,

$$m_\rho^2(T^2, M^2) = -\partial \ln M^2 R(T^2, M^2) / \partial (1/M^2). \quad (6.23)$$

This expression still depends on the Borel mass M and the continuum threshold s_0 . Fixing s_0 at 1.7 GeV², the standard vacuum value, we obtain ‘‘Borel curves’’ for m_ρ (the ρ -mass versus Borel mass) at every temperature. The ρ -mass is then obtained by looking for the stability plateau in these curves, i.e. choosing M^2 such that $\partial m_\rho(M^2)/\partial M^2 = 0$. In fact, this is equivalent to demanding independence of the artificially introduced scale M^2 for observables, i.e., defining $\tau = 1/M^2$, we demand

$$\tau \partial m_\rho^2 / \partial \tau = 0 \quad (6.24)$$

to determine M^2 . This was used implicitly in deriving (6.23).

We do not have a handle on possible changes to the continuum threshold in this approach. However, we have checked that, as the resonance mass drops, it becomes more and more insensitive to the value of s_0 . Generally, we expect s_0 to drop. For simplicity, however, we have kept it constant in this calculation. This procedure yields fig. 6.4, the ρ -mass as a function of temperature. The smooth behavior of the ρ -mass, dropping with temperature, is the result of a delicate balancing between the dropping quark condensate $\langle \bar{q}q \rangle^2$ on the one hand, and the gluon contribution on the other. These two contributions enter in the expression for the ρ -mass with opposite signs. While the gluon condensate itself does not change with temperature (as suggested by lattice calculations mentioned earlier in this report), the Wilson coefficient of this contribution, $C_{G^2}(T^2, M^2)$ on the contrary does change, vanishing as $M \rightarrow 0$ (see ref. [124] for details). The decrease of the Borel parameter with increasing temperature occurs as a consequence of eq. (6.23). As mentioned earlier, the ρ mass is read off from (6.23) by looking for the minimum of the curve, at which point the ρ mass is independent of the Borel parameter. This minimum shifts to lower Borel masses when the quark condensate is reduced. This is consistent with the general idea [41] that the Borel mass parameter should roughly coincide with the resonance mass. The Wilson coefficient of the quark condensate contribution is unaffected by temperature. We thus encounter the interesting situation where the dominance of the hard scale $\langle G^2 \rangle$, which because it contributes attractively could end up governing the approach of m_ρ to zero and force premature chiral restoration, is thwarted by its

Wilson coefficient. Indeed, it is precisely chiral restoration that forces M^2 to drop, and with it the gluonic Wilson coefficient.

The final result, fig. 6.4, essentially validates one of the scaling assumptions in (2.1), as we indeed find (compare fig. 6.3)

$$m_\rho(T)/m_\rho(0) \simeq \langle \bar{q}q \rangle^{1/3}(T)/\langle \bar{q}q \rangle^{1/3}(0). \quad (6.25)$$

Thus, although the ρ mass depends intrinsically on the two independent scales $\langle \bar{q}q \rangle^{1/3}$ and $\langle G^2 \rangle^{1/4}$, the condensates and Wilson coefficients conspire in such a way that the scaling relation (2.1), which reflects the assumption of a single scale, is approximately valid.

6.2. The nucleon at finite temperature

The extension of the finite-temperature QCD sum-rule approach to the nucleon [116] provides a unique tool to investigate nucleon properties under extreme conditions. While finite-density effects have been estimated earlier [21], care must be taken in the finite-temperature case to consistently take into account the black-body (perturbative) contributions from the condensates. This is done in the manner outlined in refs. [115, 116] and the preceding section, using the Matsubara approach. We probe the nucleon channel (neglecting quark masses, we do not differentiate between the proton and the neutron) by considering the correlator of nucleon currents

$$\Pi(q^2) = i \int_0^\beta dx_0 \int d^3x e^{iqx} \langle 0 | T_\tau (\eta_N(x) \bar{\eta}_N(0)) | 0 \rangle, \quad (6.26)$$

where $\eta_N(x)$ is the usual Ioffe current. If the source is at rest in the heat bath, $\mathbf{q} \rightarrow \mathbf{0}$, the correlator can be decomposed into two invariant structure functions,

$$\Pi(q^2) = \not{q} \Pi_1(q^2) + \Pi_2(q^2), \quad (6.27)$$

for each of which we can write fixed- $|\mathbf{q}|$ dispersion relations evaluated at $\mathbf{q} = \mathbf{0}$ with $Q^2 = -q_0^2$,

$$\Pi_{1,2}(Q^2) = \frac{1}{\pi} \int \frac{\text{Im} \Pi_{(1,2)}(\omega)}{\omega^2 + Q^2} d\omega^2. \quad (6.28)$$

Again, we obtain an expression for the l.h.s. of the sum rules (6.28) by exploiting the short distance expansion of the correlator and neglecting corrections of higher order in $1/Q^2$. We show in fig. 6.5 the terms kept in the expansion of each structure function. As we shall see, a formula

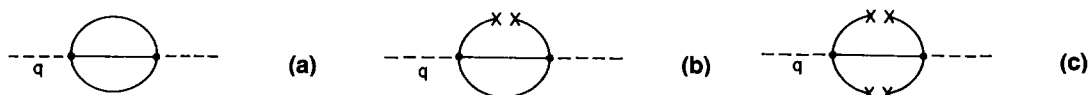


Fig. 6.5. (a) Leading perturbative contribution in the OPE for the nucleon channel, coefficient C_1 , (b) contribution of the quark condensate $C_{\bar{q}q}$, (c) contribution of the square condensate $C_{(\bar{q}q)^2}$.

for the nucleon mass is obtained by equating the ratios of the l.h.s. and the r.h.s. of the sum rules. After Borel transformation we obtain for the ratio of l.h.s.'s

$$\frac{\hat{L}_M \Pi_2(Q^2)}{\hat{L}_M \Pi_1(Q^2)} = \frac{2aM^2[1 - 64(T^4/M^4) \int x^3 dx n_F(x) e^{-4x^2 T^2/M^2}]}{M^4 + \frac{4}{3}a^2/M^2 + \frac{56}{3}\pi^4 T^4 f(T^2/M^2)}, \quad (6.29)$$

with $a = -2(2\pi)^2(\bar{q}q)$. The function $f(T^2/M^2)$ appearing in (6.29) is a slowly varying function of temperature reflecting the contribution of the diagram in fig. 6.5a. Its explicit form can be found in ref. [116]. At low temperatures

$$f(T^2/M^2) = 1 - \frac{2096}{147}\pi^2 T^2/M^2 + O(T^4/M^4). \quad (6.30)$$

For the r.h.s. of the sum rule, we need information about the absorptive part of the correlator for *all* ranges of momentum transfer, $0 < s < \infty$. This, of course, is not available, neither through perturbative techniques, nor from experiment. We therefore have to rely on established knowledge of low-energy hadron dynamics to parametrize $\text{Im} \Pi(s)$. For instance, it is clear that to lowest order the correlator is dominated by the propagation of a single nucleon, i.e.,

$$\Pi(q^2) \sim S(q^2) = \frac{\not{q} + m_N}{q^2 - m_N^2}. \quad (6.31)$$

If we denote by λ_N the overlap between the nucleon state and the vacuum [$u(p)$ is the nucleon wavefunction],

$$\langle 0 | \eta_N(x) | N(p) \rangle = \lambda_N u(p) e^{-ipx}, \quad (6.32)$$

then

$$\text{Im} \Pi(q^2) = \lambda_N^2 (\not{q} + m_N) \pi \delta(q^2 - m_N^2), \quad (6.33)$$

$$\hat{L}_M \Pi_2(Q^2) / \hat{L}_M \Pi_1(Q^2) = m_N, \quad (6.34)$$

which together with (6.29) results in the formula for the nucleon mass (as in the zero temperature case).

At very high momentum transfer, $s \rightarrow \infty$, we expect the correlator to be dominated by the effects of the propagation of free quarks. However, we shall neglect this here as our use of the Borel transform effectively cuts down the influence of the large momentum transfer region. We would like to note however that the conventional approach to nucleon sum rules [25] makes use of just this contribution to the nucleon correlator, introducing an additional parameter s_0 , which is interpreted as the threshold value for the momentum transfer. As the nucleon mass depends strongly on this parameter, and the optimal value $\sqrt{s_0} \sim 1.5 \text{ GeV}$ signaling the onset of perturbative dominance of the correlator seems rather low, we would like to propose a different approach that seems to be more appropriate at temperatures below T_c . At intermediate momentum transfers we expect corrections to the lowest order contribution (6.33) to arise through πN -dynamics. Indeed, as the pion energy $\epsilon_\pi \approx 2.7 T$, a pion at $T = 100 \text{ MeV}$ has just the right energy to excite the Δ resonance. Thus, we believe that the dominant correction to the nucleon propagator is given by the $\pi\Delta$ self-energy, fig. 6.6.

Dressing the nucleon propagator with this diagram introduces a continuum in the nucleon channel, with a threshold given by $s_0 = (M_\Delta + m_\pi)^2$. This describes nucleon ‘‘loss’’ through the process $N \rightarrow \pi\Delta$. At finite temperature, a new channel opens up due to the presence of pions from the heat

$$\Sigma_{\pi\Delta}(\not{p}) = \begin{array}{c} \pi \\ \text{---} \\ \Delta \end{array}$$

Fig. 6.6. $\pi\Delta$ -loop contribution to the nucleon self-energy.

bath: $\pi^*N \rightarrow \Delta$ (π^* denoting a ‘‘hot’’ pion). This process generates a finite width for the nucleon. As we shall see later on, this is the most important effect of the pionic heat bath, as to lowest order the nucleon pole is not affected. If we denote by $\Sigma(\not{p})$ the contribution of the self-energy (fig. 6.6), we can write the renormalized nucleon propagator as

$$iS_R(\not{p}) = \frac{i}{\not{p} - m_N - i \text{Im} \Sigma(\not{p}) + i\epsilon}, \quad (6.35)$$

while

$$\text{Im} \Pi(q^2) = \lambda_N^2 \text{Im} S_R(q^2). \quad (6.36)$$

The pole in the above propagator includes the renormalization at zero temperature and finite-temperature effects due to the real part of the self-energy. It is precisely this change in the pole of the propagator that we are attempting to extract with the sum-rule procedure.

In order to obtain the $\pi\Delta$ self-energy, we use an effective $\pi N\Delta$ interaction

$$\mathcal{L}_{\text{int}} = \frac{g}{m_\pi} \left(\bar{Z}_{\mu\alpha}^a \partial_\mu \pi^a \psi_\alpha + \text{h.c.} \right) \quad (6.37)$$

with $g^2 = 4.68$ (to reproduce $\Gamma_\Delta = 115$ MeV) and a Rarita–Schwinger field $Z_{\mu\alpha}^a$. Putting only the pion at temperature and in the limit $\not{p} \rightarrow \mathbf{0}$ we obtain

$$\text{Im} \Sigma = (\alpha \not{p} + M_\Delta) \sigma(p^2) \quad (6.38)$$

with

$$\begin{aligned} \sigma(p_0^2) = & -\frac{2}{3} \frac{g^2}{m_\pi^2} \theta(p_0) \frac{[(p_0^2 - s_+)(p_0^2 - s_-)]^{3/2}}{32\pi M_\Delta^2 p_0^2} \\ & \times \left\{ \theta(p_0^2 - s_+) [1 + n_B(\frac{1}{2}z p_0)] + \theta(s_- - p_0^2) n_B(-\frac{1}{2}z p_0) \right\} \end{aligned} \quad (6.39)$$

and the definitions

$$s_\pm = (M_\Delta \pm m_\pi)^2, \quad z = \frac{p_0^2 - M_\Delta^2 + m_\pi^2}{p_0^2} = 2(1 - \alpha). \quad (6.40)$$

Also, $n_B(x)$ is the bosonic distribution function

$$n_B(x) = 1/(1 + e^x). \quad (6.41)$$

Finally, defining

$$\mu^2 = \alpha^2 p_0^2 - M_\Delta^2 = \frac{1}{4p_0^2} (p_0^2 - s_+)(p_0^2 - s_-)$$

allows us to write

$$\text{Im } \Pi_1(s) = \lambda_N^2 \rho_1(s), \quad \text{Im } \Pi_2(s) = \lambda_N^2 m_N \rho_2(s), \quad (6.42)$$

with

$$\rho_1(s) = -\sigma(s) \frac{\alpha(s + m_N^2 + \mu^2 \sigma^2) + 2m_N M_\Delta}{(s - m_N^2 + \mu^2 \sigma^2)^2 + 4s\sigma^2(\alpha m_N + M_\Delta)^2}, \quad (6.43)$$

$$\rho_2(s) = -\sigma(s) \frac{(M_\Delta/m_N)(s + m_N^2 - \mu^2 \sigma^2) + 2\alpha s}{(s - m_N^2 + \mu^2 \sigma^2)^2 + 4s\sigma^2(\alpha m_N + M_\Delta)^2}. \quad (6.44)$$

For $T \rightarrow 0$, the spectral distributions $\rho_{1(2)}$ are reduced to Dirac delta-functions at $s = m_N^2$ and a continuum starting at $s = s_+$. For $T \neq 0$ the delta-function acquires a width, which increases rapidly with temperature (see ref. [116]). With this continuum model as input for the r.h.s., we can write

$$\frac{\hat{L}_M \Pi_2(Q^2)}{\hat{L}_M \Pi_1(Q^2)} = \frac{\int_0^\infty e^{-s/M^2} \rho_2(s) ds}{\int_0^\infty e^{-s/M^2} \rho_1(s) ds}, \quad (6.45)$$

which now depends implicitly on m_N . However, it turns out that, although the width can be sizable near T_c , (6.45) does not differ significantly from m_N . This is due partially to the absolute size of the self-energy correction (being small) and due to the fact that the integral over the resonance is practically independent of the width. Therefore, the normalized integral below s_- can for all purposes be approximated by 1, and we have

$$\frac{\hat{L}_M \Pi_2(Q^2)}{\hat{L}_M \Pi_1(Q^2)} \simeq \frac{m_N + \int_{s_+}^\infty e^{-s/M^2} \rho_2(s) ds}{1 + \int_{s_+}^\infty e^{-s/M^2} \rho_1(s) ds} \equiv Z m_N. \quad (6.46)$$

Numerically, $Z \simeq 1$ below T_c . Thus, the continuum model presented here has a negligible effect on the pole position, unlike the perturbative continuum model, which shifts the mass by several percent [25]

An expression for the nucleon width can be obtained by defining

$$\gamma_N = -2(\text{Im } S_R(p_0 = m_N))^{-1}. \quad (6.47)$$

Using (6.35), (6.38), (6.39) we obtain

$$\gamma_N = \frac{1}{3\pi} \frac{g^2}{m_\pi^2} \frac{E_N + m_N}{M_\Delta} |q_\pi|^3 n_B(\omega_\Delta/T) = 4\Gamma_\Delta (M_\Delta/m_N)^3 n_B(\omega_\Delta/T). \quad (6.48)$$

Here, $\omega_\Delta = (M_\Delta^2 - m_N^2 - m_\pi^2)/(2m_N)$, and $|q_\pi|$ is the pion momentum in the nucleon rest frame. Γ_Δ is the width of the Δ (in the Δ rest frame!) calculated from (6.37) in the tree approximation. Indeed, the width obtained using the nonrelativistic approximation (6.47) coincides with the nucleon width obtained directly from (6.37) in the Born approximation. It differs by a kinematical factor of (M_Δ/m_N) from the one obtained by Leutwyler and Smilga [125], however.

We have plotted the nucleon mass for two extreme scenarios, namely for a quark condensate *independent of temperature* (we call this scenario the “first order scenario”) and for a picture in which the quark condensate drops smoothly with temperature as $\langle \bar{q}q \rangle(T) = \langle \bar{q}q \rangle(0) [1 - (T/T_c)^2]^{1/2}$

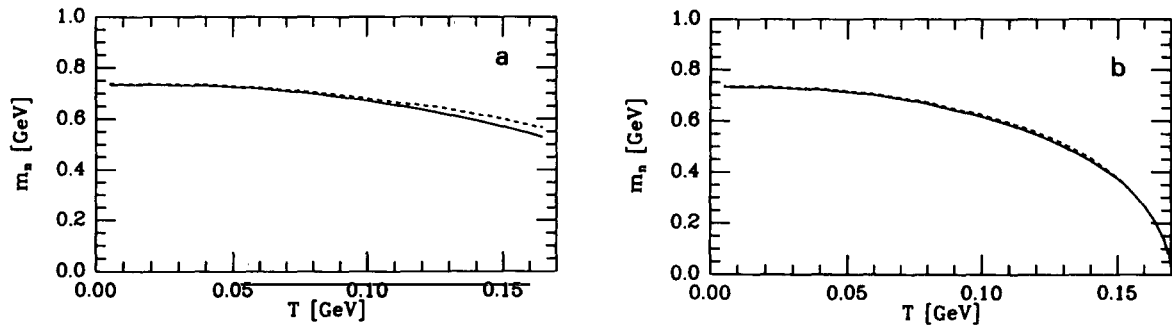


Fig. 6.7. (a) Nucleon mass versus temperature for a temperature independent quark condensate. Solid line: without continuum corrections, dashed line: including the $\pi\Delta$ continuum. (b) Same as (a) but with a condensate dropping as $[1 - (T/T_c)^2]^{1/2}$, with $T_c = 170$ MeV.

(see fig. 6.3). The latter is dubbed the “second order scenario”. The full lines in fig. 6.7 show the result of a calculation without continuum corrections, while the dashed lines include the above-mentioned $\pi\Delta$ self-energy correction. Figure 6.7a illustrates the first-order scenario, fig. 6.7b the second-order one.

We conclude this section by noting that these calculations support the general scaling idea promulgated throughout this report: The relation $m_N^*/m_N \simeq (\langle\bar{q}q\rangle^*)^{1/3}/(\langle\bar{q}q\rangle)^{1/3}$ is approximately valid, even if taking into account finite temperature corrections to the perturbative contribution (in the l.h.s.), or corrections due to the pionic heat bath (in the r.h.s.). We expect the inclusion of gluonic condensates, such as $\langle\langle G_{\mu\nu}G^{\mu\nu}\rangle\rangle$, or the mixed one $\langle\langle\bar{q}(\lambda^a/2)\sigma_{\mu\nu}G_{\mu\nu}^a q\rangle\rangle$ not to affect this conclusion significantly. For the former condensate we expect a similar mechanism as for the ρ -meson to suppress its effect. The mixed condensate usually enters at the same level as the ordinary quark condensate, and its value is often linked to it.

7. QCD sum rules at finite density and the nuclear many-body problem

QCD sum rules at finite density offer the opportunity to study nuclear matter and the problem of nuclear binding from a conceptionally new perspective, to a certain order in an expansion in terms of the chemical potential or the density. The finite-density case differs from the discussion of finite temperature in that condensates other than those present in the vacuum become relevant already at low densities, most prominent in this respect being, of course, the quark number density $\langle q^\dagger q \rangle$, which increases with density. Also, it seems that in the discussion of finite-density effects, the expectation values of the operators appearing in the expansion of the “left-hand side” should be saturated with hadronic states, rather than quark and gluon ones as was done in the preceding section. As always, the choice is one of convenience. While the result should be independent of the basis chosen if the OPE is not truncated, truncation is necessary in any physical application. Ultimately, a comparison of the two approaches should decide which is the most convenient, and at what scale.

7.1. Vector-meson masses

Finite-density sum rules were seriously considered first by Drukarev and Levin [126]. While mainly concerned with the problem of nuclear matter, they obtained a convenient way of estimating the decrease in the scalar condensate $\langle \bar{q}q \rangle^*$ with increasing density, which turns out to be quite general. Starting with the pion–nucleon sigma term [see (4.3)]

$$\Sigma_{\pi N} = (m_u + m_d) \langle N | \bar{q}q | N \rangle \quad (7.1)$$

the scalar condensate saturated with a single nucleon state can be expressed as

$$\langle N | \bar{q}q | N \rangle = \Sigma_{\pi N} / (m_u + m_d) \simeq 4, \quad (7.2)$$

using $\Sigma_{\pi N} \simeq 46$ MeV and $m_u + m_d = 11$ – 12 MeV.

Up to nuclear matter density ρ_0 , nuclei or nuclear matter can be approximated by a dilute gas of well separated nucleons. To linear order in the density then, the change in the scalar condensate can be estimated via

$$\langle \bar{q}q \rangle^* - \langle \bar{q}q \rangle \simeq \langle N | \bar{q}q | N \rangle \rho = \frac{\Sigma_{\pi N}}{(m_u + m_d)} \rho, \quad (7.3)$$

which yields

$$\frac{\langle \bar{q}q \rangle^*}{\langle \bar{q}q \rangle} = 1 - \frac{\Sigma_{\pi N}}{(m_u + m_d)} \frac{\rho}{|\langle \bar{q}q \rangle|} = 1 - \frac{\Sigma_{\pi N}}{f_\pi^2 m_\pi^2} \rho, \quad (7.4)$$

where in the last step we have used the Gell-Mann–Oakes–Renner relation. We obtain for the decrease of the quark condensate at nuclear matter density $\rho_0 = 0.17 \text{ fm}^{-3}$,

$$\langle \bar{q}q \rangle^* / \langle \bar{q}q \rangle = 0.63 \quad (7.5)$$

to within 10–15%. Universal scaling (2.1) in this case then predicts for the vector meson mass at $\rho = \rho_0$

$$m_V^* / m_V \simeq [(\langle \bar{q}q \rangle^* / \langle \bar{q}q \rangle)]^{1/3} = 0.86. \quad (7.6)$$

This result of course is subject to corrections that violate scaling. In this case these corrections come mainly from the gluon condensate contribution and leading- and higher-twist corrections, the latter being essentially nonlocal corrections to the quark condensate. For the gluon condensate Hatsuda and Lee [29] find

$$\langle (\alpha_s / \pi) G^2 \rangle^* = \langle (\alpha_s / \pi) G^2 \rangle_0 - \frac{8}{9} m_N^{(0)} \rho \quad (7.7)$$

from the trace anomaly in the chiral limit, where $m_N^{(0)}$ is the nucleon mass at zero density. The gluon condensate is thus much less affected, dropping by about 8% at nuclear matter density.

Higher-twist corrections are potentially a much more important source of scaling violations. In the common lore [29, 126, 127], these corrections, which typically appear from the Taylor expansion of the bilinear $\langle \bar{q}(x)q(0) \rangle$ in powers of x , are obtained either using measured quark distribution functions or estimated using suitable models, and then used on the left-hand side (the ‘‘QCD side’’) of the sum rule. The terms arising from the twist expansion essentially depict processes

where an increasing number of valence quarks are interacting with the source, leaving a hole in the surrounding matter. Summed to all orders, terms of this nature build up the excitation of particle-hole pairs in nuclear matter, each particle or hole consisting of three quarks or antiquarks. On the hadronic side of the (transverse) sum rule, the absorption due to such processes is described by the giant-dipole resonance (GDR) in nuclei, and as a consequence this should be included in the spectrum at finite density [128]. It is conceivable that the contributions on the left- and right-hand side of the sum rule are of similar magnitude, in which case higher-twist corrections would *not* play an appreciable role in hadron masses, as the effects on the l.h.s. and the r.h.s would counterbalance.

The calculation of Hatsuda and Lee [29], which does not take into account absorption from the GDR, reveals that the leading-twist correction comes in at about half the strength of the gluon condensate. This accelerates the scaling [as opposed to (7.6)] and they find

$$m_V^*/m_V \simeq 0.82. \quad (7.8)$$

This was obtained assuming factorization for the four-quark condensate at finite density, which may be an ad hoc assumption. Indeed, this assumption is questioned in ref. [127]. There is to date no reliable model calculation to check this; however, a simple estimate may be obtained from the Skyrmion-crystal model [129]. In this case, $\langle \bar{q}q \rangle$ is proportional to the expectation value of the sigma field. Assuming [in rough agreement with (7.5)]

$$\langle \bar{q}q \rangle^*/\langle \bar{q}q \rangle = \langle \sigma \rangle^*/\langle \sigma \rangle \simeq \frac{2}{3}, \quad (7.9)$$

the Skyrmion crystal model gives

$$\langle \sigma^2 \rangle^* = \frac{27}{20} \langle \sigma \rangle^{*2}, \quad (7.10)$$

which suggests only a modest violation of factorization. In fact, the violation appearing in the vector-meson mass, which goes as the sixth root of $\langle \sigma^2 \rangle^*$, is only about 5% as compared to $[\langle \sigma \rangle^*/\langle \sigma \rangle]^{1/3}$ as implied by Brown-Rho scaling.

The shift in the nucleon mass (see below) cannot be derived from universal scaling in the above naive manner, as the vector condensate is essential in this case. Appearance of the vector condensate naturally breaks universal scaling. The density of nucleons is trivially (and to lowest order) related to the quark number density as

$$\rho_N = \frac{3}{2} \langle N | q^\dagger q | N \rangle. \quad (7.11)$$

7.2. Nucleon mass and nuclear matter equation of state

The previous considerations set the stage for an investigation of the nuclear matter equation of state and the binding problem in the context of QCD sum rules, as first considered by Drukarev and Levin [126] and Drukarev and Ryskin [130]. This approach was recently taken up by Cohen et al. [131].

In extending the analysis of the nucleon mass in the QCD sum-rule approach to finite density we have to first observe that the matter provides for a preferred frame, and we can define the four-velocity of the nuclear medium

$$u_\mu = (1, 0) \quad (7.12)$$

in the rest-frame. The correlator of nucleon currents can then be written in terms of three invariant structure functions,

$$\Pi(q) = \not{q} \Pi_1(q^2, q \cdot u) + \Pi_2(q^2, q \cdot u) + \not{u} \Pi_u(q^2, q \cdot u). \quad (7.13)$$

The coordinate space propagator in the presence of condensates is

$$\begin{aligned} \langle 0|T\{q_i^a(x)\bar{q}_j^b(0)\}|0\rangle &= \frac{i}{2\pi^2}\delta^{ab}\frac{x^\mu}{x^4}(\gamma_\mu)_{ij} - \frac{1}{4N_c}\delta^{ab}(\gamma_\mu)_{ij}\langle 0|\bar{q}\gamma^\mu q|0\rangle^* \\ &\quad - \frac{1}{4N_c}\delta^{ab}\delta_{ij}\langle 0|\bar{q}q|0\rangle^* + \dots, \end{aligned} \quad (7.14)$$

keeping only the most singular terms. In matter, the second term involves the vector condensate

$$\langle 0|\bar{q}\gamma^\mu q|0\rangle^* \simeq \langle N|q^\dagger q|N\rangle = \frac{3}{2}\rho. \quad (7.15)$$

In this section, we neglect isospin breaking, i.e., we assume

$$\langle 0|\bar{u}u|0\rangle^* = \langle 0|\bar{d}d|0\rangle^* = \langle 0|\bar{q}q|0\rangle^* \quad (7.16)$$

and similarly for the vector condensates. Isospin breaking in finite-density QCD sum rules has been considered in refs. [132, 24], and more recently by Drukarev and Ryskin [133]

In the spirit of Landau Fermi liquid theory, we choose for the phenomenological (right-hand) side of the sum rule a quasi-particle pole structure:

$$\Pi(q) \simeq \lambda_N^{*2} \frac{1}{(q^\mu - \Sigma_V^\mu)\gamma_\mu - (m_N + \Sigma_S)}, \quad (7.17)$$

where λ_N^* is the coupling strength of the source $\eta_N(x)$ to the nucleon quasi-particle *in medium* [compare eq. (6.32)], and Σ_V^μ and Σ_S are the vector and scalar self-energies. We shall in the following suppress the Lorentz index on the vector self-energy as we deal only with the time-like component of the vector potential here (having gone to the nuclear-matter rest-frame). The phenomenological representation of the invariant structure functions is then

$$\Pi_1(q^2, q_0) = -\lambda_N^{*2} \frac{1}{q^2 - 2q_0\Sigma_V + \Sigma_V^2 - m_N^{*2}}, \quad (7.18)$$

$$\Pi_2(q^2, q_0) = -\lambda_N^{*2} \frac{m_N^*}{q^2 - 2q_0\Sigma_V + \Sigma_V^2 - m_N^{*2}}, \quad (7.19)$$

$$\Pi_u(q^2, q_0) = \lambda_N^{*2} \frac{\Sigma_V}{q^2 - 2q_0\Sigma_V + \Sigma_V^2 - m_N^{*2}}, \quad (7.20)$$

where

$$m_N^* = m_N + \Sigma_S. \quad (7.21)$$

In the finite-density case, the invariant functions depend both on q^2 and on $q \cdot u = q_0$. The Borel transformation is carried out with respect to $Q^2 = -q^2$, at constant q_0 . Equating the Borel transforms of the theoretical and phenomenological descriptions yields the relations

$$\lambda_N^{*2} e^{-\mu^2/M^2} = \frac{1}{32\pi^4} M^6 - \frac{1}{3\pi^2} q_0 M^2 \langle q^\dagger q \rangle^*, \quad (7.22)$$

$$\lambda_N^{*2} m_N^* e^{-\mu^2/M^2} = -\frac{1}{4\pi^2} M^4 \langle \bar{q}q \rangle^*, \quad (7.23)$$

$$\lambda_N^{*2} \Sigma_V e^{-\mu^2/M^2} = \frac{2}{3\pi^2} M^4 \langle q^\dagger q \rangle^*, \quad (7.24)$$

where $\mu^2 = m_N^{*2} - \Sigma_V^2 + 2q_0\Sigma_V$. The term involving q_0 on the right-hand side of eq. (7.22) is of the same order as the higher-twist corrections in deep inelastic scattering, and we neglect it in the following considerations^{*)}. In detailed calculations [127], other terms involving corrections for the nonlocality of the gluon condensate at finite density, which are of comparable size, enter. Neglecting those, the scalar and vector fields decouple, as can be seen by dividing (7.23) and (7.24) by (7.22), to yield

$$m_N^* = -8\pi^2 \langle \bar{q}q \rangle^* / M^2, \quad (7.25)$$

$$\Sigma_V^* = 64\pi^2 \langle q^\dagger q \rangle^* / 3M^2 \simeq (32\pi^2 / M^2) \rho. \quad (7.26)$$

The first of these equations is the well-known Ioffe formula (for $M = m_N$), while the second one determines the vector self-energy. Note that with (7.21) we have to this order

$$\Sigma_S = \frac{8\pi^2}{M^2} (\langle \bar{q}q \rangle_0 - \langle \bar{q}q \rangle^*) \simeq -\frac{8\pi^2}{M^2} \frac{\Sigma_{\pi N}}{(m_u + m_d)} \rho, \quad (7.27)$$

where we used (7.3). Together with our estimate (7.2) we come to the remarkable conclusion that, to this order,

$$\Sigma_V \simeq |\Sigma_S|. \quad (7.28)$$

Taking $\Sigma_{\pi N} / (m_u + m_d) = 4$ and the Borel mass $M \simeq m_N$ in eqs. (7.26) and (7.27) we arrive at the common value for Σ_V and $|\Sigma_S|$ at nuclear matter density

$$\Sigma_V = |\Sigma_S| \simeq 490 \text{ MeV}. \quad (7.29)$$

Large scalar and vector mean fields are the main feature of Walecka mean field theories [134], although in that context they are somewhat smaller than those of (7.29), i.e.,

$$\Sigma_S \simeq -350 \text{ MeV}, \quad \Sigma_V \simeq 275 \text{ MeV}, \quad (7.30)$$

at nuclear matter density. Of course, we must have Σ_V smaller than $|\Sigma_S|$ to bind nuclear matter (see next section).

Even though Walecka theory is only a more or less ad hoc effective theory, Brockmann and Toki [135], e.g., have shown that for $\rho = \rho_0$ the mean fields emerging from a relativistic Brueckner–Hartree–Fock calculation, starting from the Bonn potential for the nucleon–nucleon interaction match those of Walecka theory closely. We would therefore like to understand the discrepancy in the mean fields emerging from Walecka theory and from the sum-rule arguments.

In the Walecka theory, the mean fields are given by

$$\Sigma_S = -(g_S^2 / m_S^2) \rho_S, \quad \Sigma_V = (g_V^2 / m_V^2) \rho. \quad (7.31)$$

Most of the difference between the fields (7.29) and (7.30) can be understood by letting $m_S \rightarrow m_S^*$ and $m_V \rightarrow m_V^*$ in the Walecka theory. If we take for example following eq. (5.16)

$$m_N^* / m_N = m_S^* / m_S = m_V^* / m_V = 0.8 (\rho = \rho_0), \quad (7.32)$$

then substituting the bare masses with in-medium ones increases the Walecka mean fields by $\geq 50\%$. It is in fact clear from our earlier arguments (based on ref. [126]) that the large mean fields emerge

^{*)} For $q_0 \sim M$, it gives only $\sim 1/6$ of the first term on the right-hand side in (7.22).

directly from QCD, yet it may appear problematical to have a scalar mean field of $\sim 50\%$ of m_N . However, the work of Brown, Mütter and Prakash [83] has shown that the effective mass m_N^* is *not* simply related to m_N by $m_N^* = m_N + \Sigma_S$ as it is in the Walecka model, which in its usual formulation only deals with valence particles. This is discussed more thoroughly in Brown and Machleidt [136].

7.3. Saturation of nuclear matter

To linear order in the density, the calculation of Drukarev and Levin [126] yields scalar and vector potentials of roughly equal order of magnitude, and to this order saturation cannot be achieved. To higher order in the density ρ , saturation (i.e. nuclear binding) is then achieved by incorporating $\rho^{4/3}$ effects. Indeed, the authors calculate the contribution of fig. 7.1, the one-pion exchange process between the source nucleon, and a nucleon from the surrounding matter. In effect, this process produces a deficit of pions in nuclei, simply because there is a Pauli blocking of part of the lowest order self-energy in nuclei as opposed to free nucleons (see fig. 7.1b). The contribution from the above process can be written in such a way that one obtains the pion-number *deficit* multiplied by the $\langle \bar{q}q \rangle$ content of the pion $\langle \pi | \bar{q}q | \pi \rangle$. This latter number turns out to be rather large,

$$\langle \pi | \bar{q}q | \pi \rangle \simeq 12, \quad (7.33)$$

as can be obtained in a model-independent way, using chiral symmetry alone [126, 137]. Thus, this “pionic Sigma-term” Σ_π is considerably larger than the nucleonic one, where we found $\langle N | \bar{q}q | N \rangle \simeq 4$. In effect, this contribution cuts down the $\bar{q}q$ content of nuclear matter, which decreases the scalar mean field, and saturation is achieved.

The problem with this mechanism is that independent calculations [138, 139] give a pion excess in nuclei, rather than a decrease, which would increase the $\bar{q}q$ content of nuclear matter, and, as this leads to an increase in the scalar mean field, saturation would be lost. Moreover, higher order diagrams (such as, e.g., the two-pion exchange graph) are likely to contribute at the same order. Thus, to date finite-density QCD sum-rule calculations do *not* lead to saturation, simply because a consistent calculation of higher order effects is as yet unfeasible.

We note that this situation is somewhat analogous to the Brown, Mütter and Prakash calculation [83]. As already mentioned earlier, in this approach saturation was enforced in an ad hoc manner by introducing a two-loop term in the effective theory, which proves to be unsatisfactory from a fundamental point of view.

In effect, the QCD sum-rule calculations [126] work at tree level only, in that the high- Q^2 limit suppresses soft-pion processes which are important at larger distances. In this sense, there cannot be an Adler–Weisberger relation to this order in QCD sum-rule calculations, i.e., $g_A = 1$. Thus, vector and axial couplings are identical to this order. Loop corrections to g_A , however, do introduce $g_A \neq 1$. As is shown by Brown and Machleidt [136], this suffices to achieve saturation, and moreover, finite density effects that change nucleon and vector meson masses are counterbalanced by a change in $g_A(\rho)$ up to $\rho = \rho_0$, as we point out below.

There are many experimental indications that g_A decreases from its vacuum value $g_A = 1.26$ with increasing density, mainly from observations of missing Gamow–Teller strength (see, e.g., ref. [140]). Theoretical calculations by Rho [106] and by Ohta and Wakamatsu [107] suggest that g_A drops to unity at nuclear matter density, in the manner of eq. (5.19). In fact, this decrease has been confirmed recently by Drukarev and Levin [109]. In particular, it is shown in these calculations that changes in the quark condensate at the mean field level have little influence on the

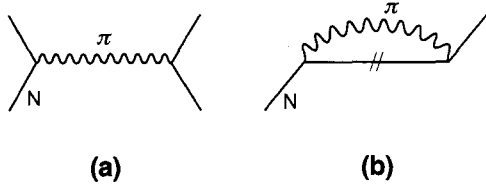


Fig. 7.1. (a) One-pion exchange interaction in nuclear matter, which is equivalent to (b) the Pauli blocking of processes where both nucleons lie below the Fermi surface.

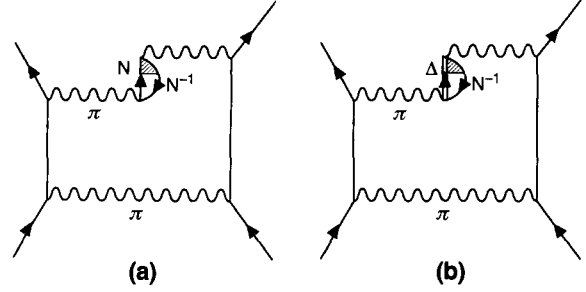


Fig. 7.2. (a) Two-pion exchange loop. (b) Correlated pion pair, through virtual- ρ exchange in the t -channel.

dependence of g_A on ρ , as most of the dependence can be traced to isobar-hole diagrams, namely those considered in refs. [106, 107].

From the mean-field relation (3.21) noted in ref. [21] and from the comparison of eq. (3.21) with (3.29) setting $M = m_\sigma$ in the latter, one finds [24]

$$g_{\sigma NN}^2/4\pi = 3\pi, \quad (7.34)$$

essentially the tree-level coupling of $g_{\sigma NN}$. This coupling must then be multiplied by the loop correction to obtain the full coupling,

$$g_{\sigma NN}^2/4\pi = (g_{\sigma NN}^2/4\pi)_{\text{tree}} g_A^2 \simeq 14.7 \quad (7.35)$$

for zero density ($g_A = 1.26$). Of course, $g_{\pi NN}$ is treated in the same way, because of chiral invariance.

Such loop corrections have not previously been included in nuclear matter calculations. If g_A were to drop with density according to eq. (5.19), it would cut down the scalar attraction by $\sim 1/3$, leaving the vector repulsion that results from the gauge coupling g_V and which is not affected by strong-interaction renormalizations. Clearly then, eqs. (5.19) and (5.20) cannot be used as such in this context, rather, we expect that a momentum-averaged g_A has to be used instead [136]. Very detailed calculations have been carried out by Mull et al. [141], which qualitatively confirm the approach taken in ref. [136].

Consider the two-pion exchange loop, fig. 7.2. The Rho-Ohta-Wakamatsu mechanism amounts to introducing isobar-hole modifications into the pion propagator, and we generalize this so as to include, also, nucleon-particle-nucleon-hole insertions. The process in fig. 7.2a, with or without the inclusion of the rescattering, fig. 7.2b, then gets a factor $\langle g_A(\rho, k) \rangle^2$, where the average is taken over the loop momentum k . The k -dependence of g_A brings in large cancellations, so that the $\langle g_A(\rho, k) \rangle$ decreases only slightly by nuclear matter density. The decrease is parameterized by Brown and Machleidt to be

$$(g_A)_{\text{eff}} = \langle g_A(\rho, k) \rangle = 1/[1 + b_{\text{eff}}(\rho/\rho_0)], \quad (7.36)$$

where $b_{\text{eff}} \simeq 0.03-0.05$ and the brackets indicate an averaging over the momentum k . This form for $(g_A)_{\text{eff}}$ is the same as that of eq. (5.19), but b_{eff} here gives a density dependence which is an order of magnitude weaker. Nonetheless, because of the near cancellation between scalar and vector mean fields, this is sufficient to achieve saturation.

The schematic arguments given here can be made quantitative with the approach of Mull et al. and Durso et al. [141]. Specifically they have shown that particle–hole insertions in the pion lines produce a substantial density-dependent repulsion. As a consequence, the nucleon effective mass does not have to drop until the attractive scalar mean field decouples sufficiently to give saturation. The loop correction works together with the decoupling of the scalar mean field in order to produce saturation at a higher m_N^* .

Let us summarize the results of this section. Drukarev and Levin [126] obtained very large values for Σ_V and $|\Sigma_S|$ straightforwardly to lowest order in the QCD sum-rule formalism. Large, but not quite so large, potentials are also obtained in Walecka theory, which can in fact be reproduced from a rather detailed calculation [135] beginning from the nucleon–nucleon potential. In the latter calculation, scalar interactions are substantially reduced due to short range correlations resulting from vector-meson exchange, but built up again by exchange terms from pion exchange, etc. Introduction of density-dependent meson masses into the Brockmann–Toki calculation brings the scalar and vector mean fields closer to those obtained in the QCD sum-rule formalism. Saturation is facilitated by density-dependent corrections to the pion propagator, which can be expressed in terms of a density- and momentum-dependent $g_A(\rho, k)$.

8. The hadron to quark/gluon transition

In this section we turn to aspects of the QCD phase transition proper. Recent evidence, numerical and theoretical, strongly suggests that the transition for two-flavor QCD is of second order, while it would be of first order for three or more massless flavors. Indeed, the strange quark mass seems to interpolate between the two possibilities, and it appears that it is sufficiently heavy that the transition is of second order. Wilczek has presented an analysis of this situation [142], and suggests modeling the critical behavior of QCD with a theory belonging to the same universality class. The order parameter in question being the chiral condensate, he suggests to consider the Landau–Ginzburg free energy

$$\mathcal{F} = \text{Tr}(\partial_i M^\dagger \partial_i M) + \mu^2 \text{Tr} M^\dagger M + \lambda_1 \text{Tr}(M^\dagger M)^2 + \lambda_2 (\text{Tr} M^\dagger M)^2, \quad (8.1)$$

where μ^2 is the temperature-dependent renormalized mass-squared, while λ_1 and λ_2 parameterize the strength of the quartic couplings. For two flavors, M may be taken to be

$$M = \sigma + i\boldsymbol{\tau} \cdot \boldsymbol{\pi}, \quad (8.2)$$

which brings us back to the linear sigma model of Gell-Mann and Levy, the nonlinear version of which we studied extensively in section 2. Interestingly, the linear model is equivalent to the standard $O(4)$ invariant $n = 4$ Heisenberg magnet, whose critical behavior has been studied extensively [143]. For three flavors, however, the situation is more complicated, and it appears that then the transition is first order. Seeing that the critical behavior of the Landau–Ginzburg free energy shares many features with the QCD case, it seems to be more than just a convenient playground. Specifically, the model predicts that in the two-flavor case the second-order behavior changes into a smooth cross-over for finite, but small, quark masses, just what is observed in recent two-flavor simulations [6, 144]. The advantage of this approach is that this model can be studied by standard renormalization group techniques, and the effects of temperature and density, as well as that of massive flavors are reflected in a renormalization of the coupling constants and mass parameters. This was indeed the main conclusion of the analysis presented in section 2, outside of

the renormalization group approach. In this section we would like to take the scaling of hadron masses for granted, and explore phenomenologically its consequences for the hadron to quark/gluon transition. It is intuitively obvious that dropping hadron masses near T_c will affect significantly the nature of the transition between the hadronic and the quark/gluon phase, as the effective number of degrees of freedom on the hadronic side is strongly mass dependent. The scenario presented here takes dropping hadron masses into account explicitly [145, 146].

We first develop a scenario which involves modifying the Hagedorn [147, 148] scenario of a maximum hadron temperature in order to take into account effects of scaling hadron masses, eq. (2.1). This lowers the maximum hadron temperature still more from the Hagedorn temperature T_H . The minimum temperature for stability of the quark/gluon plasma must be high enough so that the pressure is greater than zero, $P_{QG} > 0$; otherwise there would be a dynamical instability and the quark/gluon plasma would collapse. Naively, this turns out to be greater than the hadron temperature, i.e.,

$$(T_{QG})_{\min} > (T_H)_{\max} . \quad (8.3)$$

If this were so, there would be a phase gap between the maximum hadron temperature and the minimum quark/gluon one.

We shall first develop this scenario, although many people have pointed out that the Hagedorn scenario must be modified, and we shall discuss ways in which to modify it. Nonetheless, the scenario leading to (8.3) is instructive in telling us that the chiral symmetry restoration transition is not that of deconfinement. The following section may thus be considered academic in the sense that it explores consequences of premises that are most likely not realized. Yet, it seems to us instructive, and amusing.

8.1. *The Hagedorn scenario*

It is by now well established that increasing the temperature in the hadronic phase will ultimately restore the chiral symmetry that is spontaneously broken via a condensate of quarks. We have no doubt that such a chiral symmetry restoring transition takes place. Indeed, lattice gauge calculations are consistent with the realization of chiral symmetry above $T_{\chi SR}$ by massless hadrons, as we shall discuss later on.

Well below the chiral symmetry restoring temperature, $T_{\chi SR}$, the hadronic phase is sufficiently well described by taking into account the lowest mass degrees of freedom, namely the scalar, pseudoscalar and vector mesons, as well as the lowest mass baryons. Once the temperature becomes comparable to the pion mass, however, higher lying states can be populated, and a simple description using only a finite number of degrees of freedom seems to be inadequate. It has been suggested [147, 148] that the hadronic phase in this regime is better described by an exponentially rising density of states, the so called Hagedorn model. The celebrated consequence of this model is of course the occurrence of a maximal temperature T_0 for the hadronic phase, which comes about because from some temperature $T < T_0$ on it becomes thermodynamically more favorable to populate higher mass states instead of increasing the kinetic energy of the lower lying ones. Thus, T_0 can never be reached. While this conclusion may have seemed startling at the time of its inception, it is not really surprising, as we do not expect a hadronic phase at high temperatures anyhow, being aware of the quark/gluon substructure of hadrons. Rather, we expect the Hagedorn model to break down close to T_0 , when the energy density of the phase is so high that the quark/gluon substructure becomes apparent. Nevertheless we believe the Hagedorn density of states to be a reliable description of the

hadronic phase below T_0 , which we shall take to be $T_{\chi\text{SR}}$ without loss of generality^{*)}.

The Hagedorn density of states is usually parameterized as

$$\rho(m) = cm^{-a}e^{m/T_{\chi\text{SR}}}, \quad (8.4)$$

where the parameters c and a can be adjusted to fit the experimentally known resonances. Good fits can be obtained with $a \leq 3$ and $c = 0.01\text{--}0.03$ (see, for example, refs. [12, 13]). Our conclusions do not depend on the precise value of these constants, as they do not influence the size of the phase gap.

The main thrust of this report has been the exploration of the consequences of the scaling assumption (2.1), which has been established approximately from various points of view. It will be implemented here in the following way. The energy density of the ‘‘Hagedorn phase’’ can be written as

$$\epsilon_H(T) = \int_M^\infty dm \rho(m) \epsilon_H(m), \quad (8.5)$$

where M is a low mass cutoff and $\epsilon_H(m)$ is the energy density of hadrons of mass m . It is in the latter quantity that the temperature dependent masses appear, as

$$\epsilon_H(m) \sim \int \frac{d^3k}{(2\pi)^3} \varepsilon(k) n_F(\varepsilon), \quad (8.6)$$

with $n_F(\varepsilon)$ the Fermi distribution function, and

$$\varepsilon(k) = \sqrt{k^2 + m^{*2}}. \quad (8.7)$$

In a nonrelativistic Boltzmann approximation the energy density of hadrons of mass $m^* \gg T$ is then

$$\epsilon_H(m) = (m^*T/2\pi)^{3/2} m^* e^{-m^*/T}, \quad (8.8)$$

such that the total energy density is, using (8.8) and (8.4) in (8.5) ^{**)} ,

$$\epsilon_H(T) \simeq c \left(\frac{T}{2\pi} \right)^{3/2} \Phi^{a-1}(T) \int_M^\infty dm^* (m^*)^{5/2-a} e^{m^*/T_{\chi\text{SR}} - m^*/T}, \quad (8.9)$$

with the definition

$$T_{\chi\text{SR}}^* = \Phi(T) T_{\chi\text{SR}} = (1 - T^2/T_{\chi\text{SR}}^2)^{1/3} T_{\chi\text{SR}}. \quad (8.10)$$

Above we have taken a parametrization of the $\Phi(T)$ suggested by results presented in section 2. This parametrization fits approximately the calculation of Gerber and Leutwyler [149]. The latter was carried out in chiral perturbation theory and as such cannot include effects due to higher mass

^{*)} In general a transition temperature is associated with a certain scale. We have argued in section 3 that there are in fact two such scales. However, only one, the scale set by the quark condensate, is soft, such that there can be only one critical temperature in that regime.

^{**)} It is crucial here that the Hagedorn density of states is temperature *independent*.

hadrons, like the ρ and A_1 . From (8.9) it is apparent that $\epsilon_H(T)$ can be made arbitrarily large if $a < 3.5$, as seems to be the case from fits to the observed spectrum. This happens at a temperature

$$(T_H)_{\max} = T_{\chi\text{SR}}^* \quad (8.11)$$

or

$$(T_H)_{\max}/T_{\chi\text{SR}} = \left(1 - (T_H)_{\max}^2/T_{\chi\text{SR}}^2\right)^{1/3} \simeq 0.755. \quad (8.12)$$

If we take for $T_{\chi\text{SR}}$ the value suggested by Gerber and Leutwyler, $T_{\chi\text{SR}} = 170$ MeV, we obtain as a maximum temperature for the hadronic phase $(T_H)_{\max} \simeq 128$ MeV. We would like to stress that this is a genuine effect of the scaling relation (2.1). Let us further note that at $T = (T_H)_{\max}$ the hadron masses have dropped only by about 25%. This drop does not depend sensitively on the specific form of $\Phi(T)$, as most parameterizations of $\Phi(T)$ differ significantly only close to $T_{\chi\text{SR}}$. Let us now investigate the high temperature side of the system.

For a phase of unconfined quarks and gluons, a calculation of the thermodynamic potential to lowest order in the quark–gluon coupling constant reveals an energy density given by

$$\epsilon_{\text{QG}} = \left(16 + \frac{21}{2}N_f\right)\frac{\pi^2}{30}T^4 + B, \quad (8.13)$$

where B is the bag constant, or vacuum energy difference, and N_f is the number of light quark flavors. As we pointed out in section 3, B is associated with the gluon condensate, and represents an attractive potential in the sense that the condensation of gluons shifts the vacuum energy upwards by B . From the QCD trace anomaly we determined the value of B (eq. 3.9) for two flavors to be

$$B^{1/4} = 245 \text{ MeV}. \quad (8.14)$$

Let us stress again that the bag constant is a vacuum energy *difference*. In the perturbative regime with unconfined gluons and quarks the vacuum has energy $\epsilon = B$ at zero temperature.

Consider then the phase with unconfined quarks and gluons, with an energy density given by (8.13) and a pressure

$$P_{\text{QG}} = \left(16 + \frac{21}{2}N_f\right)\frac{\pi^2}{90}T^4 - B. \quad (8.15)$$

In order for this phase to be stable, the pressure in this phase must be positive,

$$P_{\text{QG}} \geq 0. \quad (8.16)$$

This puts a constraint on the temperature of the quark/gluon phase, as with N_f flavors we find

$$(T_{\text{QG}})_{\min} \simeq 218 \left(\frac{33 - 2N_f}{32 + 21N_f}\right)^{1/4} \text{ MeV}. \quad (8.17)$$

This minimum temperature turns out to be appreciably higher than the maximum hadron temperature $(T_H)_{\max}$: for two flavors we find from eq. (8.17)

$$(T_{\text{QG}})_{\min} \simeq 172 \text{ MeV}; \quad (8.18)$$

hence the phase gap. In obtaining the latter we have neglected the effect of degrees of freedom that are common to both phases ($\gamma, \nu, e^\pm, \dots$), as they are also not present in the lattice simulations. These will be important for the physics of the early universe, however. Perturbative corrections of order g^2 [150] on the other hand, where g is the quark–gluon coupling constant, lower the pressure in the quark/gluon phase by $\sim 28\%$, which would raise $(T_{\text{QG}})_{\text{min}}$ to 186 MeV.

We are thus led to the conclusion that with these assumptions, hadronic and quark/gluon phases *could never coexist at the same temperature*, as the phases would be separated by a gap of 30–40 MeV. This implies that no transition could take place from the hadronic to the quark/gluon phase via equilibrium processes. If the hadronic phase is heated adiabatically, the high lying states are populated and the “Hagedorn wall” builds up. Of course, this is not what happens in a heavy-ion collision, where the time scales are much too small to build up the massive resonances. Before we turn to this scenario, however, we would like to explore a little further the equilibrium situation.

While the Hagedorn description of the hadronic phase seems to be reliable up to temperatures close to $(T_H)_{\text{max}}$, it is clear that this description will break down as soon as enough energy is pumped into the system to reveal the quark/gluon substructure of the hadronic states. While we do not know precisely at what temperature the description breaks down, it is possible to construct a “phase jump”, which presumably occurs through nonequilibrium processes via tunneling, from the hadronic phase to a new phase at a higher temperature. The requirements for the occurrence of the jump are rather severe: since the temperature in the two phases cannot be the same, we require pressure and energy density to be equal, though at different temperatures. Thus:

$$\epsilon_H(T_H) = \epsilon_{\text{QG}}(T_{\text{QG}}), \quad P_H(T_H) = P_{\text{QG}}(T_{\text{QG}}). \quad (8.19)$$

This implies that the “net ram pressure” in both phases must be equal,

$$\epsilon - 3P = 4B. \quad (8.20)$$

In the hadronic phase the pressure is negligible; the scenario then seems to be such that if the energy density in the hadronic phase approaches $4B$, the system may “break out” of the Hagedorn equation of state and jump to a quark/gluon phase without changing energy density or pressure, and thus without latent heat. In fact, a detailed calculation shows that this energy density is achieved just slightly below $(T_H)_{\text{max}}$, and the system would end up in the quark/gluon phase with a temperature *just above* $(T_{\text{QG}})_{\text{min}}$. This phase, however, is not stable. As discussed in refs. [145, 146], modifications in the Hagedorn picture, for example due to the excluded volumes of the particles, make this phase jump only a curiosity.

8.2. Lattice gauge simulations

There is by now an extensive amount of data from lattice gauge calculations in the pure glue sector with no dynamical quarks, which shows a clear signal for a first order phase transition at T_{gauge} . This temperature is easily calculated setting $N_f = 0$ in the previous formulae. We thus get

$$16 \frac{\pi^2}{90} T_{\text{gauge}}^4 - B = 0. \quad (8.21)$$

Note that B is evaluated for $N_f = 0$ in this case. We then find

$$T_{\text{gauge}} = 220 \text{ MeV}. \quad (8.22)$$

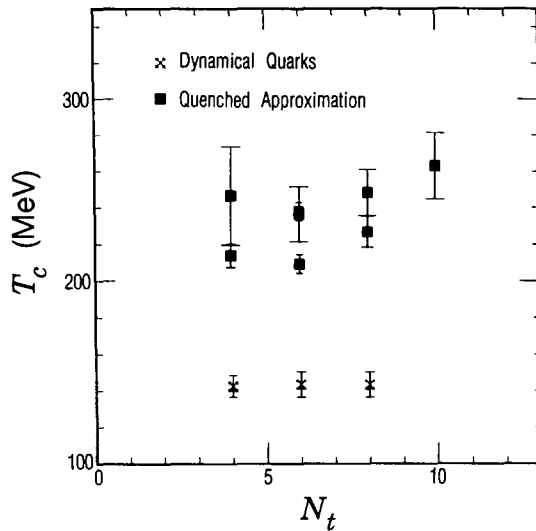


Fig. 8.1. T_c in MeV as function of the N_t , the number of time slices. The fancy crosses are for two flavors of dynamical quarks (from ref. [144]).

This is just the central value from lattice gauge calculations as summarized by Bernard et al. [144] (see fig. 8.1), although the error bars shown are large. The critical temperature of Gerber and Leutwyler [149], $T_{\chi SR} = 170$ MeV, is a bit above the central value for the two-flavor chiral restoration temperature found in lattice gauge calculations, but again the error bars are large. Note, however, that the effects of hadron mass scaling, which are not included in the latter authors' calculation, would bring their temperature even below 140 MeV, if estimated as in eq. (8.11) and following. Recent calculations [10] find $T_{\chi SR} \simeq 140$ MeV. In any case, our values for $T_{\chi SR}$ and T_{gauge} are in reasonable agreement with those obtained in the lattice calculations.

Another set of data obtained from lattice gauge calculations is that of screening masses [8, 7]. In these calculations the prominent feature is the parity doubling, which presumably should be associated with chiral symmetry restoration. In particular, it is apparent that the $N(\frac{1}{2}-)$ at 1535 MeV becomes degenerate with the nucleon at just the same temperature at which the A_1 joins the ρ in the vector meson spectrum. Similarly, the σ -meson is brought together with the pion with extrapolation to zero quark mass, even though the annihilation process which couples the glueball to the two-pion correlated state (the σ) is omitted in the calculation.

In the simulation by De Tar and Kogut [8] four flavors of staggered fermions are used to extract screening masses on a 6×10^3 lattice. It is well known that the four-flavor world investigated there shows a much stronger signal than the two-flavor one, and that the transition temperature is much less in the four-flavor case. There is a simple way of understanding why $T_{\chi SR}(N_f = 4) < T_{\chi SR}(N_f = 2)$, which invokes the parametrization of the quark condensate by Gerber and Leutwyler [149], which results from chiral perturbation theory taking into account only pions at finite temperature. Then

$$\frac{\langle 0|\bar{q}q|0\rangle^*}{\langle 0|\bar{q}q|0\rangle} = 1 - \frac{N_f^2 - 1}{N_f} \frac{T^2}{12f_\pi^2}. \quad (8.23)$$

The way in which N_f enters is easily understood here. The N_f in the denominator arises because the total condensate is trivially proportional to the number of flavors. The $N_f^2 - 1$ in the numerator

Table 8.1

Summary of screening masses in the chiral limit with constraints. The masses are given in units of temperature. (From De Tar and Kogut [8])

β	π	σ_v	ρ_0	ρ_1	A_{10}	A_{11}	$N(\frac{1}{2}+)$	$N(\frac{1}{2}-)$
5.10	0	6.2(4)	7.4(6)	7.4(6)	9.4(5)	9.4(5)	12.9(2)	14.4(4)
5.175	2.67(2)	2.67(2)	6.9(3)	6.9(3)	6.9(3)	6.9(3)	11.2(2)	11.2(2)
5.25	4.04(4)	4.04(4)	7.3(1)	6.3(2)	7.1(1)	6.3(2)	9.3(2)	9.3(2)

comes in because the condensate is “melted” by producing pions (production of a pion involves moving a quark from the negative energy sea up to positive energies). In our scenario, heavy mesons also enter in. The most important of these are the ρ and A_1 mesons, of which there are also $N_f^2 - 1$. Note that, as their masses drop, the ρ and A_1 are more easily excited; the Boltzmann factors are not small anymore. Thus, with two flavors and only pions, (8.23) would give

$$T_{\chi\text{SR}}(N_f = 2) = 2\sqrt{2}f_\pi \simeq 250 \text{ MeV} . \quad (8.24)$$

The ratio of critical temperatures in the four-flavor world to that in the two-flavor world is, in this simple model, predicted to be

$$T_{\chi\text{SR}}(N_f = 4)/T_{\chi\text{SR}}(N_f = 2) = \sqrt{0.4} , \quad (8.25)$$

which is in fact close to the one obtained on the lattice. The normalization of temperatures, however, is off, due to the neglect of the heavier mesons in the chiral perturbation theory calculation. Inclusion of the latter brings $T_{\chi\text{SR}}$ down to about 170 MeV [149], and ultimately to $\lesssim 150$ MeV, as suggested by the above arguments and found in lattice gauge simulations. Then,

$$T_{\chi\text{SR}}(N_f = 4) = \sqrt{0.4} T_{\chi\text{SR}}(N_f = 2) \sim 89 \text{ MeV} , \quad (8.26)$$

where we used our $T_{\chi\text{SR}}(N_f = 2) \sim 140$ MeV. This seems to fit the lattice gauge simulation results quite well.

Let us now discuss results obtained in lattice QCD for the screening masses (see table 8.1). The two columns each for ρ - and A_1 -mesons correspond to their two helicity states. Results for two flavors are not very different [7], and screening masses for the two different helicity states of ρ and of A_1 are now similar. The quantities in table 8.1 are conventionally called screening masses, but we prefer to call them inverse screening lengths. When continued to Euclidean space, they really describe the energy of the lowest state with given quantum numbers. We shall assume, as is often done in lattice gauge calculations, that the screening mass measures the analytically continued, real time, energy.

In order to simulate the effects of temperature in lattice calculations, the time-like extent of the lattice is cut to $\beta = 1/T$ while the space-like extent is left untouched. Thus, with a lattice spacing a , the temperature on a lattice with N_t time slices is just $T = 1/N_t a$. In order to vary the temperature on a lattice of fixed temporal extent, one adjusts the quark–gluon coupling strength g , as it is believed that the lattice spacing a is related to the (inverse) coupling strength $\beta = 6/g^2$ by the asymptotic scaling relation. From $\partial A_L/\partial a = 0$ and the definition of the QCD beta-function one obtains the usual scaling relation (quoted here for two flavors)

$$aA_L = (8\pi^2\beta/29)^{345/841} \exp(-4\pi^2\beta/29) . \quad (8.27)$$

In the above, A_L is the ultraviolet lattice regulator. The asymptotic scaling relationship of course holds true only at weak coupling, i.e. in the continuum limit. It is expected, however, that some

relation exists between the coupling strength and the lattice spacing in the pre-asymptotic scaling regime, though this cannot be obtained by perturbative renormalization group techniques. As most lattice calculations show that the observables do not follow an asymptotic scaling behavior in the region of couplings probed, a certain amount of skepticism with regard to the normalization of lattice results is in order. Let us nevertheless try to understand the results for the screening masses. In these calculations, the quantity “measured” is the coefficient in the exponent of the equal-time Green’s function with appropriate quantum numbers, at finite temperature. Some care has to be taken to extract the physical particle mass from this number, though. For a massless noninteracting quark, the equal-time finite-temperature Euclidean Green’s function reads^{*)}

$$G(\mathbf{x} - \mathbf{y}, t) = T \sum_n \int \frac{d^3p}{(2\pi)^3} \frac{1}{\omega_n^2 + \mathbf{p}^2} e^{i\mathbf{p} \cdot (\mathbf{x} - \mathbf{y})}, \quad (8.28)$$

where the sum goes over the fermionic Matsubara frequencies

$$\omega_n = 2\pi T(n + \frac{1}{2}). \quad (8.29)$$

Integrating over angles and taking the residue in the $d\mathbf{p}$ integration shows that

$$G(t, \mathbf{x} - \mathbf{y}) = \frac{T}{2\pi} \sum_n \frac{e^{-\omega_n |\mathbf{x} - \mathbf{y}|}}{\omega_n |\mathbf{x} - \mathbf{y}|}. \quad (8.30)$$

Consequently, by looking at the large $r = |\mathbf{x} - \mathbf{y}|$ behavior we find the “screening mass” to be just the Matsubara frequency. As we expect to pick up only the lowest frequency in this analysis, the “screening mass” for a massless quark at finite temperature would be $\omega_0 = \pi T$; a system of n_q massless quarks would show a screening exponent $\omega_0 = n_q \pi T$. A look at the results obtained by De Tar and Kogut [8], reproduced in our table 8.1, and by Gottlieb et al. [7] show that this is precisely what lattice calculations show at high temperature. Thus, the ρ_1 and A_{11} screening masses are essentially $2\pi T$, while that of the $N(\frac{1}{2}+)$, $N(\frac{1}{2}-)$ doublet is $3\pi T$ (once T reaches $T_{\chi\text{SR}}$). The fact that these screening masses have reached their asymptotic value at the rather low temperature $T = T_{\chi\text{SR}}$ is important. In the case of the π - and σ -mesons, the screening mass is substantially below 2π . This indicates that interactions are still important at $T = T_{\chi\text{SR}}$, as will be discussed in detail in the next subsection. The degeneracy of the π and σ screening masses leaves no question that chiral symmetry has been restored.

Note also that, had a remnant nonscaling mass—either bare or dynamically generated—persisted above T_c , the screening exponent would have been

$$\omega_{\text{scr}} = \sqrt{\omega_0^2 + m_0^2} \simeq \omega_0 + \frac{1}{2} m_0^2 / \omega_0, \quad (8.31)$$

where m_0 denotes the nonscaling mass. Thus, a remnant mass would lead to deviations from the linear behavior $\omega_0 = n_q \pi T$. These deviations, if present, are not resolved by the present accuracy of lattice simulations.

We conclude then that these lattice results corroborate the idea of dropping vector meson and nucleon masses, and are consistent with vanishing masses close to T_c . With this in mind let us calculate the pressure in the hadronic phase exerted by these nearly massless particles. Taking only the π , ρ and A_1 we obtain

$$P(\pi, \rho, A_1) = 21 \frac{\pi^2}{90} T^4, \quad (8.32)$$

^{*)} For simplicity, we neglect the spin of the quark.

which by itself already equals the pressure from the quarks. From the $N(\frac{1}{2}+)$ and $N(\frac{1}{2}-)$ and their antiparticles we obtain further

$$P \left[N(\frac{1}{2}+) + N(\frac{1}{2}-) \right] = \frac{7}{8} \times 16 \frac{\pi^2}{90} T^4, \quad (8.33)$$

where the $7/8$ arises from the fermionic nature of the particles. This pressure almost matches the one coming from the gluons. However, it seems unreasonable to keep adding up hadron degrees of freedom, which results in the Hagedorn scenario as described in section 8.1. Rather, it seems more physical to limit the degrees of freedom much in the same way as in the Debye theory of solids, as done in ref. [146]. In Debye's theory of the heat capacity, the phonon spectrum is cut off when the number of phonons reaches $3N$, where N is the number of atoms. The argument is that the number of degrees of freedom in the effective excitations (vibrations) should not exceed that of the underlying constituents (atoms). In the same fashion, if we consider the underlying constituents in QCD to be quarks and gluons, then the number of degrees of freedom in the effective excitations, the hadrons, should not exceed that in quarks and gluons. We include the gluons in this computation, because deep inelastic scattering shows half of the momentum inside hadrons to be due to gluons.

The effective number of degrees of freedom for a free gas of quarks and gluons turns out to be 40 (in the case of two flavors). In ref. [146], the limitation on the number of degrees of freedom is implemented by introducing a temperature dependent excluded volume.

In lowest-order approximation, the pressure equation for the phase transition is

$$g_{\text{eff}}(H) \frac{\pi^2}{90} T^4 = 37 \frac{\pi^2}{90} T^4 - B, \quad (8.34)$$

where $g_{\text{eff}}(H)$ denotes the effective number of degrees of freedom in the hadronic phase^{*)},

$$g_{\text{eff}}(H) \leq 40. \quad (8.35)$$

As we have discussed, lattice gauge simulations already indicate that nearly enough hadrons go essentially massless as $T \rightarrow T_{\chi\text{SR}}$ to saturate the limit mentioned above. It is more difficult to ascertain what the effects of the remaining interactions between quarks and antiquarks are on the effective number of degrees of freedom on the quark/gluon side. In section 8.3 we shall construct a scenario which fits results of lattice gauge calculations for $T \geq T_{\chi\text{SR}}$. This scenario indicates that one should continue to count the effective degrees of freedom as (hot) hadrons, as T passes from below through the region of chiral restoration. A condition not unlike that of eq. (8.35) will arise out of the dynamics of the scenario.

We would now like to compare the predictions of our scenario with results of lattice simulations. In fig. 8.2 we show the results of Kogut et al. [6] for the energy density, as a function of $\beta = 6/g^2$ [which can tentatively be converted to temperature using relation (8.27)] of up and down dynamical quarks, as well as that of the energy density of strange quarks.

We interpret these results as follows: At about $\beta \sim 5.30$ the production of hadrons increases, since the hadron mass has dropped appreciably (see section 8.1). By $\beta \sim 5.40$ the rapid increase in up and down quark energy has ended. The energy is still about 30% below black-body. This is just the reduction that would be expected from $\mathcal{O}(g^2)$ corrections [150] with $\alpha_s = 0.29 \pm 0.11$,

^{*)} The factor 37 on the right hand side of eq. (8.34) arises in the usual way by multiplying the 24 quark and antiquark degrees of freedom by a factor $7/8$ to take into account their fermionic nature, and adding the 16 gluonic degrees of freedom.

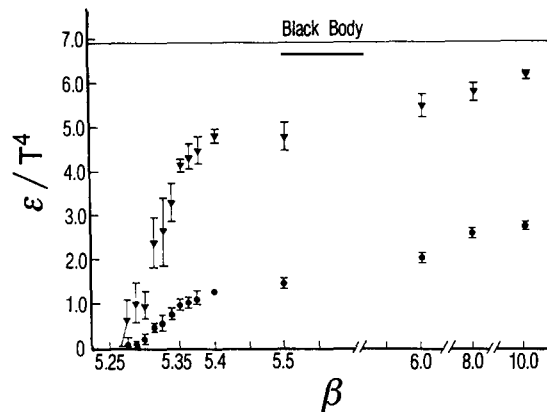


Fig. 8.2. Isodoublet ($\epsilon_{u,d}/T^4$, triangles) and strange (ϵ_s/T^4 , circles) energy densities versus coupling $\beta = 6/g^2$. The data have been corrected for free massless field finite-size effects. (From ref. [6])

as noted earlier, following eq. (8.18). Although we shall argue in section 8.3 that the system is not perturbative in this region, we might expect perturbative estimates to give us the correct order of magnitude for effects from interactions. These corrections should decrease in magnitude with increasing temperature, and the combined quark and gluon energies should go to the sum of the black-body energies. Unfortunately, the accuracy in the present lattice results is insufficient to single out the energy in gluons, and we are unable to divide the energy in hadrons into that in quarks and gluons separately. From the fact that deep inelastic scattering shows that the hadron momentum is about equally distributed between quarks and gluons, we might expect the energy production to be also roughly equally divided. Taking eq. (8.35) literally, this would appear to give nearly the same as the black-body radiation calculated for the 21 equivalent degrees of freedom in quarks and slightly ($\sim 1/4$) more than the black-body radiation calculated for the 16 degrees of freedom in gluons. Thus, if the true degrees of freedom are hadronic at this stage, we expect lattice gauge simulations to overestimate the energy density stored in gluons, by about 21/16.

To sum up, according to the arguments leading up to eq. (8.35) the sum of energies in quarks and gluons should be the same as that calculated from black-body production of hadrons with the limitation (8.35), but it may not be sensible to divide this energy density up into quark and gluon degrees of freedom due to the absence of deconfinement. Another interesting aspect of fig. 8.2 is the smooth rise in the energy density contained in the quarks. An estimate for the temperature difference between $\beta = 5.3$ to 5.4 using asymptotic scaling (8.27) gives $\Delta T \sim 18$ MeV. We believe that this should be accurate to within a factor ~ 2 . It is clear that the rise in energy is not as abrupt as would be expected in a first-order transition. In fact, Kogut et al. conclude that their results “suggest that there is no transition at all, and that there is only a smooth cross-over between hadronic matter and the quark–gluon plasma [...]”. A smooth cross-over would be consistent with a second-order chiral symmetry restoring phase transition.

8.3. Dynamical confinement

Earlier we have mentioned that several lattice QCD results hint at nontrivial effects in the high temperature phase. Indeed, it was proposed some time ago by De Tar [151,152] that the high temperature phase might be “dynamically confined”, in the sense that the long range fluctuations

are color singlet modes, and that the poles and cuts in the linear response functions of the hadronic phase go over smoothly into those of the high temperature one. The suggestions of Hatsuda and Kunihiro [153–155] are similar in nature. These scenarios of dynamical confinement presuppose a QCD phase transition of second order. In this subsection we would like to show how a simple picture of quasi-free quarks interacting at high temperature solely through magnetic current–current interactions (the electric ones being screened) can unify seemingly unrelated lattice results.

One of the most important aspects of the high temperature phase is the loss of relativistic covariance due to the presence of the heat bath. It is this feature that allows a situation where electric interactions are screened while the magnetic ones are untouched. In a relativistically covariant description this statement is of course empty, as one can be traded for the other just by choosing a different inertial system. In the high temperature limit, however, inertial systems are *not* equivalent. Nevertheless, the system is still Lorentz *invariant*, of course. The most important aspect of the lattice results on the other hand is the Euclidean formulation of the problem. Temperature is introduced formally as imaginary time, such that the original Minkowski metric is replaced by a flat three-dimensional one, with no time coordinate but a temperature instead. Consequently, this approach can only reveal static, or time averaged (steady state) properties of the system. In other words, lattice calculations cannot provide information about the time development of observables, or about the spectrum of excitations. On the other hand, one may investigate *equal-time* correlation functions measuring correlations in the spatial direction at finite temperature. This leads to information about the momentum spectrum.

Early evidence showed chiral restoration as realized by parity doubled hadrons above T_c (see table 8.1). While this could be interpreted as supporting the idea of dynamical confinement, the arguments of the last section pointed to a picture where the quarks propagate freely with their masses given by the lowest Matsubara frequencies. However, recent lattice calculations [10, 156, 157] show results for the Bethe–Salpeter wave function for π and ρ mesons at a temperature $T > T_c$ that do not support this. Rather, those results show unambiguously that there are strong correlations present even at these high temperatures. It is those correlations that we would like to understand in the following.

To be specific, let us develop the formalism for the interaction of charges and currents in Euclidean space–time. Below, we will essentially follow Koch et al. [158].

In Euclidean space, the Dirac equation for a massless particle has the following form (γ_μ^E are the Euclidean γ matrices):

$$\gamma_\mu^E \partial_\mu \psi = 0, \quad (8.36)$$

and is solved by the ansatz

$$\psi(x) = \psi_0 e^{-i(2n+1)\pi T x_0} e^{-i\mathbf{p}\cdot\mathbf{x}}, \quad (8.37)$$

where the dependence in the 0-direction is due to the antiperiodic boundary conditions on fermion wave functions which result from finite temperature. The frequencies

$$\omega_n = (2n + 1)\pi T \quad (8.38)$$

are the fermionic Matsubara frequencies. We noted earlier that only ω_0 contributes to the screening mass for massless quarks.

We shall now consider a simplified situation where the interaction between the quarks is entirely magnetic in character, i.e., is the interaction between the magnetostatic fields of the quark currents.

We neglect any color-electric effects because of the screening. This is an unusual situation, rarely encountered in classical electrodynamics, as magnetic effects are usually down by v/c as compared to the electric ones. To reduce it to more familiar grounds, we will introduce a relabeling of the (t, z) -coordinates in Euclidean space that changes electric into magnetic fields and vice versa. This will convert the magnetic current-current interaction to a static potential with a Coulomb-like and a string-like piece, the string tension of this potential, however, not arising from the time-like Wilson loops, but rather from the space-like ones. Due to the periodicity in the z -direction, the Coulomb-like potential will turn out to be logarithmic.

Under this transformation ($t \leftrightarrow z$), the Euclidean Dirac equation is invariant. The wave function, however, changes to

$$\psi(x) = \psi_0 e^{-i(2n+1)\pi T z} e^{-ip_0 x_0} e^{-i\mathbf{p}_\perp \cdot \mathbf{x}_\perp}. \quad (8.39)$$

The antiperiodicity is now in the z -direction. The Dirac equation is solved by

$$p_0 = \pm i \sqrt{p_z^2 + p_\perp^2} = \pm i \sqrt{[(2n+1)\pi T]^2 + p_\perp^2} = -iE, \quad (8.40)$$

with E real. The wave function then takes the form

$$\psi(x) = \psi_0 e^{-Ex_0} e^{-i(2n+1)\pi T z} e^{-i\mathbf{p}_\perp \cdot \mathbf{x}_\perp}. \quad (8.41)$$

Close inspection of the effective Dirac equation reveals, as postulated earlier, the effective quark mass,

$$m_{\text{eff}} = \sqrt{m_{\text{dyn}}^2 + [(2n+1)\pi T]^2}, \quad (8.42)$$

where we have allowed for a putative dynamically generated quark mass m_{dyn} . From (8.42) it is clear that this effective quark mass is quite large at the temperatures that we are considering. Therefore, we may treat the bound state problem nonrelativistically by solving the Schrödinger equation

$$(p_\perp^2/2m_{\text{eff}} - V)\psi = E\psi, \quad (8.43)$$

where we introduced a static interquark potential V . Let us first discuss the potential induced by the periodicity in the z -direction (the former time direction). The potential of a periodic array of these charges can be written as (for electrodynamics)

$$\Phi = \frac{e}{4\pi} \left[\frac{1}{r} - 2 \sum_{n=1}^{\infty} \left(\frac{1}{\sqrt{x^2 + y^2 + (n\beta - z)^2}} - \frac{1}{n\beta} \right) \right]. \quad (8.44)$$

We would like to stress again that we do not consider magnetic effects as they are considered to be screened (remember that we have effectively exchanged electric and magnetic fields via the (z, t) interchange). In the large- T limit we simply obtain the Coulomb potential in two dimensions (potential of a charged wire)

$$\Phi(r_\perp) = -(e/2\pi\beta) \ln(r_\perp/2\beta). \quad (8.45)$$

A similar potential has been obtained in QCD₃ by Hansson and Zahed [160], investigating essentially the same problem. The above potential is the analog of the one-gluon exchange interquark

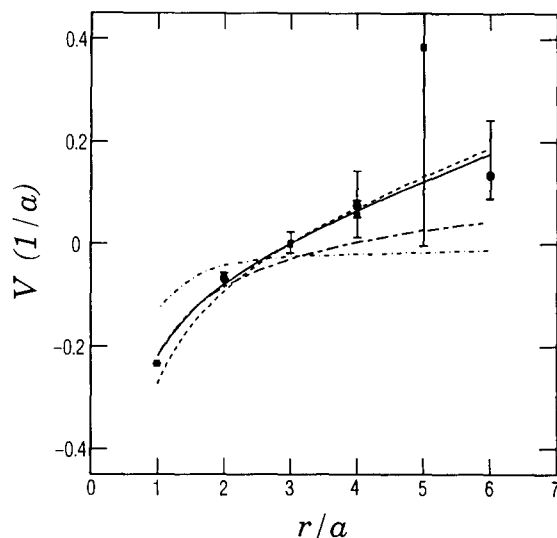


Fig. 8.3. Manousakis-Polonyi potential from ref. [9]. The finite temperature ($T > T_c$) space-like potential corresponds to the full line, the zero temperature time-like potential to the dashed line. The dashed-dotted line represents the finite temperature ($T > T_c$) space-like potential and the short-dashed line the modified Coulomb potential according to eq. (8.44)

potential in the real world. However, it is known that this is not sufficient to reproduce bound-state properties even at zero temperature, and a linearly rising piece has to be added. The usual string tension σ appearing in these potentials is related to the correlation of time-like Wilson loops, and therefore vanishes in the high temperature limit (disordering of the Wilson loop). The only remaining correlation is that of space-like Wilson loops, which are not related to a static interquark potential [161]. In the (t, z) inverted world, however, this is the correlator that acts as the confinement criterion, and therefore we should add to the logarithmic potential derived above a linearly rising potential with a string tension obtained from the correlation of the *space-like* Wilson loops. The latter was estimated from lattice calculations performed for pure glue by Manousakis and Polonyi [9]. They calculated the correlation function of two space-like Polyakov lines for $T \sim 2T_c$, where T_c is the pure gauge transition temperature. We show their results in fig. 8.3. The correlation function of time-like Polyakov loops gives roughly the same potential as the correlation of time-like Wilson loops. The potential due to the latter is denoted by the dotted line, and seems to approach zero with distance rather rapidly, indicating screening. As the time-like direction is compressed with increasing temperature, the electric modes move more and more into the high-frequency region and decouple, leaving effectively a three-dimensional confining theory with magnetic interactions, as observed long ago [161]. Also in fig. 8.3 are shown the results of Polonyi and Manousakis for the correlation function of space-like Polyakov loops at $T \sim 2T_c$. According to the arguments raised above, this correlation function is interpreted as the potential $V(R)$ between a heavy quark and antiquark (heavy in this context meaning large *effective* mass) in a world where the (t, z) relabeling is performed. Let us now parameterize this static potential $V(R)$ as

$$V(R) = -b/R + \sigma_{\text{sp}}R + c, \quad (8.46)$$

with the values

$$b = 0.184 \pm 0.02, \quad \sqrt{\sigma_{\text{sp}}} = 0.22 \pm 0.03 \text{ a}^{-1}, \quad (8.47)$$

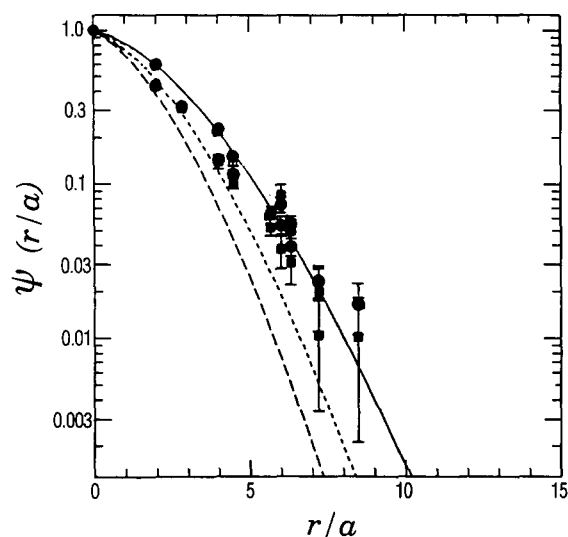


Fig. 8.4. Wave function for the ρ -meson as a function of r/a ($a = 0.22$ fm) for different temperatures. The curves correspond to wave functions obtained with the confining potential Eq. (8.46). Temperatures: 150 MeV (full line), 250 MeV (short-dashed line) and 350 MeV (long-dashed) line. Data are from ref. [10] and correspond roughly to $T \sim 210$ MeV.

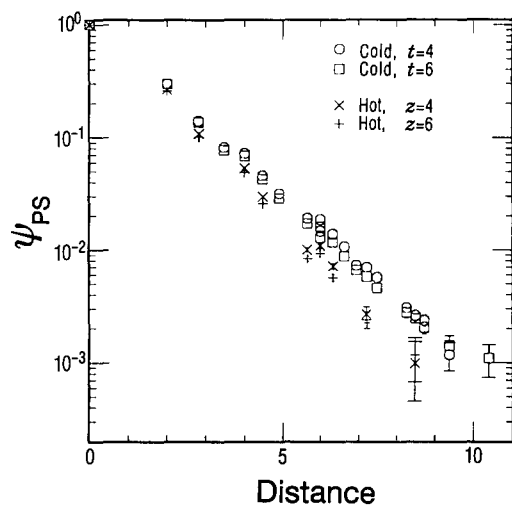


Fig. 8.5. The pion wave function at $T = 0$ (“cold”, $t = 4, 6$) and the screening pion correlation function at $T \simeq 1.5T_c$. For the “cold” case two Euclidean times are plotted, to show that the wave function is roughly independent of the number of time slices used, while for the hot case two values of z are shown (from ref. [10]).

where the space-like string tension is given in lattice units. The constant c remains undetermined. The physical zero-temperature static potential, measured by time-like Wilson loops [159], also shown in fig. 8.3, can be parameterized by

$$b = \frac{1}{12}\pi, \quad \sqrt{\sigma} = 0.22 \pm 0.02 a^{-1}. \quad (8.48)$$

From the known value of $\sigma = (400 \text{ MeV})^2$, we deduce that $a = 0.1$ fm in the Manousakis and Polonyi calculation.

The persistence of the (space-like) string tension at temperatures above T_c implies that magnetic modes are still confined; indeed, they should be as the compression of the time-like direction does not affect the magnetic fields. The potential (8.46) should therefore be thought of as originating from interactions mediated by these modes. The space-like string tension σ_{sp} above T_c is calculated to be about the same as the zero-temperature string tension (8.48), suggesting that magnetic screening is negligible at these temperatures, within the accuracy of these lattice results.

The full potential (8.46) can now be used to solve the (temperature-dependent) Schrödinger equation (8.43) to obtain the bound state wave functions in the QCD case. We thus obtain fig. 8.4, where we have plotted the wave functions obtained for three temperatures together with results from lattice QCD calculations [10]. The latter (in the pseudoscalar channel) are redisplayed in fig. 8.5 for a temperature $T = 1.5T_c$ (which here corresponds to $T \approx 220$ MeV) together with a measurement of the same quantity on a symmetric lattice ($T = 0$). These wave functions are obtained by measuring the *spatial* correlation of quarks and antiquarks at equal time, a distance z downstream of a “hot” wall from which the initial quark and antiquark are boiled off in a completely uncorrelated state. As the quarks are carried downstream, only the lowest energy eigenvalue will

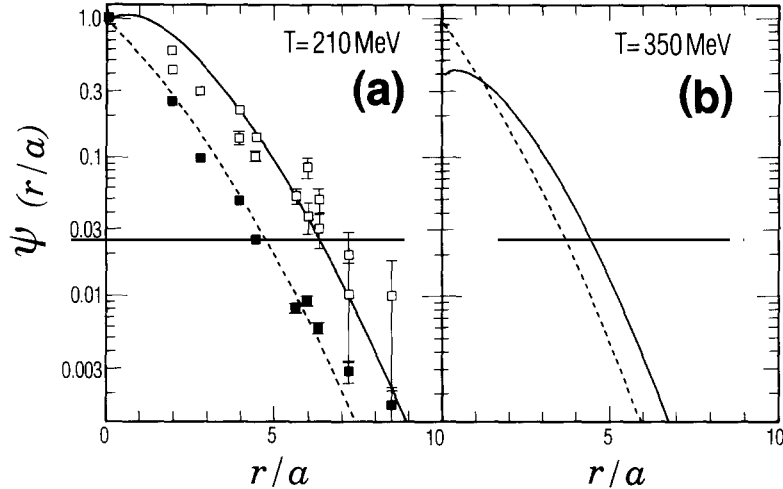


Fig. 8.6. Wave functions for the ρ and π at (a) $T=210$ MeV and (b) $T=350$ MeV as a function of r/a ($a=0.23$ fm). The full line corresponds to the ρ with spin quantum number $S_z = \pm 1$. The dashed line represents the pion and the ρ ($S_z = 0$) wave functions. In (a) arbitrary normalization was used, while in (b) all wave functions have the same normalization. Data are from ref. [10].

survive, and correlations build up due to the current–current interaction. Also, any transverse momentum of the quarks is suppressed at large z , as from the uncertainty relation in this space we find $p_\perp \sim 1/\sqrt{Tz}$, and the momenta of quark and antiquark are effectively parallel at large z . This reflects the binding in the original space. As is obvious from these plots, the hot wave function cannot be distinguished from the cold one, a quite striking result, which may be explained by the simple model presented above.

We can also add a spin–spin Breit–Fermi-type interaction that will split the π and ρ channels [160, 158]. The resulting wave functions are plotted in figs. 8.6a and 8.6b as the solid (ρ with spin $S_z \pm 1$) and dashed (π and ρ with $S_z = 0$) lines, at 210 MeV and 350 MeV, respectively*).

To summarize the results of figs. 8.4–8.6, a space-like string tension as obtained by Manoussakis and Polonyi can explain the strong correlations found by Bernard et al. In this picture, a Breit–Fermi interaction (with $\alpha_s = 0.25$) splits the ρ and π wave functions. Note that a purely logarithmic confining potential as arising from the replications would not suffice to reproduce the wave functions observed on the lattice; a linearly rising potential with $\sigma \sim \sigma_{sp}$ is required at all temperatures. We are thus led to believe that the states in these channels do *not* propagate in the plasma as weakly interacting quarks, as suggested recently [162, 163]. As noted following eq. (8.31), the proximity of these screening masses to $n_q \pi T$ indicates that the dynamically generated quark mass has become negligibly small (as compared to $n_q \pi T$, to the accuracy of the lattice data); the lowest Matsubara frequency $\omega_0 = \pi T$ here plays the role of a “thermal mass” or “chiral mass”**) for the quark. Since it becomes large as T increases, interactions can produce the correlations that are observed. Nevertheless, the size of the system does not seem to be determined by the temperature or any other soft scale, but rather by a hard scale, presumably that of deconfinement [157].

We would like to propose an intuitive picture of the high temperature phase based on the above observations. We saw that current–current interactions persist above T_c and force any quark–

*) These temperatures are chosen to facilitate the comparison with the lattice calculations of the same quantities.

**) The “chiral mass” is very different from a bare mass in the sense that it does not break chiral symmetry.

antiquark pair (and maybe every three-quark state) to correlate into color singlets. As the quarks are moving in the heat bath, the strings connecting them for color neutrality are constantly breaking and reforming, which can be interpreted as hadrons going in and out of the heat bath. The energetic advantage of color neutrality was emphasized in the context of dense strange matter by Bethe, Brown, and Cooperstein [72]. This picture seems to suggest that the relevant degrees of freedom are still hadronic, as suggested by the original deconfinement model of DeTar, and an equation of state describing massless hadrons might be appropriate. This, however, raises the specter of a maximum temperature again, as it seems as if we can construct an infinite tower of states with different angular momenta in each channel, since there is no deconfinement. The average distance between quark and antiquark is of the order T^{-1} , thus once a quark moves beyond that distance it is likely to be replaced by another one, closer to the former partner. This “quark promiscuity” assures that the maximum angular momentum of a quark–antiquark pair is roughly

$$J_{\max} \sim T^{-1} \times \pi T = \pi, \quad (8.49)$$

thus only bound states with angular momentum $J = 0, 1, 2$ are likely to survive. Thus, the density of states in this phase is not exponentially rising, and there is no maximum temperature. However, the number of states with these momenta exceeds the number of degrees of freedom in the quark/gluon phase. Consequently, not all of these can be realized, since the condition (8.35) must be enforced.

Our picture for $T > T_{\chi\text{SR}}$ has a formal resemblance to the string flip model [164, 165], but the apparent similarity is somewhat misleading. In the string flip model with time-like strings, chiral symmetry is broken, since the quarks flip helicity as they bounce back from a maximally stretched string. In our case, for $T > T_{\chi\text{SR}}$, we are in a chirally restored phase. The correlated quark and antiquark must therefore conserve helicity. In fact, before the change of variables $z \leftrightarrow t$, the interaction between quark and antiquark is magnetic, i.e., a current–current interaction.

9. Conclusions

Our main objective in this report was to bring together a variety of theoretical approaches and experimental information that support the notion of a “benign”, nondramatic change in the properties of nuclear matter under extreme conditions. As temperature and density change, so do the microscopic, and ultimately macroscopic, scales that govern the behavior of such matter; most notable among these is the dropping of hadron masses. The latter is very natural in a picture of chiral symmetry restoration that is not first order; intuitively we expect at a certain point of the transition to have the choice to describe the hadron in either language: the hadronic one or the quark one. In the absence of chiral-symmetry breaking this is most natural if the mass of the hadron in question is essentially the sum of the bare-quark masses that make up the color-singlet.

We have explored here not only how such a change in hadron masses can occur in various formulations, but also the ramifications of such behavior in intermediate to high-energy regimes, from nuclear structure to heavy-ion collisions to neutron stars. In most applications it would show that, while hadron masses are a convenient way to parameterize the change in related observables, it is really the quark and gluon condensates that play the key role in chiral-symmetry and scaling-symmetry restoration. There is still much to be learned about the subtle relationship between these symmetries and the condensates, as it is they who mirror the changes in the nonperturbative vacuum. A good description of the latter therefore is essential to further our understanding of matter under extreme conditions. Dramatic progress was indeed achieved using QCD sum rules,

lattice gauge theory, and the instanton-liquid model, to name but some of the front-runners. These approaches are still being pursued and should yield more valuable information. Yet it seems that we are still far from a satisfactory understanding of nonperturbative QCD, at any temperature or density. Indeed, the exploration of the different temperature and density regimes can be viewed as part of the ongoing effort of exploring nonperturbative QCD, using all available tools. Certainly, relativistic heavy-ion collision experiments are a keystone to this concerted effort, and large-scale projects such as RHIC should yield a wealth of puzzling details that further our understanding and spark new insights. At the same time the need for large-scale computing facilities and logistics is more and more obvious, not only on the hardware side. New and more powerful algorithms may emerge from such efforts, and together with the next generation of machines this should give the community a third solid leg to stand on, next to the analytical and the experimental one.

Acknowledgements

We would like to thank Steve Koonin for the hospitality at the Kellogg Radiation Laboratory, Caltech, where part of this work was written up. For discussions and advice we are grateful to H.A. Bethe, T. Hatsuda, V. Koch, B.L. Ioffe, A.D. Jackson, M. Prakash, E.V. Shuryak, W. Weise, C. Weiss, and I. Zahed. This work was supported in part by the U.S. Dept. of Energy Grant No. DE-FG02-88ER40388.

References

- [1] G.E. Brown, C.B. Dover, P.B. Siegel and W. Weise, *Phys. Rev. Lett.* 60 (1988) 2723.
- [2] G.E. Brown and M. Rho, *Phys. Lett. B* 222 (1989) 324.
- [3] G.E. Brown and M. Rho, *Phys. Lett. B* 237 (1990) 3.
- [4] F.R. Brown et al., *Phys. Rev. Lett.* 65 (1990) 2491.
- [5] S. Gottlieb, W. Liu, R.L. Renken, R.L. Sugar and D. Toussaint, *Phys. Rev. D* 41 (1990) 622.
- [6] J.B. Kogut et al., *Phys. Lett. B* 263 (1991) 101.
- [7] C. Bernard, M.C. Ogilvie, T.A. DeGrand, C. DeTar, S. Gottlieb, A. Krasnitz, R.L. Sugar and D. Toussaint, *Phys. Rev. D* 45 (1992) 3854.
- [8] C. De Tar and J.B. Kogut, *Phys. Rev. D* 36 (1987) 2828.
- [9] E. Manousakis and J. Polonyi, *Phys. Rev. Lett.* 58 (1987) 847.
- [10] C. Bernard, T.A. DeGrand, C.E. De Tar, S. Gottlieb, A. Krasnitz, M.C. Ogilvie, R.L. Sugar and D. Toussaint, *Phys. Rev. Lett.* 68 (1992) 2125.
- [11] G.E. Brown and M. Rho, *Phys. Rev. Lett.* 66 (1991) 2720.
- [12] B.A. Campbell, J. Ellis and K.A. Olive, *Phys. Lett. B* 235 (1990) 325.
- [13] B.A. Campbell, J. Ellis and K.A. Olive, *Nucl. Phys. B* 345 (1990) 57.
- [14] D.B. Kaplan and A.E. Nelson, *Phys. Lett. B* 175 (1986) 57.
- [15] A.E. Nelson and D.B. Kaplan, *Phys. Lett. B* 192 (1987) 193.
- [16] T.L. Ainsworth, G.E. Brown, M. Prakash and W. Weise, *Phys. Lett. B* 200 (1988) 413.
- [17] G.E. Brown, *Prog. Theor. Phys. Suppl.* 91 (1987) 85.
- [18] G.E. Brown, *Nucl. Phys. A* 488 (1988) 689c.
- [19] G.E. Brown, *Z. Phys. C* 38 (1988) 291.
- [20] G.E. Brown, *Nucl. Phys. A* 507 (1990) 251c.
- [21] G.E. Brown, *Nucl. Phys. A* 522 (1991) 397c.
- [22] V. Bernard, U.-G. Meißner and I. Zahed, *Phys. Rev. Lett.* 59 (1987) 966; *Phys. Rev. D* 36 (1987) 819.
- [23] V. Bernard and U.-G. Meißner, *Nucl. Phys. A* 489 (1988) 647; *Phys. Rev. D* 38 (1988) 1551.
- [24] C. Adami and G.E. Brown, *Z. Phys. A* 340 (1991) 93.
- [25] B.L. Ioffe, *Nucl. Phys. B* 188 (1981) 317.
- [26] M. Wakamatsu and W. Weise *Z. Phys. A* 331 (1988) 173.

- [27] K. Kusaka and W. Weise, *Phys. Lett. B* 288 (1992) 6.
- [28] G. Ripka and M. Jaminon, *Ann. Phys. (NY)* 218 (1992) 51.
- [29] T. Hatsuda and S.H. Lee, *Phys. Rev. C* 46 (1992) R34.
- [30] T. Hatsuda, Y. Koike and S.H. Lee, *Nucl. Phys. B* 394 (1993) 221.
- [31] S. Coleman and E. Weinberg, *Phys. Rev. D* 7 (1973) 1888.
- [32] J. Ellis, *Nucl. Phys. B* 22 (1970) 478.
- [33] J. Collins, A. Duncan and S. Joglekar, *Phys. Rev. D* 16 (1977) 438;
N.K. Nielsen, *Nucl. Phys. B* 120 (1977) 212.
- [34] J. Schechter, *Phys. Rev. D* 21 (1980) 3393.
- [35] E.V. Shuryak, *Nucl. Phys. B* 203 (1982) 93, 116, 140.
- [36] M.A. Nowak, J.J.M. Verbaarschot and I. Zahed, *Nucl. Phys. B* 321 (1989) 387.
- [37] H. Gomm, P. Jain, R. Johnson and J. Schechter, *Phys. Rev. D* 33 (1986) 3476.
- [38] H. Forkel, A.D. Jackson, M. Rho, C. Weiss, A. Wirzba and H. Bang, *Nucl. Phys. A* 504 (1989) 818.
- [39] H. Reinhardt and B.V. Dang, *Phys. Rev. D* 38 (1988) 2881.
- [40] C.G. Callan Jr., R. Dashen and D.J. Gross, *Phys. Rev. D* 17 (1978) 2717.
- [41] M.A. Shifman, A.I. Vainshtein and V.I. Zakharov, *Nucl. Phys. B* 147 (1979) 385, 448.
- [42] M. Bando, T. Kugo and K. Yamawaki, *Phys. Rep.* 164 (1988) 217.
- [43] J.J. Sakurai, *Currents and Mesons* (Univ. of Chicago Press, Chicago and London, 1969).
- [44] T.H.R. Skyrme, *Nucl. Phys.* 31 (1962) 556;
E. Witten, *Nucl. Phys. B* 223 (1983) 422, 433.
- [45] E.V. Shuryak, *Phys. Lett. B* 107 (1981) 103.
- [46] E.V. Shuryak, *Nucl. Phys. B* 203 (1982) 93.
- [47] E.V. Shuryak, *Phys. Lett. B* 79 (1978) 135.
- [48] Y. Nambu and G. Jona-Lasinio, *Phys. Rev* 122 (1961) 345.
- [49] M. Jaminon, G. Ripka and P. Stassart, *Nucl. Phys. A* 504 (1989) 733;
T. Hatsuda and T. Kunihiro, *Phys. Lett. B* 198 (1987) 126;
R. Allkofer, P.A. Amundsen and H. Reinhardt, *Phys. Lett. B* 218 (1988) 75.
- [50] M. Lutz, S. Klimt and W. Weise, *Nucl. Phys. A* 542 (1992) 521.
- [51] G.E. Brown, *Phys. Rep.* 163 (1988) 167.
- [52] S. Li, R.S. Bhalerao and R.K. Bhaduri, *Int. J. Mod. Phys. A* 6 (1991) 501.
- [53] M. Asakawa and K. Yazaki, *Nucl. Phys. A* 504 (1989) 668.
- [54] E. Jenkins and A. Manohar, *Phys. Lett. B* 255 (1991) 562; *B* 259 (1991) 353.
- [55] E. Jenkins, *Nucl. Phys. B* 368 (1991) 190.
- [56] L.J. Reinders, H. Rubinstein and S. Yazaki, *Phys. Rep.* 127 (1985) 1.
- [57] L.J. Reinders, *Acta Phys. Pol. B* 15 (1984) 329.
- [58] C. De Tar and T. Kunihiro, *Phys. Rev. D* 39 (1989) 2805.
- [59] G.E. Brown, V. Koch and M. Rho, *Nucl. Phys. A* 535 (1991) 701.
- [60] J. Gasser, H. Leutwyler and M.E. Sainio, *Phys. Lett. B* 253 (1991) 252.
- [61] J. Delorme, M. Ericson and T.E.O. Ericson, *Phys. Lett. B* 291 (1992) 379.
- [62] S. Fubini and G. Furlan, *Ann. Phys. (NY)* 48 (1968) 322.
- [63] G.E. Brown, C.-H. Lee, M. Rho and V. Thorsson, in preparation.
- [64] A. Müller-Groeling, K. Holinde and J. Speth, *Nucl. Phys. A* 513 (1990) 557.
- [65] R. Büttgen, K. Holinde, A. Müller-Groeling, J. Speth and P. Wyborny, *Nucl. Phys. A* 506 (1990) 586.
- [66] V. Vento, M. Rho and G.E. Brown, *Phys. Lett. B* 108 (1981) 285.
- [67] K. Holinde, in: *American Institute of Physics Conf. Proc. No. 224*, eds. B.F. Gibson, W.R. Gibbs and M.B. Johnson (1990) p. 101.
- [68] G.E. Brown, K. Kubodera and M. Rho, *Phys. Lett. B* 192 (1987) 273.
- [69] H.D. Politzer and M.B. Wise, *Phys. Lett. B* 273 (1991) 156.
- [70] G.E. Brown, K. Kubodera, M. Rho and V. Thorsson, *Phys. Lett. B* 291 (1992) 355.
- [71] G. Baym and D.K. Campbell, in: *Mesons and Nuclei*, Vol. 3, eds. M. Rho and D. Wilkinson (North-Holland, Amsterdam, 1979).
- [72] H.A. Bethe, G.E. Brown and J. Cooperstein, *Nucl. Phys. A* 462 (1987) 791.
- [73] G.E. Brown, in: *Proc. First Symp. on Nuclear Physics of the Universe* (Oak Ridge, TN, 1992), eds. D.H. Feng, M. Guidry and M. Strayer (World Scientific, Singapore).
- [74] G.E. Brown, S.W. Bruenn and J.C. Wheeler, *Comments Astrophys.* 16 (1992) 153;
G.E. Brown and H.A. Bethe, *Astrophys. J.*, to be published.
- [75] J.W. Harris and NA35 Collab., *Nucl. Phys. A* 498 (1989) 133c.

- [76] J. Schukraft, invited talk at Workshop on Quark Gluon Plasma Signatures (Strasbourg, France, 1990), CERN preprint PPE/91-04.
- [77] C.M. Ko, Z.G. Wu, L.H. Xia and G.E. Brown, in: Proc. Workshop on Heavy Ion Physics at the AGS (1990), ed. O. Hansen, p. 361;
C.M. Ko, Z.G. Wu, L.H. Xia and G.E. Brown, Phys. Rev. Lett. 66 (1991) 2577;
G.E. Brown, C.M. Ko, Z.G. Wu and L.H. Xia, Phys. Rev. C 43 (1991) 1881.
- [78] J. Rafelski and B. Müller, Phys. Rev. Lett. 48 (1982) 1066;
J. Rafelski, Nucl. Phys. A 418 (1984) 215c.
- [79] T. Abbott et al., Phys. Rev. Lett. 64 (1990) 847.
- [80] G.E. Brown, J. Stachel and G.M. Welke, Phys. Lett. B 253 (1991) 19.
- [81] NA35 Collab., Johann Wolfgang Goethe University Frankfurt preprint (1990).
- [82] D. Lissauer and E.V. Shuryak, Phys. Lett. B 253 (1991) 15.
- [83] G.E. Brown, H. Müther and M. Prakash, Nucl. Phys. A 506 (1990) 413.
- [84] G.E. Brown, W. Weise, G. Baym and J. Speth, Comments Nucl. Part. Phys. 17 (1987) 39.
- [85] P.B. Siegel, W.B. Kaufmann and W.R. Gibbs, Phys. Rev. C 31 (1985) 2184.
- [86] D. Marlow et al., Phys. Rev. C 25 (1982) 2619.
- [87] Y. Mardor et al., Phys. Rev. Lett. 65 (1990) 2110;
R. Krauss, Texas A&M Univ. Ph.D. Thesis (1991).
- [88] C.M. Chen and D.J. Ernst, Phys. Rev. C 45 (1992) 2019.
- [89] Q. Daffner, Diplomarbeit, Regensburg Univ. (1990), unpublished;
J. Labarsouque, Nucl. Phys. A 506 (1990) 539.
- [90] J. Alster, in: Proc. Intern. Symp. on Hypernuclear and Strange Particle Physics (Shimoda, Japan, 1991), Nucl. Phys. A 547 (1992).
- [91] A. Gal, private communication.
- [92] W.R. Gibbs, B.F. Gibson and G.J. Stephenson, Phys. Rev. Lett. 39 (1977) 1316.
- [93] N.M. Hintz et al., Phys. Rev. C 30 (1984) 1976;
see also: N.M. Hintz et al., Univ. of Minn. Summary Progr. Rept. 1984-87, p. 112, unpublished.
- [94] G.E. Brown, A. Sethi and N.M. Hintz, Phys. Rev. C 44 (1991) 2653.
- [95] J. Tjon and S.J. Wallace, preliminary results, shown in ref. [94].
- [96] I. Sick, Phys. Lett. B 157 (1985) 13.
- [97] G.E. Brown, M. Rho and W. Weise, Nucl. Phys. A 454 (1986) 669.
- [98] M. Soyeur, G.E. Brown and M. Rho, Nucl. Phys. A 553 (1993) 355.
- [99] B. Buck and F. Perez, Phys. Rev. Lett. 54 (1988) 707.
- [100] J. Bartel et al., Nucl. Phys. A 386 (1982) 79.
- [101] K. Kubodera and M. Rho, Phys. Rev. Lett. 67 (1991) 3479.
- [102] E.K. Warburton, Phys. Rev. Lett. 66 (1991) 1823; Phys. Rev. C 44 (1991) 233;
I.S. Towner and E.K. Warburton, Phys. Lett. B 294 (1992) 1.
- [103] K. Kubodera, J. Delorme and M. Rho, Phys. Rev. Lett. 40 (1978) 755.
- [104] M. Kirchbach and H. Reinhardt, Phys. Lett. B 208 (1988) 79.
- [105] T. Park, D.-P. Min and M. Rho, Phys. Rep. 233 (1993) 341.
- [106] M. Rho, Nucl. Phys. A 231 (1974) 493.
- [107] K. Ohta and M. Wakamatsu, Nucl. Phys. A 234 (1975) 445.
- [108] T. Cohen and L. Kisslinger, Univ. of Maryland preprint (1991), unpublished.
- [109] E.G. Drukarev and E.M. Levin, Nucl. Phys. A 532 (1991) 695.
- [110] J. Ahrens, Nucl. Phys. A 446 (1985) 229c.
- [111] J. Ahrens, L.S. Ferreira and W. Weise, Nucl. Phys. A 485 (1988) 621.
- [112] G.E. Brown, S.K. Klimt, M. Rho and W. Weise, Z. Phys. A 331 (1988) 139 (see appendix).
- [113] S.E. Koonin, C.W. Johnson and P. Vogel, Phys. Rev. Lett. 69 (1992) 1163.
- [114] A.I. Bochkarev and M.E. Shaposhnikov, Nucl. Phys. B 268 (1986) 220.
- [115] C. Adami, T. Hatsuda and I. Zahed, Phys. Rev. D 43 (1991) 921.
- [116] C. Adami and I. Zahed, Phys. Rev. D 45 (1992) 4312.
- [117] K.G. Wilson, Phys. Rev. 129 (1969) 1499.
- [118] A. Fetter and J.D. Walecka, Quantum Theory of Many Particle Systems (McGraw-Hill, New York, 1971).
- [119] A.A. Abrikosov, L.P. Gorkov and I.E. Dzyaloshinskii, Methods of Quantum Field Theory in Statistical Physics (Dover Publ., New York, 1963).
- [120] M. Dey, V.L. Eletsky and B.L. Ioffe, Phys. Lett. B 252 (1990) 620.
- [121] E.S. Fradkin, Proc. P.N. Lebedev Phys. Inst. 29 (1965) 3.

- [122] R.J. Furnstahl, T. Hatsuda and S.H. Lee, *Phys. Rev. D* 42 (1990) 1744.
- [123] S.H. Lee, *Phys. Rev. D* 40 (1989) 2484.
- [124] C. Adami and G.E. Brown, *Phys. Rev. D* 46 (1992) 478.
- [125] H. Leutwyler and A.V. Smilga, *Nucl. Phys. B* 342 (1990) 302.
- [126] E.G. Drukarev and E.M. Levin, *Nucl. Phys. A* 511 (1990) 679.
- [127] R.J. Furnstahl, D.K. Griegel and T.D. Cohen, *Phys. Rev. C* 46 (1992) 1507.
- [128] G.E. Brown, V. Koch and T. Schäfer, work in progress.
- [129] E. Wüst, G.E. Brown and A.D. Jackson, *Nucl. Phys. A* 468 (1987) 450.
- [130] E.G. Drukarev and M.G. Ryskin, *St. Petersburg Nuclear Physics Institute Report PNPI-1786* (1992), *Nucl. Phys. B*, to appear.
- [131] T.D. Cohen, R.J. Furnstahl and D.K. Griegel, *Phys. Rev. Lett.* 67 (1991) 961; *Phys. Rev. C* 45 (1992) 1881.
- [132] T. Hatsuda, H. Høgaasen and M. Prakash, *Phys. Rev. C* 42 (1990) 2212; *Phys. Rev. Lett.* 66 (1991) 2851.
- [133] E.G. Drukarev and M.G. Ryskin, *Isospin breaking nuclear forces in QCD sum rules and the Nolen–Schiffer anomaly*, *St. Petersburg Nuclear Physics Institute Report PNPI-1848* (1992).
- [134] B.D. Serot and J.D. Walecka, *Adv. Nucl. Phys.* 16 (1986) 1.
- [135] R. Brockmann and H. Toki, *Phys. Rev. Lett.* 68 (1992) 3408.
- [136] G.E. Brown and R. Machleidt, *Stony Brook Univ. preprint SUNY-NTG-92-30* (1992).
- [137] T. Hatsuda and T. Kunihiro, *Nucl. Phys. B* 387 (1992) 715.
- [138] B.L. Friman, V.R. Pandharipande and R.B. Wiringa, *Phys. Rev. Lett.* 51 (1983) 763.
- [139] E.L. Berger, F. Coester and R.B. Wiringa, *Phys. Rev. D* 29 (1984) 398.
- [140] C.A. Goodman, in: *Spin and Isospin in Nuclear Interactions*, eds. S.W. Wissink, C.A. Goodman and G.E. Walker (Plenum, New York and London, 1986), p. 167.
- [141] V. Mull, J. Wambach and J. Speth, *Phys. Lett. B* 286 (1992) 13;
J.W. Durso, H.C. Kim and J. Wambach, *Phys. Lett. B* 298 (1993) 267.
- [142] F. Wilczek, *Int. J. Mod. Phys. A* 7 (1992) 3911.
- [143] G. Baker, B. Nickel and D. Meiron, *Phys. Rev. D* 17 (1978) 1365.
- [144] C. Bernard, M.C. Ogilvie, T.A. DeGrand, C. DeTar, S. Gottlieb, A. Krasnitz, R.L. Sugar and D. Toussaint, *Phys. Rev. D* 45 (1992) 3854.
- [145] G.E. Brown, H.A. Bethe and P.M. Pizzochero, *Phys. Lett. B* 263 (1991) 337.
- [146] G.E. Brown, H.A. Bethe, A.D. Jackson and P.M. Pizzochero, *Nucl. Phys. A* 560 (1993) 1035.
- [147] R. Hagedorn, *Nuovo Cimento Suppl.* 3 (1965) 147.
- [148] C.J. Hamer and S.C. Frautschi, *Phys. Rev. D* 4 (1971) 2125.
- [149] P. Gerber and H. Leutwyler, *Nucl. Phys. B* 321 (1989) 387.
- [150] E.V. Shuryak, *Sov. Phys. JETP* 47 (1987) 319;
S.A. Chin, *Phys. Lett. B* 78 (1978) 522.
- [151] C. De Tar, *Phys. Rev. D* 32 (1985) 276.
- [152] C. De Tar, *Phys. Rev. D* 37 (1987) 2378.
- [153] T. Hatsuda and T. Kunihiro, *Phys. Lett. B* 145 (1984) 7.
- [154] T. Hatsuda and T. Kunihiro, *Phys. Rev. Lett.* 55 (1985) 158.
- [155] T. Hatsuda and T. Kunihiro, *Prog. Theor. Phys.* 74 (1985) 765.
- [156] C. Bernard et al., *Nucl. Phys. A* 544 (1992) 519c.
- [157] S. Schramm and M.C. Chu, *Quark-correlations in high-temperature QCD*, *Phys. Rev. D* (September 1993), to appear.
- [158] V. Koch, E. Shuryak, G.E. Brown and A.D. Jackson, *Phys. Rev. D* 46 (1992) 3169; *Erratum Phys. Rev. D* 47 (1993) 2157.
- [159] C. Bowler, C.B. Chalmers, R.D. Kenway, G.S. Pawley and D. Roweth, *Nucl. Phys. B* 284 (1987) 299.
- [160] T.H. Hansson and I. Zahed, *Nucl. Phys. B* 374 (1992) 277.
- [161] D.J. Gross, R.D. Pisarski and L.G. Yaffe, *Rev. Mod. Phys.* 53 (1981) 43.
- [162] K.D. Born, S. Gupta, A. Irbäck, F. Karsch, E. Laermann, B. Petersson and H. Satz, *Phys. Rev. Lett.* 67 (1991) 302.
- [163] A. Goksch, *Phys. Rev. Lett.* 67 (1991) 1701.
- [164] C.J. Horowitz, E. Moniz and J. Negele, *Phys. Rev. D* 31 (1985) 1689.
- [165] G. Röpke, D. Blaschke and H. Schulz, *Phys. Rev. D* 34 (1986) 3499.